

Summer 6-6-1963

# Transient Response of Linear Undamped and Lightly Damped Lumped Spring-Mass Systems by Graphica Techniques

Richard O. Brooks

Follow this and additional works at: [https://digitalrepository.unm.edu/me\\_etds](https://digitalrepository.unm.edu/me_etds)



Part of the [Mechanical Engineering Commons](#)

---

## Recommended Citation

Brooks, Richard O.. "Transient Response of Linear Undamped and Lightly Damped Lumped Spring-Mass Systems by Graphica Techniques." (1963). [https://digitalrepository.unm.edu/me\\_etds/103](https://digitalrepository.unm.edu/me_etds/103)

This Thesis is brought to you for free and open access by the Engineering ETDs at UNM Digital Repository. It has been accepted for inclusion in Mechanical Engineering ETDs by an authorized administrator of UNM Digital Repository. For more information, please contact [disc@unm.edu](mailto:disc@unm.edu).







TRANSIENT RESPONSE OF SPRING-MASS SYSTEMS - - BROOKS

378.789  
Jn30br  
1963  
cop. 2



THE LIBRARY  
UNIVERSITY OF NEW MEXICO



Call No.

378.789

Un30br

1963

cop.2

Accession  
Number

307826



A14407 262274

DATE DUE					
MAY 13 1964					
MAY - 5 RECD					
JUN - 2 1964 <i>no card</i>					
MAY 21 RECD					
FEB 18 1969					
FEB 17 RECD					
FEB 9 '86					
FEB 11 '86					
FEB 12 '86					
MAR - 3 '86					
GAYLORD					
					PRINTED IN U.S.A.











100% COTTON FIBRE  
REYNOLDS BOND  
STRENGTH



# UNIVERSITY OF NEW MEXICO LIBRARY

## MANUSCRIPT THESES

Unpublished theses submitted for the Master's and Doctor's degrees and deposited in the University of New Mexico Library are open for inspection, but are to be used only with due regard to the rights of the authors. Bibliographical references may be noted, but passages may be copied only with the permission of the authors, and proper credit must be given in subsequent written or published work. Extensive copying or publication of the thesis in whole or in part requires also the consent of the Dean of the Graduate School of the University of New Mexico.

This thesis by Richard O. Brooks  
has been used by the following persons, whose signatures attest their acceptance of the above restrictions.

A Library which borrows this thesis for use by its patrons is expected to secure the signature of each user.

NAME AND ADDRESS

DATE



## MANUSCRIPT THESIS

Unpublished theses submitted for the Master's and Doctor's degrees and deposited in the University of New Mexico Library are open for inspection, but are to be read only with due regard to the rights of the authors. Bibliographical references may be made, and passages may be copied only with the permission of the authors and proper credit must be given in abstracts, reviews or published work. Extensive copying or publication of the thesis in whole or in part requires also the consent of the Dean of the Graduate School of the University of New Mexico.

This thesis by \_\_\_\_\_  
has been used by the following persons, whose signatures are here  
accepted of the above restrictions.

A library which borrows this thesis for use by its patrons is  
expected to secure the signature of each user.

NAME AND ADDRESS

DATE



TRANSIENT RESPONSE OF LINEAR  
UNDAMPED AND LIGHTLY DAMPED LUMPED  
SPRING-MASS SYSTEMS BY GRAPHICAL TECHNIQUES

By

Richard O. Brooks

A Thesis

Submitted in Partial Fulfillment of the Requirements  
for the Degree of Master of Science  
in Mechanical Engineering

The University of New Mexico

1963





This thesis, directed and approved by the candidate's committee, has been accepted by the Graduate Committee of the University of New Mexico in partial fulfillment of the requirements for the degree of

MASTER OF SCIENCE

W. J. Parish

Dean

Date

June 10, 1963

TRANSIENT RESPONSE OF LINEAR  
UNDAMPED AND LIGHTLY DAMPED LUMPED  
SPRING-MASS SYSTEMS BY GRAPHICAL TECHNIQUES

By  
Richard O. Brooks

Thesis committee

R. C. Davis

Chairman

C. T. L. L.

Floyd O. Calvert



This thesis, directed and approved by the candidate's committee, has been accepted by the Graduate Committee of the University of New Mexico in partial fulfillment of the requirements for the degree of

MASTERS

DEGREE

1950

DATE

THESIS

1950

Thesis committee

Chairman

1950

1950



378.789  
267 30.00  
1963  
Cop. 2

#### ACKNOWLEDGMENTS

The author wishes to extend his most sincere appreciation to the various people who made this thesis possible. Many thanks to Dr. R. C. Dove, University of New Mexico, whose timely suggestions kept the analysis portions of this thesis in perspective, and to J. A. Guzman, Sandia Corporation, whose assistance in doing the experimental work was invaluable. Not to be slighted are the several typists, editors, and technical artists at Sandia Corporation who had a part in the preparation of the material.

307826





## TABLE OF CONTENTS

	Page
ACKNOWLEDGMENTS . . . . .	ii
I. INTRODUCTION . . . . .	1
II. STATEMENT OF THE PROBLEM . . . . .	4
III. LITERATURE SURVEY . . . . .	6
IV. PHASE-PLANE ANALYSIS - SINGLE-DEGREE SYSTEMS . . . . .	11
1. Undamped Systems . . . . .	12
2. Coulomb Damped Systems . . . . .	24
3. Viscously Damped Systems . . . . .	41
V. PHASE-PLANE ANALYSIS - MULTIDEGREE SYSTEMS . . . . .	58
1. Undamped Systems . . . . .	58
2. Damped Systems . . . . .	85
VI. EXPERIMENTAL INVESTIGATION . . . . .	93
1. Single-Degree System Designs . . . . .	93
2. Test Results . . . . .	100
VII. CONCLUSIONS . . . . .	115
BIBLIOGRAPHY . . . . .	122
APPENDIX . . . . .	124

CONTENTS

ACKNOWLEDGMENTS

1. INTRODUCTION

II. STATEMENT OF THE PROBLEM

III. LITERATURE SURVEY

IV. PHASE-PLANE ANALYSIS - ANALYTICAL

- 1. Unforced System
- 2. Damped System
- 3. Viscoelastic Damped System

V. PHASE-PLANE ANALYSIS - NUMERICAL

- 1. Unforced System
- 2. Damped System

VI. EXPERIMENTAL INVESTIGATION

- 1. Single-Degree System
- 2. Test Results

VII. CONCLUSIONS

BIBLIOGRAPHY

APPENDIX



## I. INTRODUCTION

Responsive motions of linear undamped and lightly damped lumped spring-mass systems subjected to transient inputs can be determined by several methods. All these methods require solving of the differential equation of motion in some manner. Practically all techniques for solving the differential equations involve higher mathematics. For single-degree systems, the analytical methods of solving the differential equation of motion include:

- (1) The classical solution (which requires finding the complementary and particular parts to a nonhomogeneous differential equation).
- (2) Duhamel's Integral (which determines responsive motions due to continuous forces acting during a specified time interval.
- (3) Laplace Transforms (which solves equations by the use of transform tables and partial fractions).

For multidegree systems, the same analytical tools can be used, but matrix operations are usually required to solve the simultaneous equations of motion. Computers frequently are used to solve these types of equations.

One method for solving a differential equation of motion which does not require higher mathematics in the solution is the graphical technique called





the "phase-plane" method. This method has been applied by several authors to a variety of problems of a transient nature. The problems have dealt almost exclusively with displacement responses of both single- and two-degree undamped systems. Discrete examples have been shown. Displacement responses of damped single-degree systems when excited by external forces have also been considered.

The field of mechanical shock testing is one in which responsive motions of undamped and lightly damped spring-mass systems to transient support excitation must frequently be determined. Most often, however, both the transient inputs and the responsive motions are in the nature of acceleration data. The input acceleration pulse shape generally is not described easily by a simple mathematical expression. Often, the input acceleration data is available only from an oscilloscope picture. Input data of this form is not easily inserted into analog or digital computers without additional time consuming work.

An investigation was therefore conducted to see if the phase-plane technique of solving transient vibration problems could be extended to determine responsive displacement-time or acceleration-time histories of a general multidegree system that is excited by a transient motion of the system's support. Any limitations of the phase-plane method found in the investigations would be beneficial in that no literature was found to say when the phase-plane method would not solve the problem.

Even though computers are now frequently used to rapidly solve response problems in mechanical shock testing, a graphical solution of the same problem





has its place in the field. The method would be used in cases where a model representing the specimen was known and a computer was not available, or where the input data was not immediately suitable for computer use and the responsive information was needed in a few hours. The method should be simple enough that a trained technician could solve the problem.





## II. STATEMENT OF THE PROBLEM

A general two-degree-of-freedom damped linear spring-mass system mounted on a shock machine is shown in Fig. 1. Excitation of the system occurs only by controlled motion of the carriage. Support excitation is a known displacement-, velocity-, or acceleration-time history. These quantities are represented by the symbols  $\lambda(t)$ ,  $\dot{\lambda}(t)$ ,  $\ddot{\lambda}(t)$ .

The masses  $m_1$  and  $m_2$  are very small in comparison with the carriage mass. Values for each spring,  $k_1$ ,  $k_2$ ,  $k_3$ , and each mass,  $m_1$  and  $m_2$ , are known from the physical design of the specimen. The location of each viscous damper,  $c_1$ ,  $c_2$ ,  $c_3$ , or friction damper,  $f_1$ ,  $f_2$ ,  $f_3$ , is known but the actual values are not. The effects of the dampers would be determined by experiment. The magnitudes of the dissipative forces of the dampers are such that in free vibration at least two complete cycles of each mass in motion will be discernible. If the  $f$ 's or  $c$ 's of the model are zero, the two-degree viscously and/or coulomb-damped model becomes undamped. Similarly, if one mass is zero, the model becomes a single-degree spring-mass system.

The problem is to develop and to find limitations of a graphical technique for finding (within reasonable accuracies) the displacement-time histories  $x(t)$ ,  $y(t)$ , and acceleration-time histories,  $\ddot{x}(t)$ ,  $\ddot{y}(t)$ , of the two masses for general known input-time histories,  $E(t)$ . The technique should require only the use of graph paper, a protractor, compass, straightedge, and knowledge of the specimen's natural period and damping characteristics.





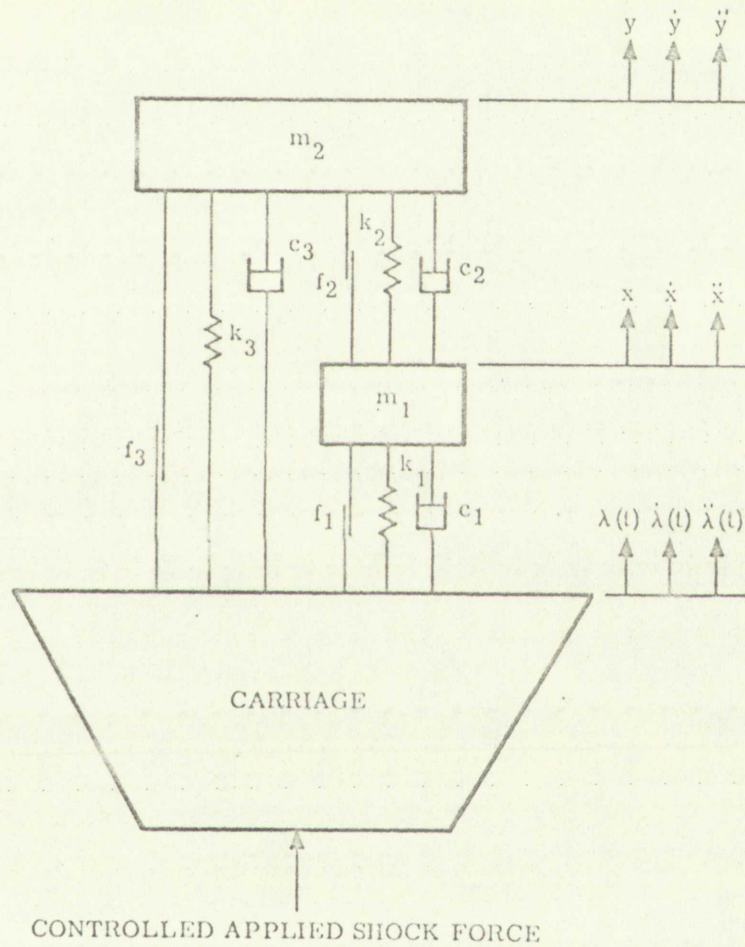
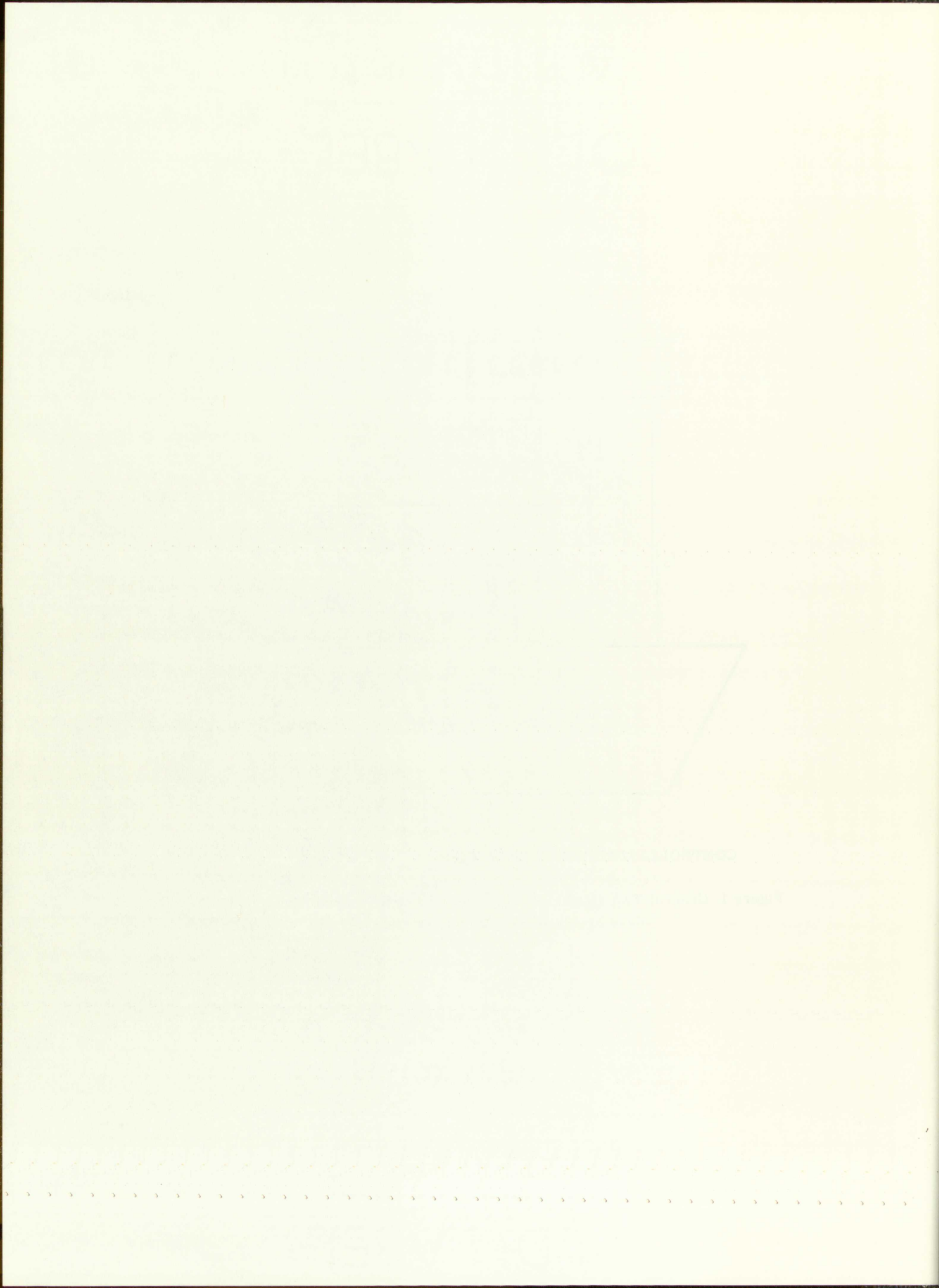


Figure 1 General Two-Degree Viscous and Coulomb Damped Spring Mass System Under Consideration





### III. LITERATURE SURVEY

This section discusses investigations conducted by several authors in the transient response of both single- and two-degree systems, undamped or damped. In most of the literature studied, certain facts became clear. Most analysis of single- and two-degree systems was performed using higher mathematics.

For single-degree undamped systems, Timoshenko and Young (1)\* developed Duhamel's Integral to obtain responsive displacements. This integral was then used to show how the "phase-plane" method worked. In all examples an external force applied to the mass in question was involved. No examples were available where the disturbance to the system was applied to the support. Jacobsen and Ayre (2) extended the information contained in Ref. (1) and presented a most comprehensive investigation on the phase-plane method of solution of single-degree undamped systems. However, again all the examples were restricted to displacement responses with either support displacement or force application directly to the mass. Jacobsen and Ayre conducted the investigation of undamped systems for various shaped input pulses throughout the range  $0 \leq \frac{t_d}{T} \leq 4$  (where  $t_d$  = pulse duration,  $T$  = specimen natural period) and plotted many types of spectra. Harris and Crede (3) indicated how the differential

---

\* Numbers in parentheses refer to bibliography.





equation of motion shown below would appear for different types of system response when a known excitation was applied to the system.

$$\frac{m}{k} \ddot{\gamma} + \gamma = E(t)$$

where

$m$  = specimen mass

$\ddot{\gamma}$  = second derivative of  $\gamma$  with respect to time

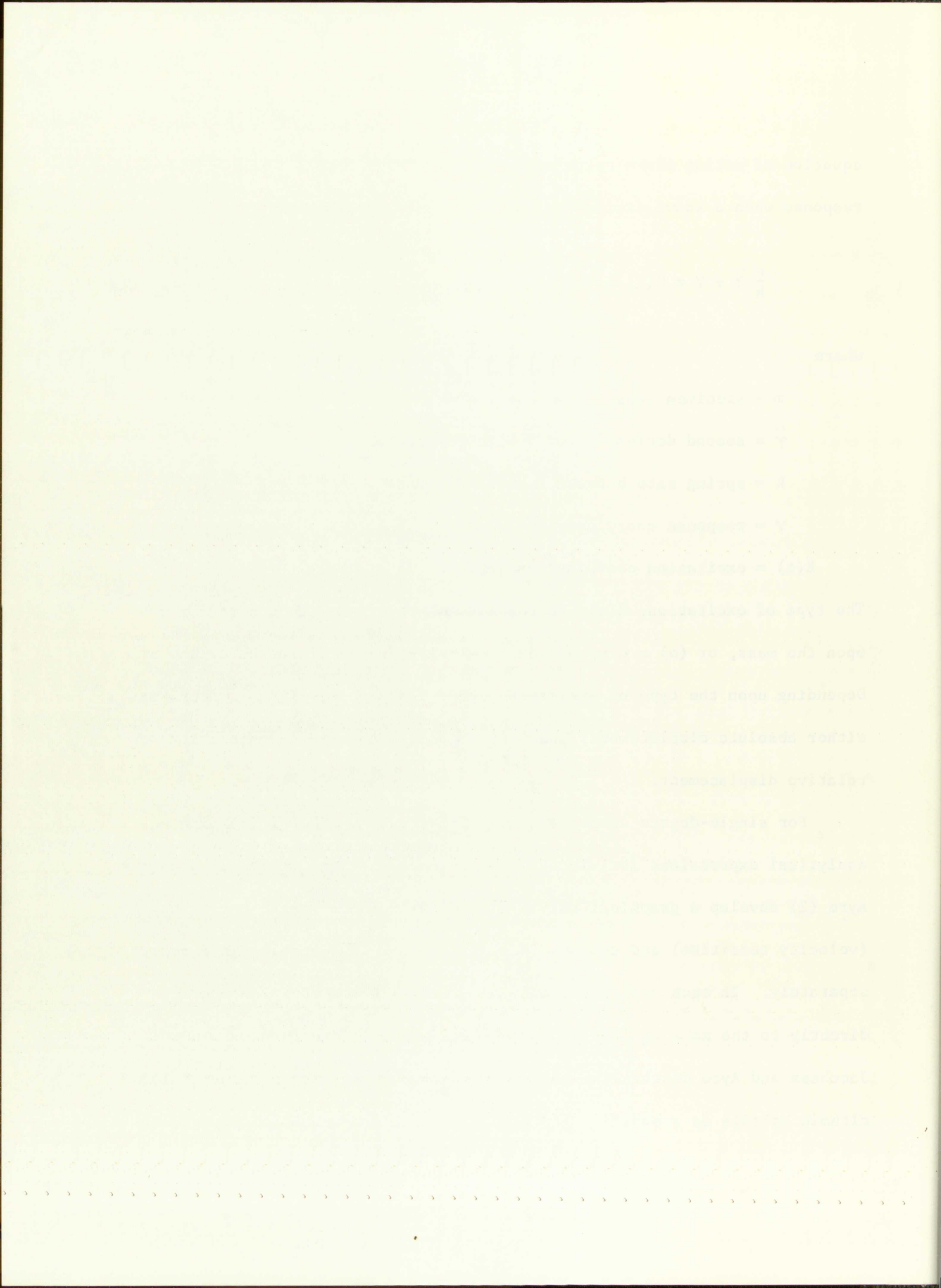
$k$  = spring rate between support and mass

$\gamma$  = response coordinate

$E(t)$  = excitation coordinate as a function of time.

The type of excitation,  $E(t)$ , to the system was either (a) a direct force upon the mass, or (b) a displacement, velocity, or acceleration of the support. Depending upon the type of excitation, the response,  $\gamma$ , of the system was either absolute displacement, absolute velocity, absolute acceleration, or relative displacement.

For single-degree damped systems, Timoshenko and Young (1) discuss analytical expressions for viscous and coulomb friction, while Jacobsen and Ayre (2) develop a graphical solution of displacements for both viscous (velocity sensitive) and coulomb (dry) friction when occurring in a system separately. In each reference, only an external force function applied directly to the mass or free vibration with support fixed was considered. Jacobsen and Ayre discuss the use of an oblique coordinate system and logarithmic spirals as a modification of the phase-plane technique to solve a





viscously damped vibration condition. They show how to construct an approximate logarithmic spiral accurate to 2% if the damping ratio is  $< 0.5$ .

Jacobsen, in another paper (4), discusses a general method of solving second-order differential equations by a phase-plane-delta displacement method. The differential equation of motion must be reduced and written in the form shown below.

$$m\ddot{x} + k(x + \delta) = 0$$

where

$$\delta = \frac{1}{k} G(x, \dot{x}, t) .$$

His method of solution required that  $\delta$  be evaluated as the phase-plane was constructed. The different values of  $\delta$  were usually obtained from auxiliary diagrams when the relationship between  $\delta$  and  $x, \dot{x}, t$  were known. The  $\delta$  values were used to find pertinent centers of the phase-plane diagram. A similar type "delta" method was applied to the problem in this thesis. Bishop (5) used phase-plane displacements for a force-excited viscously damped system by using a different type of oblique coordinate system than Jacobsen and Ayre used. Bishop's coordinate system was much easier to use than Jacobsen and Ayre's in converting data from the phase-plane plots to the displacement-time history plot. However, all of Bishop's examples (like those of the previous authors) did not show examples of support excitation through the viscous damper.





Considering an undamped two-degree system arrangement similar to the system shown in Fig. 1, no author had any pertinent data on the phase-plane method. Jacobsen and Ayre, as well as Timoshenko and Young, developed the solutions of the equations of motion analytically when external forces were applied directly to either or both of the two masses. Jacobsen and Ayre illustrated an actual problem utilizing a different half-sine input force pulse applied to each mass. Their solution was modified and used for comparison of a problem of support excitation presented in this thesis. Timoshenko and Young (6) describe principal coordinates in writing differential equations of motion for free and forced vibration. These authors show how to convert principal coordinates to usable arbitrary coordinates. Ayre (7) illustrates an actual problem of single support excitation on a two-spring, two-mass system showing how to use the phase-plane displacements in principal coordinates and converting them to rectangular coordinates. He was vague, however, in his development and made no statement as to when his constants for coordinate conversion would not apply. Chu and Abramson (8) applied Jacobsen's phase-plane-delta method to multidegree vibrating systems, but their analysis did not use support excitation and did not convert the normal coordinates to rectangular coordinates. They considered only one force applied to one mass while supports were fixed.

For lightly viscously damped two-degree systems, sources of usable information become scarce. Mindlin (9) shows some shock spectra for the lightest endmost mass of a two-degree viscously damped series system that has



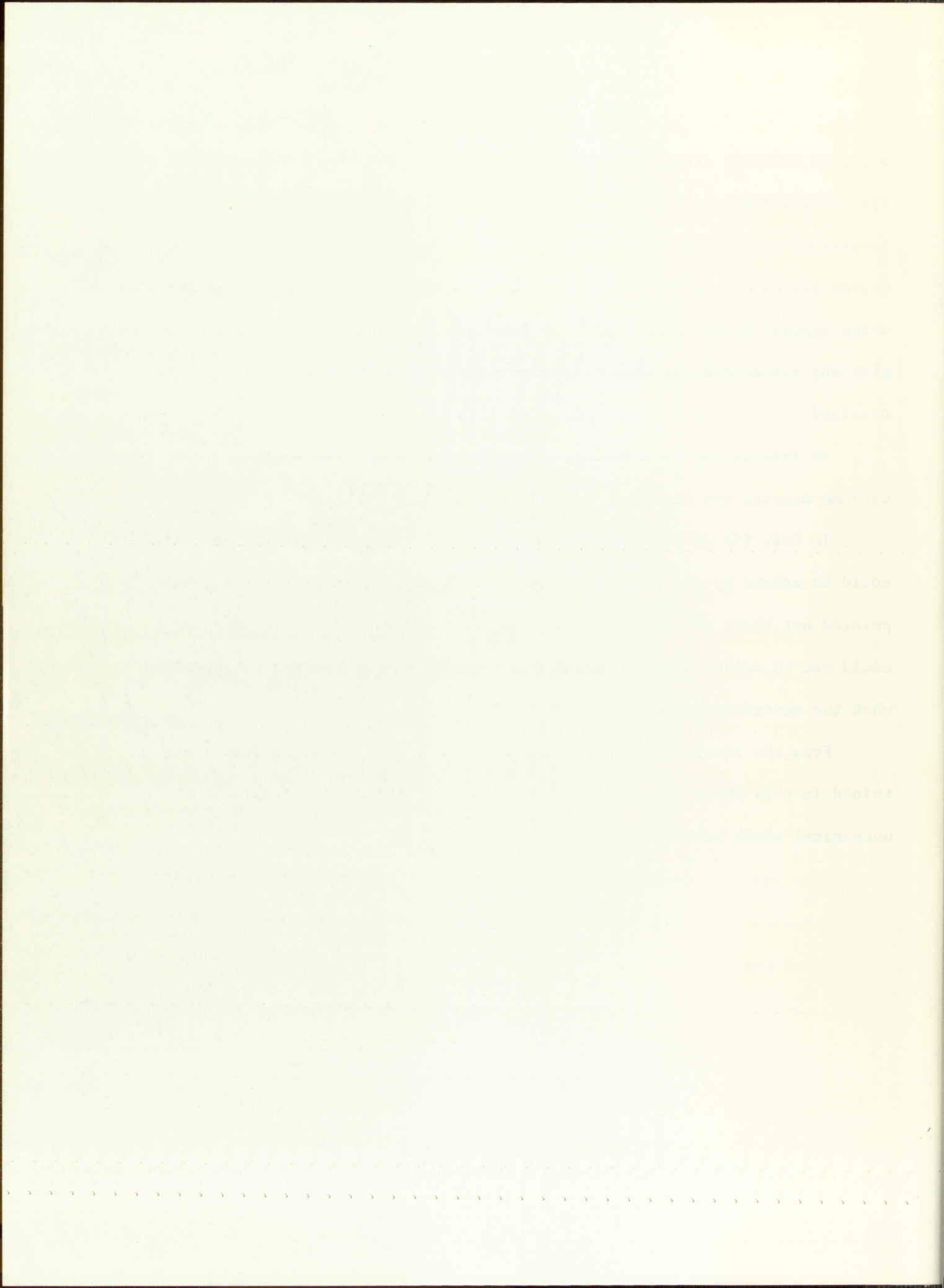


a sudden velocity change of the support. With this type of excitation the system will ring and both masses will vibrate. No data is shown for the spectra of the second mass. Hill (10) shows some spectra for a heavy two-degree system mounted on a light carriage (a three-degree system problem) which appears to be an extension of Mindlin's work. However, Hill does not give any references nor does he state any method by which his results were obtained.

No information on transient response of a two-degree system having coulomb damping was found.

In Ref. (5) it was mentioned that certain undamped multidegree systems could be solved by the phase-plane method. In this reference, it was also pointed out that, generally speaking, multidegree systems having damping could not be solved by phase-plane techniques. The author did not point out what the restrictions were.

From the literature survey conducted, it is felt that material contained in this thesis could be a worthwhile contribution to the field of mechanical shock testing.





#### IV. PHASE-PLANE ANALYSIS - SINGLE-DEGREE SYSTEMS

This section discusses the use of phase-plane techniques for three types of single-degree models, undamped, lightly coulomb damped, and lightly viscously damped. The two types of damping were selected from the many varieties of damping forces that occur in practical engineering shock and vibration problems. Four types most frequently encountered are:

1. Viscous damping - the damping force is proportional to the velocity. This describes the condition in viscous fluids. This condition is approached frequently with greasy sliding surfaces.
2. Coulomb damping - this type of damping is produced by a dry friction force. It depends only upon normal pressures.
3. Air damping - damping force is assumed to be proportional to velocity squared of the mass when high relative velocities are involved.
4. Internal hysteretic damping - the damping force is dependent upon the amplitude of motion.

Air damping at low relative velocities inside a sealed test item approaches viscous type damping. Internal hysteretic damping can be approximated by an equivalent viscous damping such that the energy dissipated per cycle is the same.





The types of support excitation considered are transient displacement, velocity step, and controlled acceleration-time histories. Vibratory motion is analyzed both for the system under the external disturbance and for free vibration after the disturbance has ceased. Quite often in the analysis, initial conditions are assumed to be zero only for the convenience offered. The analysis also holds for any given initial conditions. The effect is merely additive.

### 1. Undamped Systems

For the system in free vibration shown in Fig. 2b, the differential equation of motion is

$$m\ddot{x} + kx = 0 , \quad (1)$$

the solution being

$$x = x_0 \cos pt + \frac{\dot{x}_0}{p} \sin pt . \quad (2)$$

$x$  = responsive displacement of mass,  $m$

$k$  = spring rate

$x_0$  = initial mass displacement from equilibrium position

$\dot{x}_0$  = initial mass velocity at release

$p$  = specimen natural frequency

$t$  = time.

Fig. 2c is the displacement-time history of the free vibration. The slope of the curve at  $x_0$  represents  $\dot{x}_0$ . In Fig. 2a, a vector,  $r$ , rotates

The first assumption is that the system is in a steady state. This means that the system has been operating for a long enough time that any initial transients have died out. The second assumption is that the system is linear. This means that the output of the system is directly proportional to the input. The third assumption is that the system is time-invariant. This means that the system's behavior does not change over time. The fourth assumption is that the system is causal. This means that the system's output at any time depends only on inputs up to that time. The fifth assumption is that the system is stable. This means that the system's output remains bounded for any bounded input.

For the system in the previous figure, the input is a unit step function. The output of the system is a unit step function. The system is a first-order system. The transfer function of the system is  $G(s) = \frac{1}{s+1}$ . The system is stable. The system is causal. The system is time-invariant. The system is linear. The system is in a steady state.

The system is a first-order system. The transfer function of the system is  $G(s) = \frac{1}{s+1}$ . The system is stable. The system is causal. The system is time-invariant. The system is linear. The system is in a steady state.

(3) 
$$x = \frac{1}{s+1} u(s)$$

$x$  is a continuous displacement of mass  $m$ .  
 $u$  is a unit step function.  
 $x$  is a first-order system displacement from equilibrium position.  
 $\dot{x}$  is a first-order system velocity in velocity.  
 $\ddot{x}$  is a first-order system acceleration in acceleration.

$t = 0$  is the time when the system is first excited.  
 $t = \infty$  is the time when the system has reached a steady state.



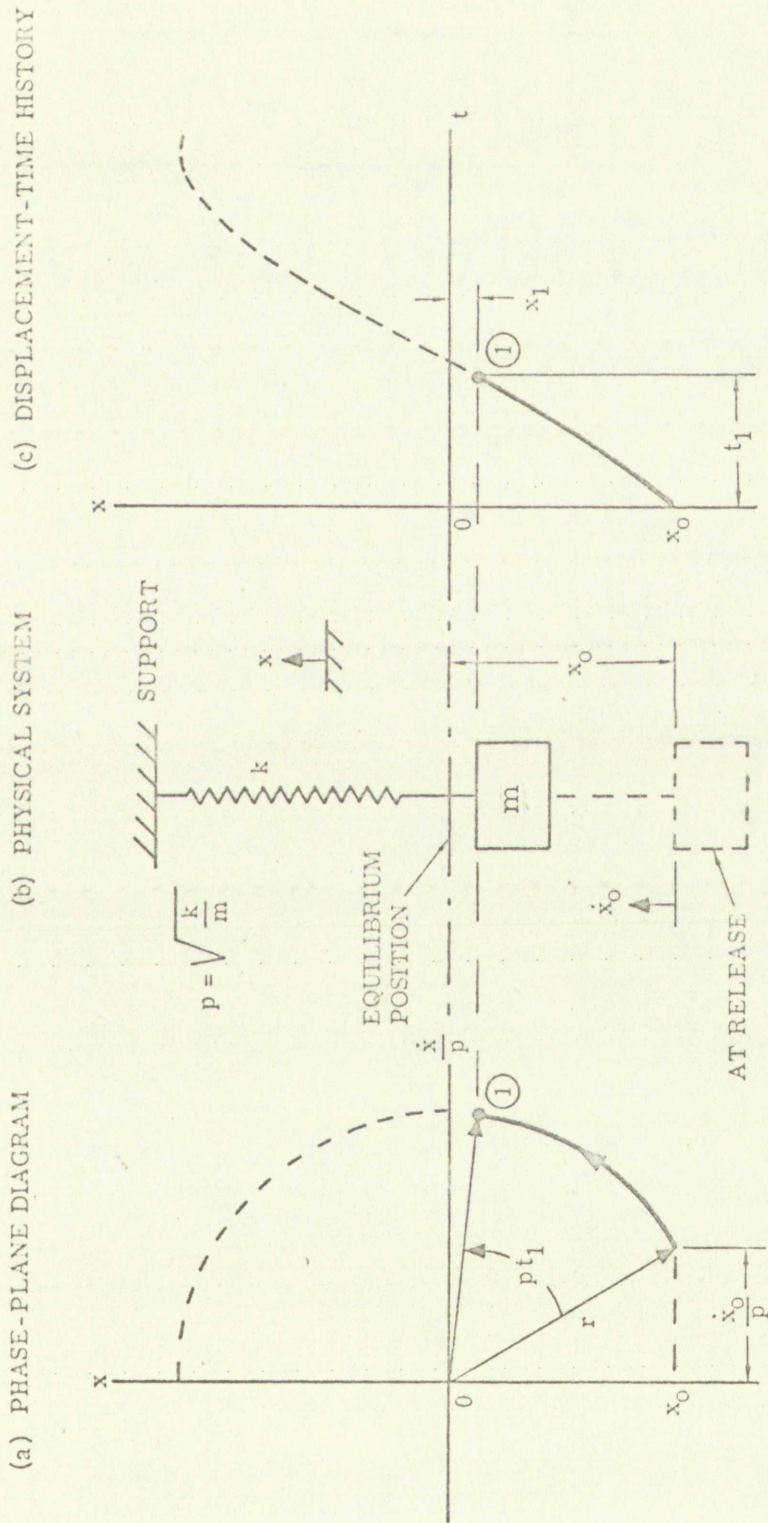


Figure 2 Typical Phase-Plane and Displacement-Time History of Simple System in Free Vibration

Q. 2. A particle starts from rest and moves with a constant acceleration of  $2 \text{ m/s}^2$ . Find the distance travelled by it in the first 5 seconds.



Q. 3. A particle starts from rest and moves with a constant acceleration of  $2 \text{ m/s}^2$ . Find the distance travelled by it in the first 5 seconds.

from  $x_0$  and  $\dot{x}_0/p$  at an angular speed of  $p$  rad/sec sweeping out a circular arc. The location of the vector terminus along the circular arc at any time after release represents a particular displacement and velocity of the mass at that time. This plot of points is referred to as the phase-plane plot of the motion of the mass at any time. The term "phase" occurs because the phasing of the displacement and velocity coordinates are fixed, and "plane" occurs because the plot is always in the plane of the paper for simple systems.

If a step disturbance,  $\lambda_i$ , of the support had occurred at time  $t = 0$ , it in effect would cause the mass to oscillate about a new equilibrium point. Also, since  $x_0$  and  $\dot{x}_0$  were arbitrary, it follows that for any initial starting conditions, a particular phase plane could be drawn for any interval of time after the start of the interval. Thus, a series of step disturbances of the base in succession could be used to make a phase-plane plot where the end conditions of one step become the initial conditions for the following step. Eqs. 1 and 2 now would be

$$m\ddot{x} + kx = k\lambda_i, \quad (1a)$$

$$x = x_* \cos pt_i + \frac{\dot{x}_*}{p} \sin pt_i + \lambda_i(1 - \cos pt_i), \quad (2a)$$





where

$\lambda_i$  = amplitude of step during interval

$t_i$  = time during interval of step

$x_{**}$  = mass displacement at start of interval

$\dot{x}_{**}$  = mass velocity at start of interval.

Fig. 3 shows how a phase-plot of a single-degree linear undamped system is generated from a stepwise transient input displacement (the input is shown as a dotted line). The center of each circular segment of the phase-plane is determined by the displacement level of each step of the transit input, namely,  $\lambda_0$ ,  $\lambda_1$ ,  $\lambda_2$ ,  $\lambda_3$ , and  $\lambda_4$ . The radius,  $r_1$ , of the first circular segment is determined by the initial starting conditions. (In the figure it is assumed that the initial displacement and initial velocity of the mass are zero; however, the same procedure would be followed for any other starting conditions.) This radius,  $r_1$ , is a rotating vector for the time interval,  $t_1$ , of the first stepwise input,  $\lambda_1$ . The counterclockwise angle through which the rotating radius vector turns is dependent upon the natural frequency,  $p$ , of the system and the time interval of the step. The conditions of motion of the system at the end of the first step interval, (1), become the new starting conditions of the system for the second step interval of the input. A new center,  $\lambda_2$ , and a new radius,  $r_2$ , are now used. The second radius vector rotates through the second angle, which is proportional to the second time interval,  $t_2$ . The end conditions of the second interval, (2),





PHASE-PLANE PLOT

SYSTEM DISP. - TIME HISTORY

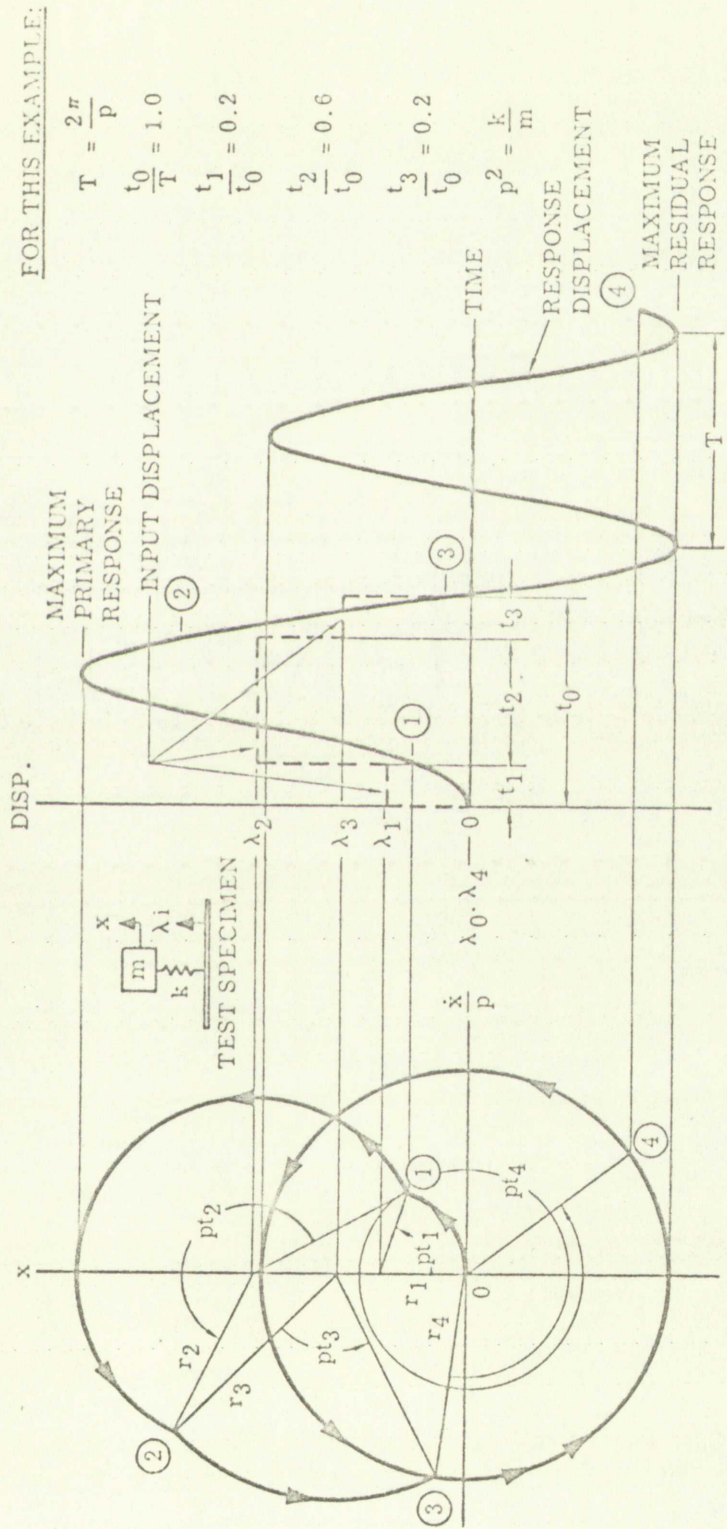


Figure 3 Response of Single Degree Linear Undamped System to Transient Input Displacement



become the starting conditions for the third step interval, etc., and the procedure is repeated as often as necessary. One can easily see, therefore, that this procedure can be applied to any transient input shape as long as the shape can be approximated by steps, each step having the same area as that portion of the input transient.

After the phase-plane plot is completed, points representing various responsive displacements from the phase-plane plot can be projected back to the displacement-time history plot which is superimposed on the transient input. Thus, the entire displacement-time history of the responding spring-mass system is shown in the right-hand side of Fig. 3.

The step method shown above can be applied to any pulse shape when the duration,  $t_d$ , is of the same order as the specimen natural period,  $T$ . The size interval of each step is dependent upon pulse shape and accuracy desired, but usually a ratio of  $\frac{t_i}{T} = \frac{1}{10}$  should be highly satisfactory. When the ratio  $\frac{t_d}{T} \approx \frac{1}{4}$ , it is satisfactory to use a single step with little error for any pulse shape.

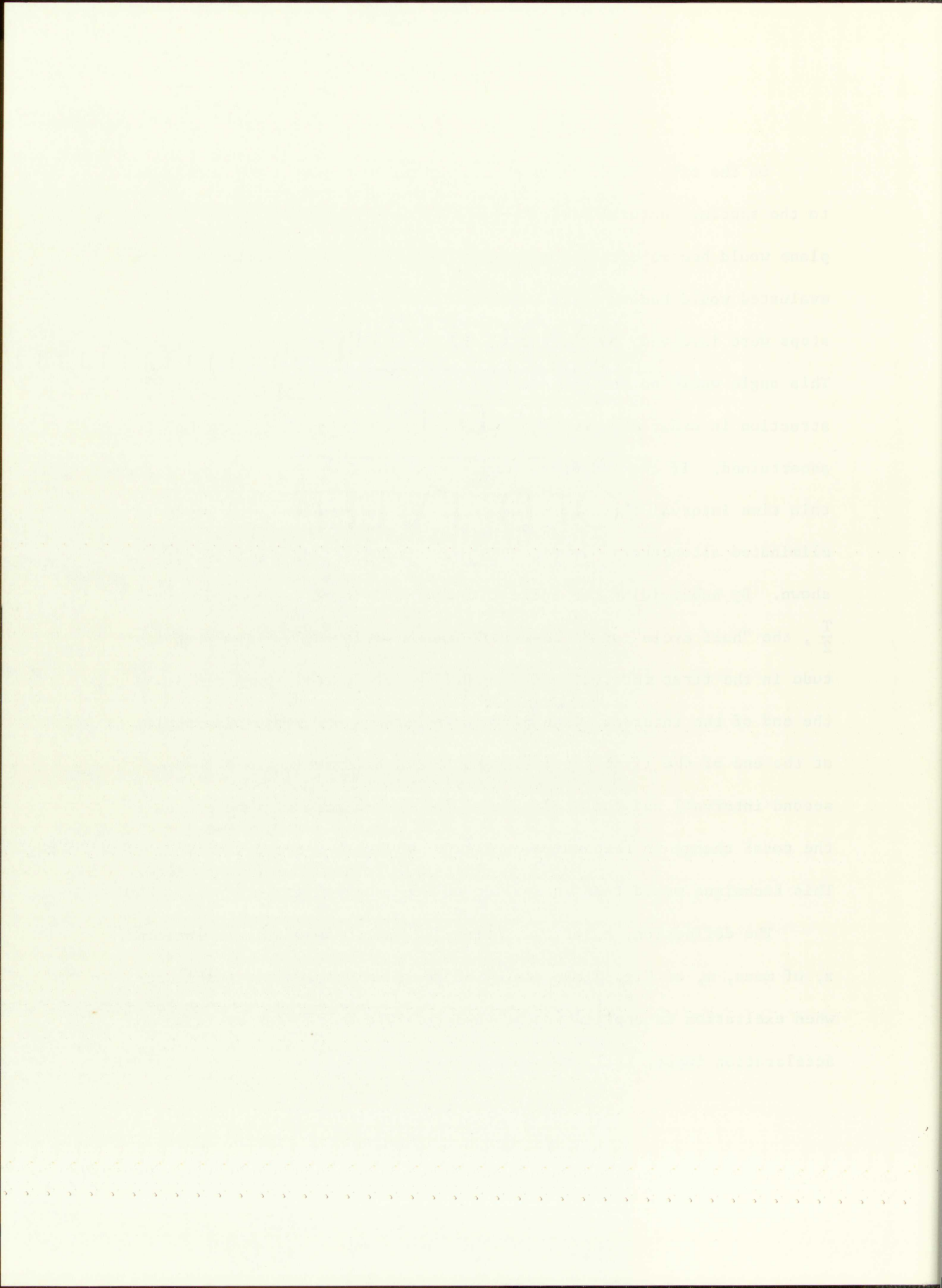
When the pulse duration is very short compared to the specimen natural period, the angles in the phase-plane construction become extremely small. It is satisfactory  $\left( \text{when } \frac{t_d}{T} < \frac{1}{10} \right)$  to assume that the support has had such a small change in position that the only effect upon the system is to essentially change the initial velocity of the mass if time is measured from the end of the impulse period.





On the other hand, if the pulse duration is very long in relation to the specimen natural period  $\left(\frac{t_d}{T} \geq 10\right)$ , then the angles in the phase-plane would become either exceedingly large or else the number of points evaluated would become quite numerous. If  $\frac{t_d}{T} = 10$  and twenty equal steps were involved, each angle in the phase plane would be 180 degrees. This angle would be the maximum angle permissible in a phase-plane construction in order that the peak amplitudes during each cycle could be ascertained. If the 180-degree angle were always used to represent a certain time interval throughout the pulse, the phase-plane plot could be eliminated altogether. In Fig. 4 a symmetrical triangle pulse input is shown. By subdividing the pulse into steps having a duration interval of  $\frac{T}{2}$ , the "half cycle" or "full-swing" method would apply. The step amplitude in the first interval would be half of the actual input amplitude at the end of the interval. The difference between the responsive amplitude at the end of the first interval (and hence the starting amplitude of the second interval) and the amplitude of the second step will be one half the total change in responsive amplitude during the second interval. This technique would then be applied to each succeeding interval.

The deflection,  $u$ , of the spring,  $k$ , and/or absolute displacement,  $x$ , of mass,  $m$ , of Fig. 2 can easily be found by phase-plane techniques when excitation is applied to the support. The excitation could be an acceleration input,  $\ddot{\lambda}(t)$ , as shown in Fig. 5.





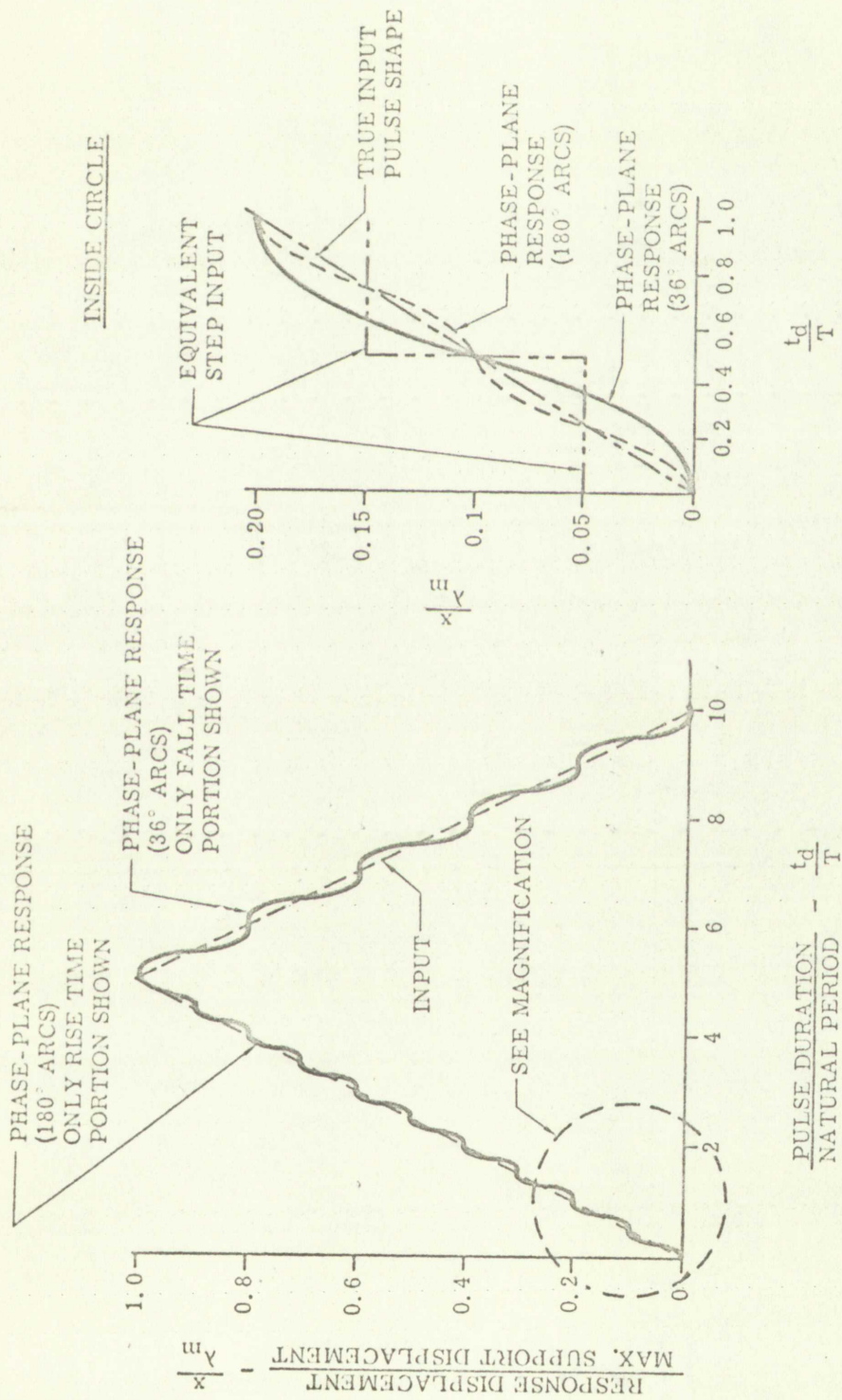


Figure 4 Comparison of Displacement-Time Histories Obtained by Phase-Plane Method Using Both  
36° Arcs and 180° Arcs (Half-Cycle)



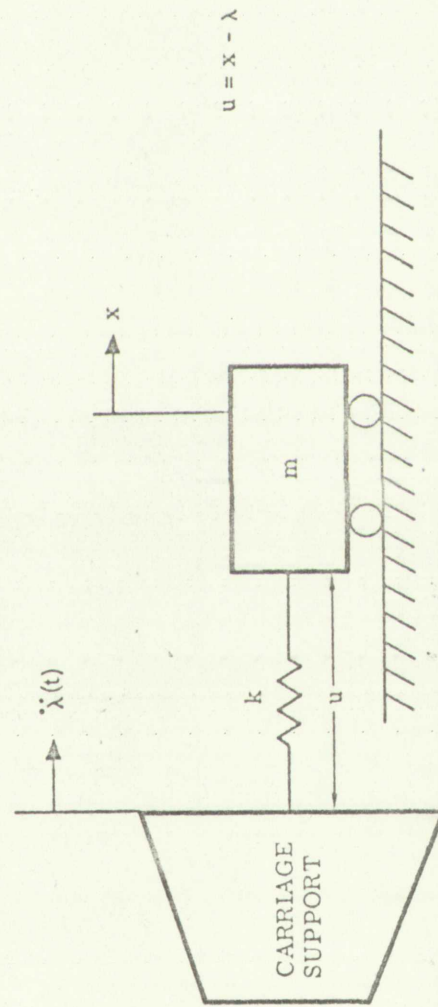


Figure 5 Single Degree Undamped System Subjected to a Known Support Acceleration





The differential equation of motion is

$$m\ddot{x} + kx = k\lambda(t) \quad (3)$$

or by substituting  $u = x - \lambda(t)$  and its derivatives

$$m[\ddot{\lambda}(t) + \ddot{u}] + k[\lambda(t) + u] = k\lambda(t) ,$$

from which the particular solution is determined from the equation

$$m\ddot{u} + ku = -m\ddot{\lambda}(t) . \quad (3a)$$

Eq. 3a is in the form of Eq. 1a, which has already been shown suitable to permit the construction of a phase-plane diagram.

Fig. 6 illustrates how the phase-plane would be used to solve a problem where  $\dot{\lambda}(t)$  is a constant velocity input. The fact that  $\ddot{\lambda}(t)$  in this problem is zero is immaterial. The purpose of the example is to show how the phase plane can be drawn to facilitate finding  $u$ . Also shown in Fig. 6 is a method for finding the absolute mass displacement,  $x$ , without drawing another phase plane. Since the support is known to have a constant velocity, it also has a ramp-type displacement in the time interval concerned. The difference in amplitudes at any time of the input displacement and the relative displacement curve is the mass displacement at that time.

The spring deflection response,  $u$ , is of most concern in shock testing in as far as structural integrity is concerned. Since shock tests are controlled by a known input acceleration, this technique is quite useful.

The displacement is specified as follows:

and a value of

is obtained from the following equation:

$$y = \frac{1}{2} \frac{v^2}{g} \sin^2 \theta$$

where  $y$  is the vertical displacement,  $v$  is the initial velocity, and  $\theta$  is the angle of projection.

(12)

where  $\theta$  is the angle of projection.

It is to be noted that the value of  $y$  is already given above.

It is also noted that the displacement is a function of time.

The displacement is a function of time and is given by

where  $y$  is the vertical displacement,  $v$  is the initial velocity, and  $\theta$  is the angle of projection.

This equation is valid for any angle of projection.

It is also noted that the displacement is a function of time.

It is also noted that the displacement is a function of time.

It is also noted that the displacement is a function of time.

It is also noted that the displacement is a function of time.

It is also noted that the displacement is a function of time.

It is also noted that the displacement is a function of time.

The vertical displacement is given by

where  $y$  is the vertical displacement,  $v$  is the initial velocity, and  $\theta$  is the angle of projection.

It is also noted that the displacement is a function of time.

where



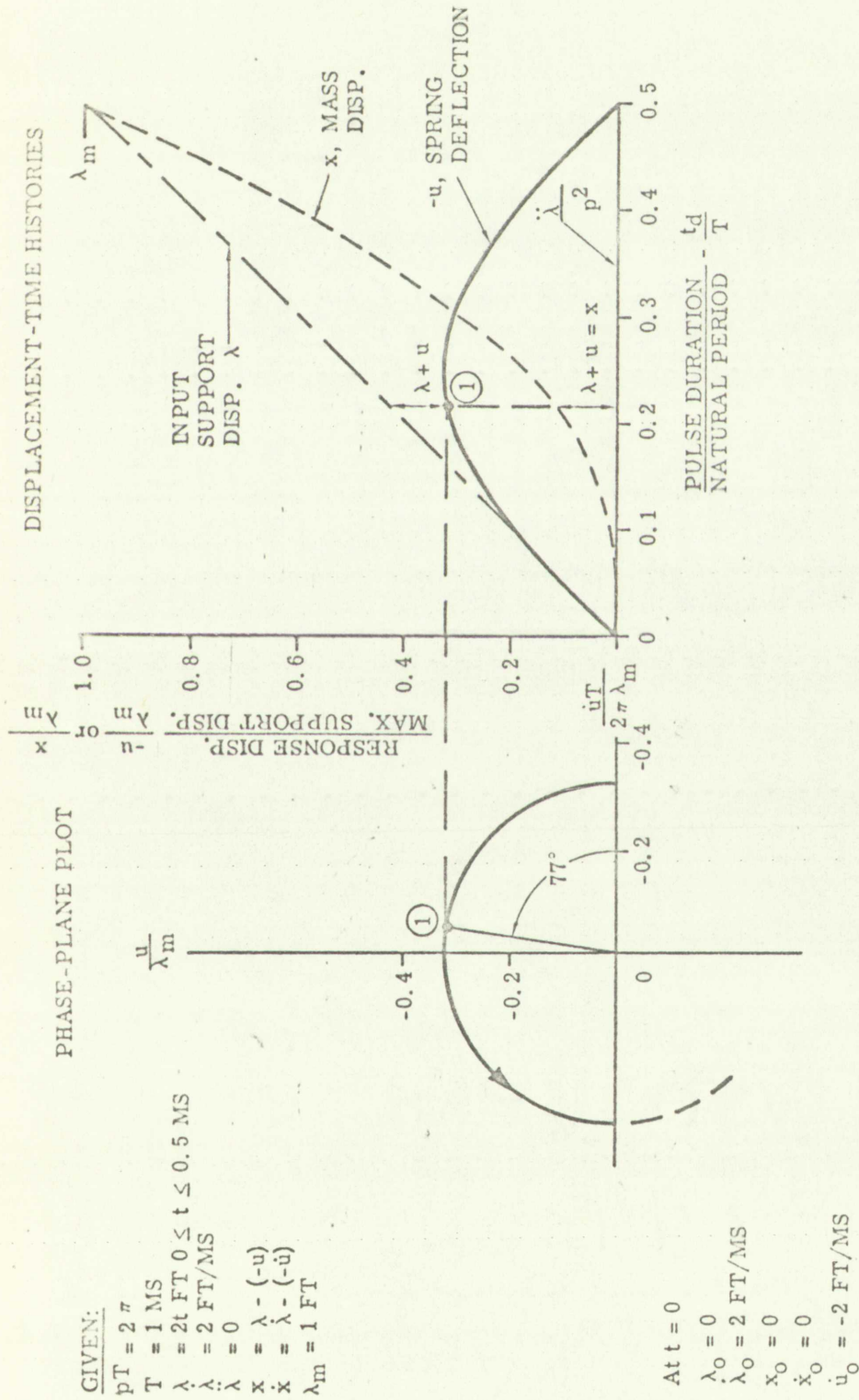


Figure 6 Spring Deflection and Mass Displacement of a Single-Degree Undamped System Having Support Excitation of Constant Velocity

DATA

DATA

DATA

DATA

DATA

DATA

DATA

Support excitation and undamped system mass response in terms of acceleration are solved in exactly the manner as discussed for displacement phase-plane analysis. All that is required is that the differential equation of motion be differentiated twice with respect to time. The format of the resulting expressions is similar to the format developed in the displacement analysis. From the general differential equation of motion of a mass with support excitation

$$\ddot{x} + p^2 x = p^2 \lambda(t) . \quad (1b)$$

Two differentiations with respect to time result in

$$\ddot{\ddot{x}} + p^2 \ddot{x} = p^2 \dot{\lambda}(t) . \quad (1c)$$

If  $\ddot{\lambda}(t)$  can be represented by a series of steps,  $\ddot{\lambda}_i$ , the general solution becomes

$$\ddot{x} = \ddot{x}_* \cos pt_i + \frac{\ddot{x}_*}{p} \sin pt_i + \ddot{\lambda}_i (1 - \cos pt_i) ; \quad (2b)$$

$\ddot{x}_*$  and  $\ddot{x}_*$  represent conditions at the start of the step,  $\ddot{\lambda}_i$  = input acceleration step.

In Fig. 3, therefore, each  $x$  is replaced by  $\ddot{x}$ , each  $\dot{x}$  by  $\ddot{\ddot{x}}$ , and each  $\lambda_i$  by  $\ddot{\lambda}_i$ .

When the support excitation is a velocity step,  $\dot{\lambda}_0$ , the initial conditions for the phase-plane construction for acceleration response are (assuming zero initial conditions)

$$\ddot{x}_0 = 0, \quad \ddot{\ddot{x}}_0 = p^2 \dot{\lambda}_0 . \quad (4)$$



2. The first condition is that the function  $f$  is continuous in  $x$  and  $y$ .

3. The second condition is that the function  $f$  is continuous in  $x$  and  $y$ .

4. The third condition is that the function  $f$  is continuous in  $x$  and  $y$ .

5. The fourth condition is that the function  $f$  is continuous in  $x$  and  $y$ .

6. The fifth condition is that the function  $f$  is continuous in  $x$  and  $y$ .

7. The sixth condition is that the function  $f$  is continuous in  $x$  and  $y$ .

8. The seventh condition is that the function  $f$  is continuous in  $x$  and  $y$ .

(2)

$$f(x, y) = p(x, y)$$

Two differential equations with respect to time  $t$  are

$$\dot{x} = f(x, y, t), \quad \dot{y} = g(x, y, t)$$

If  $f(x, y, t)$  can be represented by a series of steps  $f_i$ , the general solution

is

$$x = x_0 + \int_0^t f(x, y, t) dt, \quad y = y_0 + \int_0^t g(x, y, t) dt$$

$x_0$  and  $y_0$  represent initial conditions at the start of the step  $t = 0$ .

where  $t$  is time.

In Fig. 1, therefore, each  $x$  is replaced by  $x_i$  and  $y$  by  $y_i$ .

where  $x_i$  and  $y_i$  are

the values of  $x$  and  $y$  at the start of the step  $t_i$ .

With this notation, the general solution for the system of equations

is (assuming zero initial conditions)

Eq. 4 can be found by solving and then differentiating Eq. 1b when

$$\lambda(t) = \dot{\lambda}_0 t.$$

## 2. Coulomb Damped Systems

This type of damping is quite often one of the predominant types of friction in actual systems. The differential equation of motion of a system in free vibration is

$$m\ddot{x} + kx = -f \operatorname{sgn} \dot{x}, \quad (5)$$

where  $(\operatorname{sgn} \dot{x})$  means sign of the velocity of the mass. The general solution of Eq. 5 is

$$x = x_0 \cos pt + \frac{\dot{x}_0}{p} \sin pt - \Delta_c (\operatorname{sgn} \dot{x}) (1 - \cos pt), \quad (6)$$

where

$\Delta_c$  = equivalent frictional displacement,  $f/k$

$x_0$  = initial displacement

$\dot{x}_0$  = initial velocity.

Eq. 6 is similar to Eq. 2a, so a phase-plane diagram can be drawn.

Eq. 6 indicates that the center of the phase-plane diagram is shifted from zero a distance  $\Delta_c$  in a direction dictated by the  $\operatorname{sgn}$  of  $\dot{x}$ .





The  $\Delta_c$  term of Eq. 6 can be considered a "passive" type disturbance of the mass that changes sign every time  $\dot{x}$  changes sign. Clearly, if any other disturbance occurred directly to the mass, the  $\Delta_c$  term would only displace the neutral position to a new point where the velocity of the mass would be a maximum. When the system has an additional step forcing function applied directly to the mass, Eq. 5 must be written

$$m\ddot{x} + kx = F_i - f \operatorname{sgn} \dot{x} . \quad (7)$$

The general solution is

$$x = x_* \cos pt_i + \frac{\dot{x}_*}{p} \sin pt_i + \left( \frac{F_i}{k} - \Delta_c \operatorname{sgn} \dot{x} \right) (1 - \cos pt_i) , \quad (8)$$

where

$x_*$  = mass displacement at start of step

$\dot{x}_*$  = mass velocity at start of step

$F_i$  = step force applied to mass

$t_i$  = time during step interval.

Fig. 7 shows the graphical solution of a system when it has a coulomb damping force,  $f = \frac{1}{10} F_m$ .  $F_m$  is the maximum value of an external force applied directly to the mass (the carriage fastened to ground).

This type of solution is shown by Jacobsen and Ayre in Ref. (2).

Unfortunately, the graphical solution as shown in Fig. 7 is unsuitable when the test item is excited by a carriage displacement,  $\lambda(t)$ ,

The  $\delta$  term of Eq. 1 can be considered a "passive" type disturbance of the mass that changes its value in a random way. When  $\delta$  is not zero, the disturbance is active. In this case, the  $\delta$  term must be taken into account in the model of the system. The general solution of the system with a random disturbance  $\delta$  can be written as follows:

$$x = x_0 + \delta x_1 + \delta x_2 + \dots + \delta x_n \quad (1)$$

The general solution is

$$x = x_0 \cos p_1 t + \frac{\dot{x}_0}{p_1} \sin p_1 t + \left( \frac{\ddot{x}_0}{p_1^2} \sin p_1 t - \frac{\dot{x}_0}{p_1} \cos p_1 t \right) \cos p_1 t + \dots \quad (2)$$

where

$x_0$  = mass displacement at start of step

$\dot{x}_0$  = mass velocity at start of step

$\ddot{x}_0$  = step force applied to mass

$p_1$  = time during step interval

Fig. 1 shows the frequency solution of a system when it has a

constant damping force,  $F = \frac{1}{2} \dot{x}$ .  $\omega$  is the radian value of an external

force applied directly to the mass (the average lagtime is ignored).

This type of solution is shown by Jacobson and Sjöberg [2].

However, the general solution of the system in Fig. 1 is

valid only when the mass is not subject to a random disturbance. If

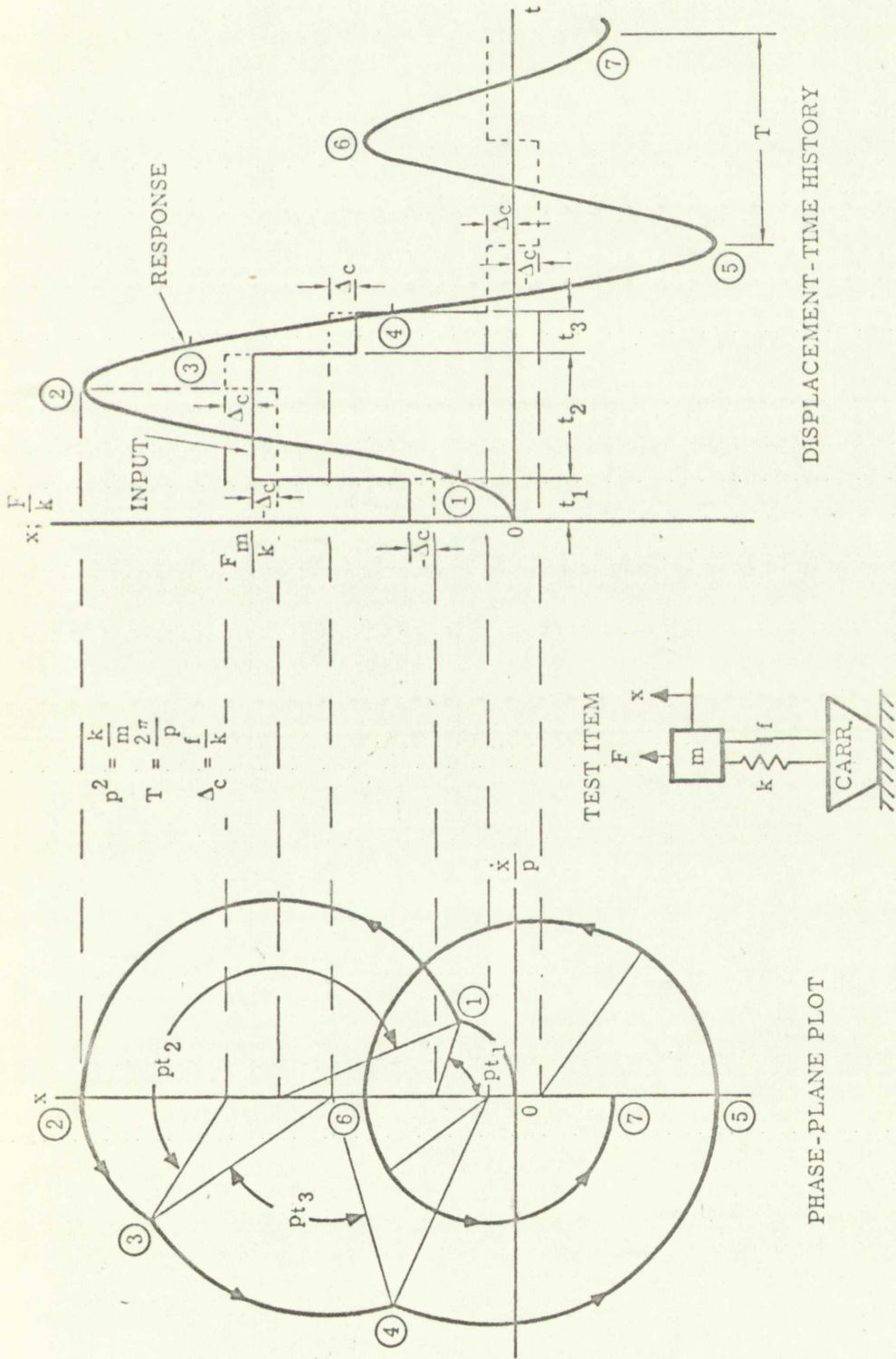


Figure 7 Response of Single-Degree Coulomb Damped System to Transient Force Pulse  
(Carriage Tied to Ground)





instead of the force  $F(t)$ . When excitation is through the support, the direction of the friction force,  $f$ , is the same as the relative velocity of the carriage to the mass  $(\dot{\lambda} - \dot{x})$ . One can see, therefore, by drawing a free body diagram of the mass that the responsive displacement of the mass occurring at  $t > 0$  in Fig. 8a should be different than displacement of mass occurring with the setup in Fig. 8b.

Eq. 7 should now be written as

$$m\ddot{x} + kx = k\lambda(t) + f \operatorname{sgn}(\dot{\lambda} - \dot{x}), \quad (9)$$

where  $\lambda(t)$  = amplitude of displacement input by support.

The general solution becomes for a step,

$$x = x_* \cos pt_i + \frac{\dot{x}_*}{p} \sin pt_i + \left[ \lambda_i + \Delta_c \operatorname{sgn}(\dot{\lambda} - \dot{x}) \right] [1 - \cos pt_i]. \quad (10)$$

Fig. 9 shows the graphical transient response of two different coulomb-damped masses subjected to a symmetrical triangle displacement of their supports. In one case the damper is tied to ground; in the other case, the damper is tied to the movable support. The phase-plane diagram for the former case is constructed in the same manner as the phase-plane diagram in Fig. 7, except that the excitation,  $F(t)$ , is replaced by  $k\lambda(t)$ .

In constructing the phase-plane for the latter case, one needs to be aware of  $\operatorname{sgn}(\dot{\lambda} - \dot{x})$  in order to decide whether to add or subtract

instead of  $\log \log n$ . When restricted to through the support, the

algorithm of the previous paper [1] is the same as the previous algorithm

of this paper in the case of a single node. The algorithm of this

paper is a generalization of the algorithm of the previous paper [1]

and is based on the same idea as the algorithm of the previous paper [1]

of this paper. The algorithm of this paper is a generalization of the

algorithm of the previous paper [1] and is based on the same idea as the

$$(3) \quad \alpha_1 + \alpha_2 + \dots + \alpha_k = 1 \text{ and } \alpha_i \geq 0$$

where  $\alpha_i$  is a coefficient of displacement along the support.

The algorithm of this paper is based on the same idea as the

algorithm of the previous paper [1] and is based on the same idea as the

$$x = x_1 \cos \theta_1 + x_2 \cos \theta_2 + \dots + x_k \cos \theta_k \quad (4)$$

Fig. 2 shows the graphical representation of two different

real-time diagrams and is based on the same idea as the

of their support. In this case the diagram is also to present in the

other case, the diagram is also to present in the same plane.

Diagram for the former case is represented in the same manner as the

phase-plane diagram in Fig. 3. A vector from the center of Fig. 3 is

represented by  $\vec{r}(t)$ .

In constructing the phase-plane diagram for the former case, one needs to

be aware of the fact that the vector  $\vec{r}(t)$  is not a vector in the phase-plane



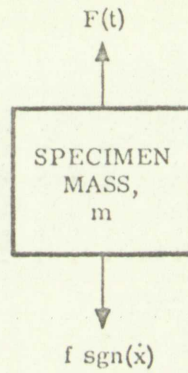


Figure 8a Free Body Diagram of Coulomb Damped Mass  
When the Support is Fixed to Ground

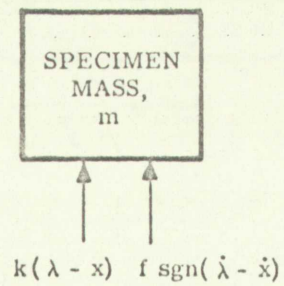
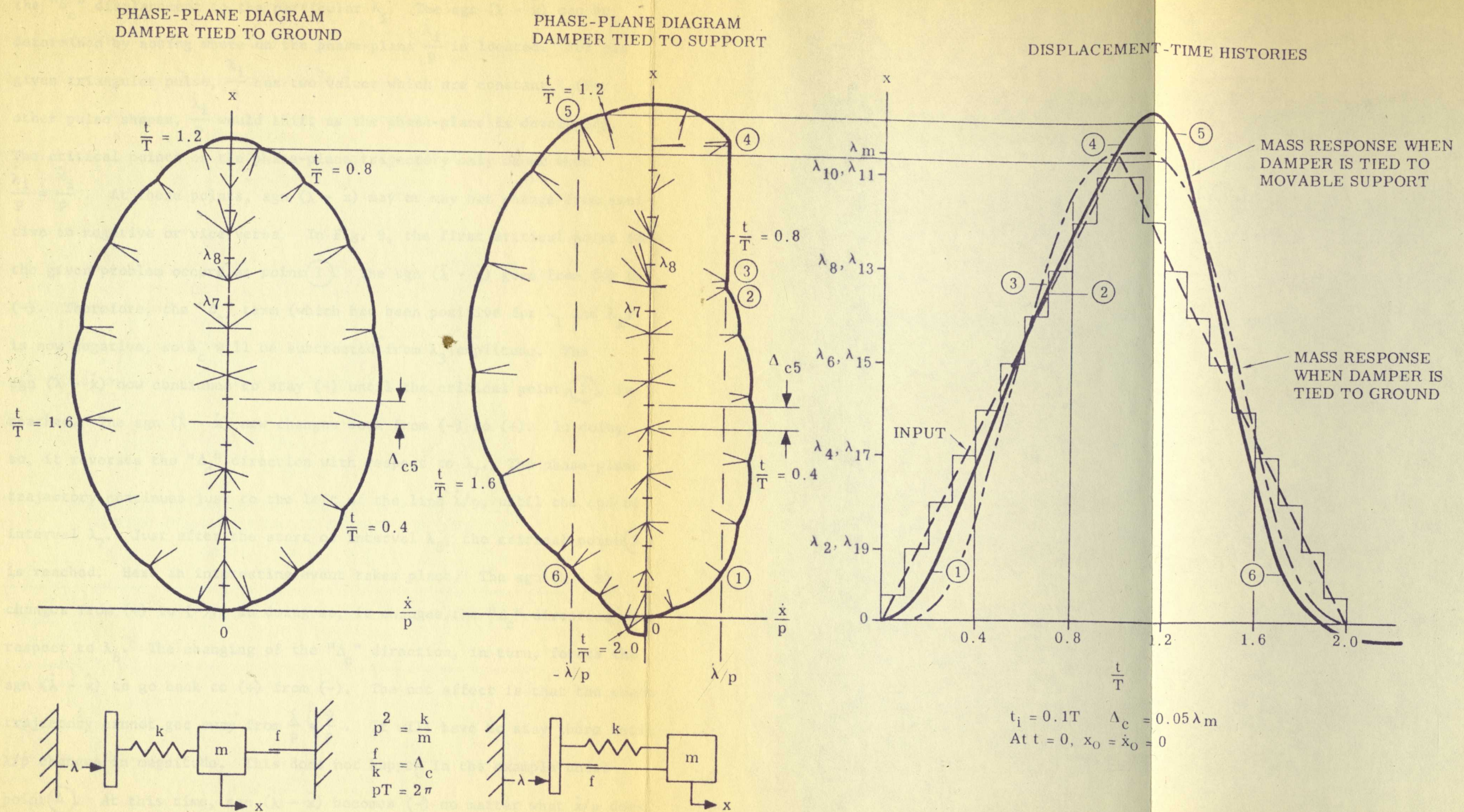


Figure 8b Free Body Diagram of a Mass Having a Coulomb Damper  
Tied to Its Support Which is Excited











the " $\Delta_c$ " displacement to the particular  $\lambda_i$ . The  $\text{sgn}(\dot{\lambda} - \dot{x})$  can be determined by noting where on the phase-plane  $\frac{\dot{\lambda}_i}{p}$  is located. For the given triangular pulse,  $\frac{\dot{\lambda}_i}{p}$  has two values which are constant. (For other pulse shapes,  $\frac{\dot{\lambda}_i}{p}$  would shift as the phase-plane is developed).

The critical points on the phase-plane trajectory only occur when  $\frac{\dot{\lambda}_i}{p} = \frac{\dot{x}_i}{p}$ . At these points,  $\text{sgn}(\dot{\lambda} - \dot{x})$  may or may not change from positive to negative or vice versa. In Fig. 9, the first critical point for the given problem occurs at point (1). The  $\text{sgn}(\dot{\lambda} - \dot{x})$  goes from (+) to (-). Therefore, the " $\Delta_c$ " term (which had been positive for  $\lambda_1$  and  $\lambda_2$ ) is now negative, so  $\Delta_c$  will be subtracted from  $\lambda_3$  amplitude. The  $\text{sgn}(\dot{\lambda} - \dot{x})$  now continues to stay (-) until the critical point, (2), is reached. The  $\text{sgn}(\dot{\lambda} - \dot{x})$  now changes back from (-) to (+). In doing so, it reverses the " $\Delta_c$ " direction with respect to  $\lambda_7$ . The phase-plane trajectory continues just to the left of the line  $\dot{\lambda}/p$ , until the end of interval  $\lambda_7$ . Just after the start of interval  $\lambda_8$ , the critical point (3) is reached. Here an interesting event takes place. The  $\text{sgn}(\dot{\lambda} - \dot{x})$  changes from (+) to (-). In doing so, it changes the " $\Delta_c$ " direction with respect to  $\lambda_8$ . The changing of the " $\Delta_c$ " direction, in turn, forces the  $\text{sgn}(\dot{\lambda} - \dot{x})$  to go back to (+) from (-). The net effect is that the phase trajectory cannot get away from  $\frac{\dot{\lambda}}{p} = \frac{\dot{x}}{p}$ . It will have to stay there until  $\dot{\lambda}/p$  changes in magnitude. This does not happen in the example until point (4). At this time,  $\text{sgn}(\dot{\lambda} - \dot{x})$  becomes (-) no matter what  $\dot{x}/p$  does. The fifth critical point occurs at point (5). Here  $\text{sgn}(\dot{\lambda} - \dot{x})$  goes from





(-) to (+). The phase trajectory continues without "stalling" at  $-\frac{\dot{x}}{p} = -\frac{\lambda}{p}$  point. The last critical point, (6), causes no trouble when the phase trajectory passes through it.

In the example shown in Fig. 9, the responsive displacement of the mass when the damper is fastened to ground while the support is movable is shown by the dash-dot line. For the case where the damper is fastened to the support, the responsive displacement of the mass is shown by the solid line. The difference in responsive peak amplitudes is approximately 8%.

A check of the accuracy of the two graphical solutions was made at  $\frac{t_d}{T} = 0.4$ , and was compared with the analytical solutions shown in Table I.

TABLE I

PHASE-PLANE AND ANALYTICAL RESPONSES OF TWO TYPES OF  
COULOMB-DAMPED SYSTEMS TO SUPPORT EXCITATION

OF FIG. 9 @  $\frac{t}{T} = 0.4$

Mass Motion	Damper Tied to Ground			Damper Tied to Support		
	Ph.-Pl.	Anal.	Percent Error*	Ph.-Pl.	Anal.	Percent Error*
Mass Disp. $\left(\frac{x}{\lambda_m}\right)$	0.22	0.21	+1.0	0.33	0.33	0
Mass Vel. $\left(\frac{\dot{x}}{p\lambda_m}\right)$	0.25	0.26	-1.0	0.21	0.22	-1.0

\* Error based on  $\lambda_m = 1$ .



The analytical equations were found using Laplace Transforms and are shown below.

For the coulomb-damped system of Fig. 9 where the damper is tied to ground

$$x = \frac{2\lambda_m}{t_d} \left( t - \frac{T}{2\pi} \sin \frac{2\pi t}{T} \right) - \Delta_c \operatorname{sgn} \dot{x} \left( 1 - \cos \frac{2\pi t}{T} \right) \quad 0 \leq t \leq T. \quad (11a)$$

For the coulomb-damped system of Fig. 9 where the damper is tied to the movable support

$$\begin{aligned} x = & x_* \cos \frac{2\pi t'}{T} + \frac{\dot{x}_* T}{2\pi} \sin \frac{2\pi t'}{T} \\ & + \left[ \lambda' + \Delta_c \operatorname{sgn} (\ddot{\lambda} - \ddot{x}) \right] \left[ 1 - \cos \frac{2\pi t'}{T} \right] \quad 0.2 \leq \frac{t}{T} \leq 0.7 \quad (11b) \\ & + \left( \frac{\lambda'' - \lambda'}{t_i} \right) \left[ t' - \frac{T}{2\pi} \sin \frac{2\pi t'}{T} \right], \end{aligned}$$

where

$x_*$  = mass displacement at critical point ①  $\left( \frac{t'}{T} = 0 \right)$

$\dot{x}_*$  = mass velocity at critical point ①

$t'$  = time measured from critical point ①  $\left( \frac{t'}{T} = \frac{t}{T} - 0.2 \right)$

$\lambda'$  = support displacement at  $\frac{t}{T} = 0.2$

$\lambda''$  = support displacement at  $\frac{t}{T} = 0.4$

$t_i$  = time interval from  $\frac{t}{T} = 0.2$  to  $\frac{t}{T} = 0.4$ .

In Table I,  $\dot{x}$ 's were found by differentiating Eqs. 11a and 11b.



The differential equations were solved using Laplace transforms and

are shown below.

For the undamped system in Fig. 1 where the spring is 100 lb/in.

is given

$$m\ddot{x} + kx = 0 \quad (1)$$

For the critically-damped system in Fig. 2 where the spring is 100 lb/in.

and the dashpot is 20 lb/in-sec

$$m\ddot{x} + c\dot{x} + kx = 0 \quad (2)$$

$$(4.13) \quad 0.02 \ddot{x} + 0.2 \dot{x} + 100x = 0 \quad (3)$$

$$\left( \frac{1}{2} \ddot{x} + \dot{x} + 100x \right) = 0 \quad (4)$$

where

$x$  = mass displacement in critical point (1/2 - 1)

$\dot{x}$  = mass velocity in critical point (1/2 - 1)

$\ddot{x}$  = time measured from critical point (1/2 - 1)

$\ddot{x}$  = support displacement at  $t = 0$

$\ddot{x}$  = support displacement at  $t = 0.1$

and  $\ddot{x}$  = support displacement at  $t = 0.2$

In Table I, the mass velocity is given in ft/sec.

Eq. 11b cannot be used between any two critical points where a "stall" occurs such as between (3) and (4), because between critical points (3) and (4) there is no relative motion between support and mass.

The method illustrated in Fig. 9 for the damper fixed to the support will apply to any range  $0.1 \leq \frac{t_d}{T} \leq \infty$  for  $\Delta_c \leq 0.2\lambda_m$ . If  $\frac{t_d}{T} < 0.1$ , a single step (whose area is equal to the pulse area) can be employed, and damping neglected; the error of both displacement and velocity of the mass at the end of the pulse is approximately 1%. For large values of  $\frac{t_d}{T}$ , unless the value of  $\Delta_c$  is extremely small, friction will stop the relative motion between mass and support within a very few cycles (e.g.,  $\frac{\Delta_c}{\lambda_m} = 0.1$ ,  $\frac{t_d}{T} = 2$ , symmetrical triangle input; friction stopped relative motion by the time  $\frac{1}{10}$  of pulse duration had elapsed).

The above technique for displacements is especially suitable for relative displacement response when the support (with damper connected) has a known acceleration input. The general solution of Eq. 9 in step input form would become

$$-u = -u_* \cos pt_i - \frac{\dot{u}_*}{p} \sin pt_i + \left[ \frac{\ddot{\lambda}_i}{p^2} - \Delta_c \operatorname{sgn}(-\dot{u}) \right] (1 - \cos pt_i) \quad (12)$$

where

$$u = x - \lambda; \quad \dot{u} = \dot{x} - \dot{\lambda}.$$

The  $\operatorname{sgn}(-\dot{u})$  can thus be observed directly from the phase-plane diagram.

(Note: Eq. 12 is only valid when  $\frac{\ddot{\lambda}_i}{p^2} > \Delta_c$ . If  $\frac{\ddot{\lambda}_i}{p^2} < \Delta_c$ ,  $-u = -\dot{u} = 0$ .)

Fig. 1. The system for which the equations of motion are derived. The system consists of two particles, 1 and 2, which are connected by a spring with stiffness  $k$  and a damper with coefficient  $c$ . The particles are also connected to fixed points by springs with stiffness  $k_1$  and  $k_2$  respectively. The displacement of particle 1 from its equilibrium position is  $x_1$  and the displacement of particle 2 is  $x_2$ . The equations of motion are:

$$m_1 \ddot{x}_1 + c(\dot{x}_1 - \dot{x}_2) + k(x_1 - x_2) + k_1 x_1 = 0$$
$$m_2 \ddot{x}_2 + c(\dot{x}_2 - \dot{x}_1) + k(x_2 - x_1) + k_2 x_2 = 0$$

The natural frequencies of the system are  $\omega_1$  and  $\omega_2$ . The damping ratio is  $\zeta$ . The system is overdamped if  $\zeta > 1$ , critically damped if  $\zeta = 1$ , and underdamped if  $\zeta < 1$ . The response of the system to a step input is given by:

$$x_1(t) = \frac{1}{\omega_d} \left[ \frac{\omega_1^2 - \omega_2^2}{\omega_1^2 - \omega_2^2} e^{-\zeta \omega_1 t} \sin \omega_d t + \frac{\omega_1^2 - \omega_2^2}{\omega_1^2 - \omega_2^2} e^{-\zeta \omega_2 t} \sin \omega_d t \right]$$

where  $\omega_d = \omega_1 \sqrt{1 - \zeta^2}$  and  $\omega_2 = \omega_1 \sqrt{1 - \zeta^2}$ . The system is overdamped if  $\zeta > 1$ , critically damped if  $\zeta = 1$ , and underdamped if  $\zeta < 1$ . The response of the system to a step input is given by:

$$x_1(t) = \frac{1}{\omega_d} \left[ \frac{\omega_1^2 - \omega_2^2}{\omega_1^2 - \omega_2^2} e^{-\zeta \omega_1 t} \sin \omega_d t + \frac{\omega_1^2 - \omega_2^2}{\omega_1^2 - \omega_2^2} e^{-\zeta \omega_2 t} \sin \omega_d t \right]$$

$$x_1(t) = \frac{1}{\omega_d} \left[ \frac{\omega_1^2 - \omega_2^2}{\omega_1^2 - \omega_2^2} e^{-\zeta \omega_1 t} \sin \omega_d t + \frac{\omega_1^2 - \omega_2^2}{\omega_1^2 - \omega_2^2} e^{-\zeta \omega_2 t} \sin \omega_d t \right] \quad (11)$$

where  $\omega_d = \omega_1 \sqrt{1 - \zeta^2}$  and  $\omega_2 = \omega_1 \sqrt{1 - \zeta^2}$ . The system is overdamped if  $\zeta > 1$ , critically damped if  $\zeta = 1$ , and underdamped if  $\zeta < 1$ . The response of the system to a step input is given by:

$$x_1(t) = \frac{1}{\omega_d} \left[ \frac{\omega_1^2 - \omega_2^2}{\omega_1^2 - \omega_2^2} e^{-\zeta \omega_1 t} \sin \omega_d t + \frac{\omega_1^2 - \omega_2^2}{\omega_1^2 - \omega_2^2} e^{-\zeta \omega_2 t} \sin \omega_d t \right]$$



In the single-degree coulomb-damped system, differences between the acceleration phase-plane analysis and the displacement analysis appear. The reason behind this is that the friction force is a constant and thus the differentiation of the equation of motion will appear different in form than for an undamped system, or, as will be seen later, one that is viscously damped. Referring to Eq. 6, the solution of the equation of motion of a free coulomb-damped system is

$$x = (x_0 + \Delta_c \operatorname{sgn} \dot{x}) \cos pt + \frac{\dot{x}_0}{p} \sin pt - \Delta_c \operatorname{sgn} \dot{x}. \quad (6)$$

Differentiating twice with respect to time,

$$\ddot{x} = -p^2(x_0 + \Delta_c \operatorname{sgn} \dot{x}) \cos pt - p\dot{x}_0 \sin pt. \quad (13)$$

Assume an example where the support is stationary and the mass has an initial displacement from the spring equilibrium position. Thus, at  $t = 0$ ,  $x = +x_0$ ,  $\dot{x} = 0$ . At a very short time,  $t = \epsilon_1$ , later when motion is just starting,  $x = +x_0$ ,  $\dot{x} = -\delta$ ,  $\ddot{x} = -p^2(x_0 - \Delta_c)$ , where  $\delta$  is a very small velocity.

The mass now has a constant friction force,  $f$ , in addition to the spring force which effectively has reduced the spring tension, or changed the equilibrium position of the spring by the distance  $\Delta_c$ . Eq. 13 would now be

$$\ddot{x}_1 = -p^2(x_0 - \Delta_c) \cos pt \quad 0 < t < \frac{\pi}{p} \quad (13a)$$



where  $\ddot{x}_1$  is acceleration of the mass during the first half cycle of response.

At  $t = \frac{\pi}{p}$ , a discontinuity occurs in Eq. 13a because  $f$  (and hence  $\Delta_c$ ) abruptly goes to zero. Immediately at  $t = \frac{\pi}{p}$ ,  $\ddot{x}_1$  decreases in magnitude by an amount  $|p^2 \Delta_c|$ . When a short interval of time,  $\epsilon_2$ , has elapsed, the  $\Delta_c$  term appears again but has changed sign. The  $\Delta_c$  term effectively further decreases the acceleration magnitude upon the mass. Now Eq. 13a becomes for the second half cycle,

$$\ddot{x}_2 = -p^2(x_1 - \Delta_c) \cos pt \quad \frac{\pi}{p} < t < \frac{2\pi}{p} \quad (13b)$$

where  $x_1 = (x_0 - 2\Delta_c)$ .

The foregoing statements are shown graphically in Fig. 10a, 10b, and 10c. Note that Fig. 10c is a mirror image of Fig. 10a, except that  $|x_1| < |x_0|$  by an amount  $|2\Delta_c|$ . For any half cycle, then, Eq. 13 becomes for this example

$$\ddot{x}_n = -p^2 \left[ x_0 + (-1)^{n-1} (2n-1) \Delta_c \operatorname{sgn} \dot{x}_n \right] \cos pt \quad \frac{(n-1)\pi}{p} < t < \frac{n\pi}{p} \quad (13c)$$

where  $n$  = half cycle of response.

In terms of constructing a phase-plane diagram and acceleration-time response Eq. 13c is better written as

$$\ddot{x}_n = \left[ \ddot{x}_0 + (-1)^{n-1} (2n-1) \ddot{\Delta}_c \operatorname{sgn} \ddot{x}_n \right] \cos pt \quad \frac{(n-1)\pi}{p} < t < \frac{n\pi}{p} \quad (13d)$$

where  $\ddot{\Delta}_c = p^2 \Delta_c = \frac{f}{m}$ .



where  $\lambda$  is a constant of the mass during the first half cycle of  
 response.  
 In a case of a system with a constant  $\lambda$ , the constant  $\lambda$  can be  
 determined from the condition that the magnitude of the response  
 magnitude at the middle of the first half cycle is equal to the  
 magnitude of the response at the end of the first half cycle.  
 Additionally, it is required that the magnitude of the response  
 at the end of the first half cycle is equal to the magnitude of the  
 response at the end of the second half cycle.

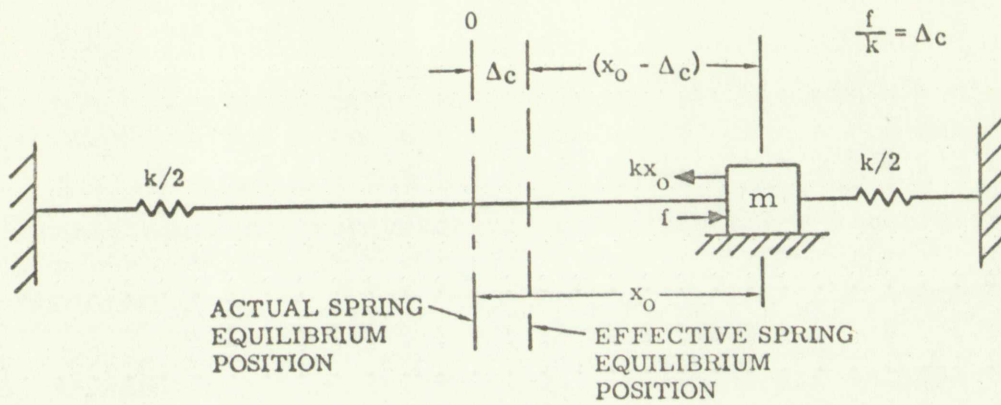
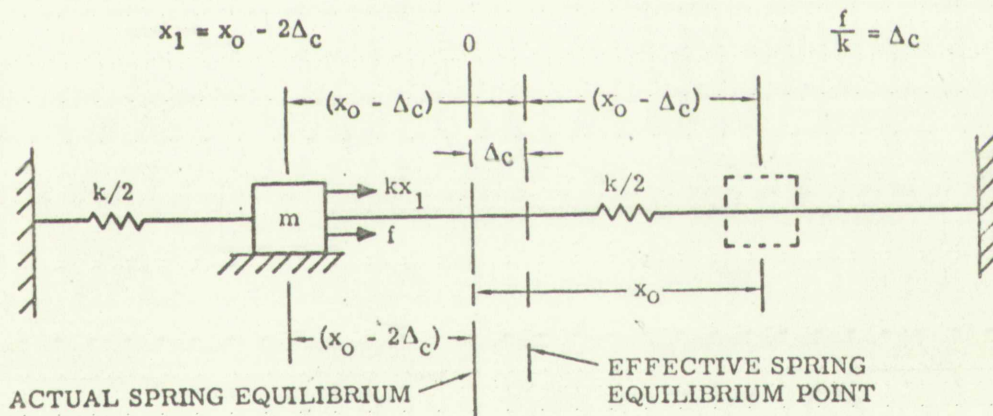
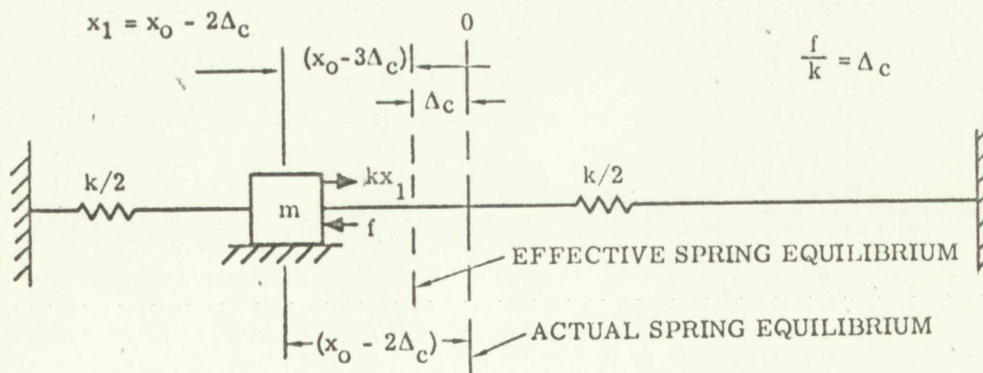
$$\lambda = -\frac{1}{2} \left( \frac{1}{\lambda_1} + \frac{1}{\lambda_2} \right) \quad \text{and} \quad \lambda = \frac{1}{2} \left( \frac{1}{\lambda_1} - \frac{1}{\lambda_2} \right) \quad (11b)$$

where  $\lambda_1 = (\lambda_1^2 - 2\lambda^2)$ .  
 The foregoing arguments are shown graphically in Fig. 11a, 11b,  
 and 11c. Note that Fig. 11c is a relative image of Fig. 11a, except that  
 $|\lambda_1| < |\lambda_2|$  by an amount  $|\lambda_1|$ . For any half cycle, then, Fig. 11b becomes  
 for this example

$$\lambda = -\frac{1}{2} \left( \frac{1}{\lambda_1} + \frac{1}{\lambda_2} \right) \quad \text{and} \quad \lambda = \frac{1}{2} \left( \frac{1}{\lambda_1} - \frac{1}{\lambda_2} \right) \quad (11c)$$

where  $\lambda$  is half cycle of response.  
 In case of constructing a stress-strain diagram and construction  
 this requires for the in particular as

$$\lambda = \left( \frac{1}{\lambda_1} + \frac{1}{\lambda_2} \right) \quad \text{and} \quad \lambda = \left( \frac{1}{\lambda_1} - \frac{1}{\lambda_2} \right)$$

Figure 10a Coulomb Damped System at  $t = \epsilon$ Figure 10b Coulomb Damped System at  $t = \frac{\pi}{p} - \epsilon$ Figure 10c Coulomb Damped System at  $t = \frac{\pi}{p} + \epsilon$

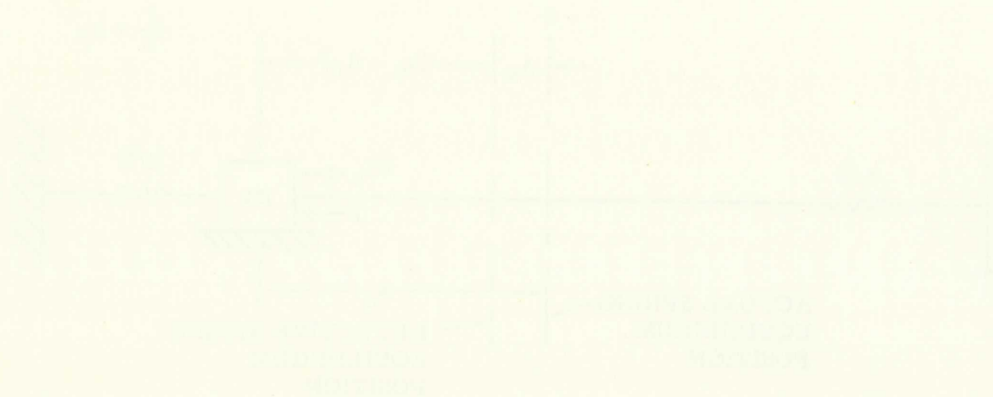


Figure 10.1 Control System Example 10.1



Figure 10.2 Control System Example 10.2

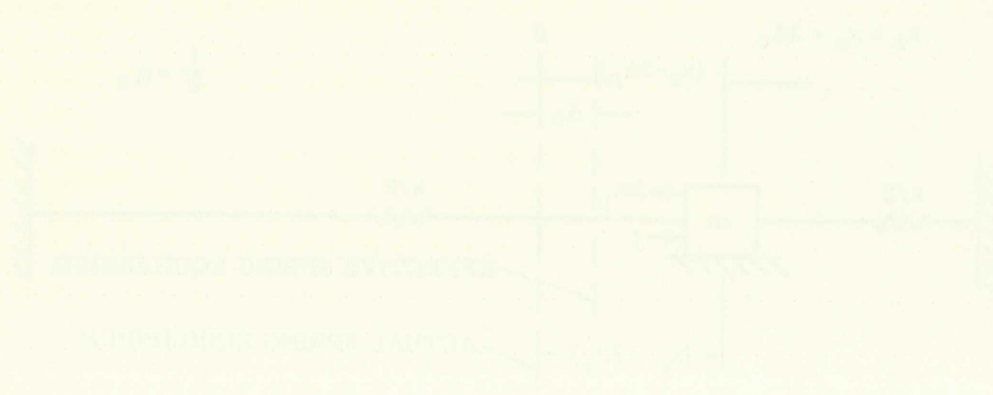


Figure 10.3 Control System Example 10.3



Eq. 13d appears as a linearly damped cosine curve having discontinuities at each peak (see Fig. 11 where, at  $t = 0$ ,  $x = -x_0$ .)

It is a simple matter to extend Eq. 13 concept to occasions when the support (with damper attached) is being accelerated from rest. Differentiating Eq. 9 twice with respect to time and considering the first interval,  $t_1$

$$\ddot{x} + p^2 \dot{x} = p^2 \ddot{\lambda}(t)_1 \quad (14)$$

where  $\ddot{\lambda}(t)_1$  is constant for the first time interval observed.

The general solution of Eq. 14 is

$$\ddot{x} = A \cos pt + B \sin pt + \ddot{\lambda}_1 (1 - \cos pt) .$$

At  $t = 0 + \epsilon_1$ ,  $\ddot{x} = p^2 \Delta_c \operatorname{sgn} (\dot{\lambda} - \dot{x})$ ,  $\ddot{x} \approx 0$ . (This occurs because the mass velocity is still zero and force is applied only through the damper.)

Then

$$A = p^2 \Delta_c \operatorname{sgn} (\dot{\lambda} - \dot{x}) \text{ and } B = 0 .$$

The solution of Eq. 14 becomes

$$\ddot{x} = \ddot{\lambda}_1 (1 - \cos pt) + p^2 \Delta_c \operatorname{sgn} (\dot{\lambda} - \dot{x}) \cos pt \quad 0 < t < \frac{\pi}{p} . \quad (15)$$

Eq. 15 represents free vibration around an input acceleration level of  $\ddot{\lambda}_1$  for the first half cycle (see Fig. 12).

Fig. 1. The dependence of the angular velocity  $\omega$  on the angular displacement  $\theta$ .

where  $\omega_0$  is the initial angular velocity,  $\theta_0$  is the initial angular displacement,  $\theta_1$  is the angular displacement at the end of the first interval,  $\theta_2$  is the angular displacement at the end of the second interval,  $\theta_3$  is the angular displacement at the end of the third interval,  $\theta_4$  is the angular displacement at the end of the fourth interval,  $\theta_5$  is the angular displacement at the end of the fifth interval,  $\theta_6$  is the angular displacement at the end of the sixth interval,  $\theta_7$  is the angular displacement at the end of the seventh interval,  $\theta_8$  is the angular displacement at the end of the eighth interval,  $\theta_9$  is the angular displacement at the end of the ninth interval,  $\theta_{10}$  is the angular displacement at the end of the tenth interval,  $\theta_{11}$  is the angular displacement at the end of the eleventh interval,  $\theta_{12}$  is the angular displacement at the end of the twelfth interval,  $\theta_{13}$  is the angular displacement at the end of the thirteenth interval,  $\theta_{14}$  is the angular displacement at the end of the fourteenth interval,  $\theta_{15}$  is the angular displacement at the end of the fifteenth interval,  $\theta_{16}$  is the angular displacement at the end of the sixteenth interval,  $\theta_{17}$  is the angular displacement at the end of the seventeenth interval,  $\theta_{18}$  is the angular displacement at the end of the eighteenth interval,  $\theta_{19}$  is the angular displacement at the end of the nineteenth interval,  $\theta_{20}$  is the angular displacement at the end of the twentieth interval,  $\theta_{21}$  is the angular displacement at the end of the twenty-first interval,  $\theta_{22}$  is the angular displacement at the end of the twenty-second interval,  $\theta_{23}$  is the angular displacement at the end of the twenty-third interval,  $\theta_{24}$  is the angular displacement at the end of the twenty-fourth interval,  $\theta_{25}$  is the angular displacement at the end of the twenty-fifth interval,  $\theta_{26}$  is the angular displacement at the end of the twenty-sixth interval,  $\theta_{27}$  is the angular displacement at the end of the twenty-seventh interval,  $\theta_{28}$  is the angular displacement at the end of the twenty-eighth interval,  $\theta_{29}$  is the angular displacement at the end of the twenty-ninth interval,  $\theta_{30}$  is the angular displacement at the end of the thirtieth interval,  $\theta_{31}$  is the angular displacement at the end of the thirty-first interval,  $\theta_{32}$  is the angular displacement at the end of the thirty-second interval,  $\theta_{33}$  is the angular displacement at the end of the thirty-third interval,  $\theta_{34}$  is the angular displacement at the end of the thirty-fourth interval,  $\theta_{35}$  is the angular displacement at the end of the thirty-fifth interval,  $\theta_{36}$  is the angular displacement at the end of the thirty-sixth interval,  $\theta_{37}$  is the angular displacement at the end of the thirty-seventh interval,  $\theta_{38}$  is the angular displacement at the end of the thirty-eighth interval,  $\theta_{39}$  is the angular displacement at the end of the thirty-ninth interval,  $\theta_{40}$  is the angular displacement at the end of the fortieth interval,  $\theta_{41}$  is the angular displacement at the end of the forty-first interval,  $\theta_{42}$  is the angular displacement at the end of the forty-second interval,  $\theta_{43}$  is the angular displacement at the end of the forty-third interval,  $\theta_{44}$  is the angular displacement at the end of the forty-fourth interval,  $\theta_{45}$  is the angular displacement at the end of the forty-fifth interval,  $\theta_{46}$  is the angular displacement at the end of the forty-sixth interval,  $\theta_{47}$  is the angular displacement at the end of the forty-seventh interval,  $\theta_{48}$  is the angular displacement at the end of the forty-eighth interval,  $\theta_{49}$  is the angular displacement at the end of the forty-ninth interval,  $\theta_{50}$  is the angular displacement at the end of the fiftieth interval,  $\theta_{51}$  is the angular displacement at the end of the fifty-first interval,  $\theta_{52}$  is the angular displacement at the end of the fifty-second interval,  $\theta_{53}$  is the angular displacement at the end of the fifty-third interval,  $\theta_{54}$  is the angular displacement at the end of the fifty-fourth interval,  $\theta_{55}$  is the angular displacement at the end of the fifty-fifth interval,  $\theta_{56}$  is the angular displacement at the end of the fifty-sixth interval,  $\theta_{57}$  is the angular displacement at the end of the fifty-seventh interval,  $\theta_{58}$  is the angular displacement at the end of the fifty-eighth interval,  $\theta_{59}$  is the angular displacement at the end of the fifty-ninth interval,  $\theta_{60}$  is the angular displacement at the end of the sixtieth interval,  $\theta_{61}$  is the angular displacement at the end of the sixty-first interval,  $\theta_{62}$  is the angular displacement at the end of the sixty-second interval,  $\theta_{63}$  is the angular displacement at the end of the sixty-third interval,  $\theta_{64}$  is the angular displacement at the end of the sixty-fourth interval,  $\theta_{65}$  is the angular displacement at the end of the sixty-fifth interval,  $\theta_{66}$  is the angular displacement at the end of the sixty-sixth interval,  $\theta_{67}$  is the angular displacement at the end of the sixty-seventh interval,  $\theta_{68}$  is the angular displacement at the end of the sixty-eighth interval,  $\theta_{69}$  is the angular displacement at the end of the sixty-ninth interval,  $\theta_{70}$  is the angular displacement at the end of the seventieth interval,  $\theta_{71}$  is the angular displacement at the end of the seventy-first interval,  $\theta_{72}$  is the angular displacement at the end of the seventy-second interval,  $\theta_{73}$  is the angular displacement at the end of the seventy-third interval,  $\theta_{74}$  is the angular displacement at the end of the seventy-fourth interval,  $\theta_{75}$  is the angular displacement at the end of the seventy-fifth interval,  $\theta_{76}$  is the angular displacement at the end of the seventy-sixth interval,  $\theta_{77}$  is the angular displacement at the end of the seventy-seventh interval,  $\theta_{78}$  is the angular displacement at the end of the seventy-eighth interval,  $\theta_{79}$  is the angular displacement at the end of the seventy-ninth interval,  $\theta_{80}$  is the angular displacement at the end of the eightieth interval,  $\theta_{81}$  is the angular displacement at the end of the eighty-first interval,  $\theta_{82}$  is the angular displacement at the end of the eighty-second interval,  $\theta_{83}$  is the angular displacement at the end of the eighty-third interval,  $\theta_{84}$  is the angular displacement at the end of the eighty-fourth interval,  $\theta_{85}$  is the angular displacement at the end of the eighty-fifth interval,  $\theta_{86}$  is the angular displacement at the end of the eighty-sixth interval,  $\theta_{87}$  is the angular displacement at the end of the eighty-seventh interval,  $\theta_{88}$  is the angular displacement at the end of the eighty-eighth interval,  $\theta_{89}$  is the angular displacement at the end of the eighty-ninth interval,  $\theta_{90}$  is the angular displacement at the end of the ninetieth interval,  $\theta_{91}$  is the angular displacement at the end of the ninety-first interval,  $\theta_{92}$  is the angular displacement at the end of the ninety-second interval,  $\theta_{93}$  is the angular displacement at the end of the ninety-third interval,  $\theta_{94}$  is the angular displacement at the end of the ninety-fourth interval,  $\theta_{95}$  is the angular displacement at the end of the ninety-fifth interval,  $\theta_{96}$  is the angular displacement at the end of the ninety-sixth interval,  $\theta_{97}$  is the angular displacement at the end of the ninety-seventh interval,  $\theta_{98}$  is the angular displacement at the end of the ninety-eighth interval,  $\theta_{99}$  is the angular displacement at the end of the ninety-ninth interval,  $\theta_{100}$  is the angular displacement at the end of the hundredth interval.

It is a simple matter to show that the angular displacement  $\theta$  is a function of time  $t$ .

The angular displacement  $\theta$  is a function of time  $t$  and angular velocity  $\omega$ .

Differentiating (1) with respect to time  $t$  and substituting the

first interval, we

(10)

where  $\theta_1$  is constant for the first time interval observed.

The general solution of Eq. (10) is

$$\ddot{\theta} = A \cos p_1 t + B \sin p_1 t + C_1 (1 - \cos p_1 t)$$

At  $t = 0$ ,  $\ddot{\theta} = 0$ ,  $\dot{\theta} = 0$ ,  $\theta = 0$ . (This occurs because the

angular velocity is still zero and hence the applied force through the damper.)

Then

$$A = p_1^2 \ddot{\theta}_1 \sin \theta_1 \quad \text{and} \quad B = 0$$

The solution of Eq. (10) becomes

(11)

$$\ddot{\theta} = \ddot{\theta}_1 (1 - \cos p_1 t) + p_1^2 \ddot{\theta}_1 \sin \theta_1 (1 - \cos p_1 t) \quad 0 < t < \frac{\pi}{p_1}$$

Fig. 12. The dependence of the angular displacement  $\theta$  on the angular velocity  $\omega$ .

At  $t = \frac{\pi}{p_1}$  for the first time interval, we

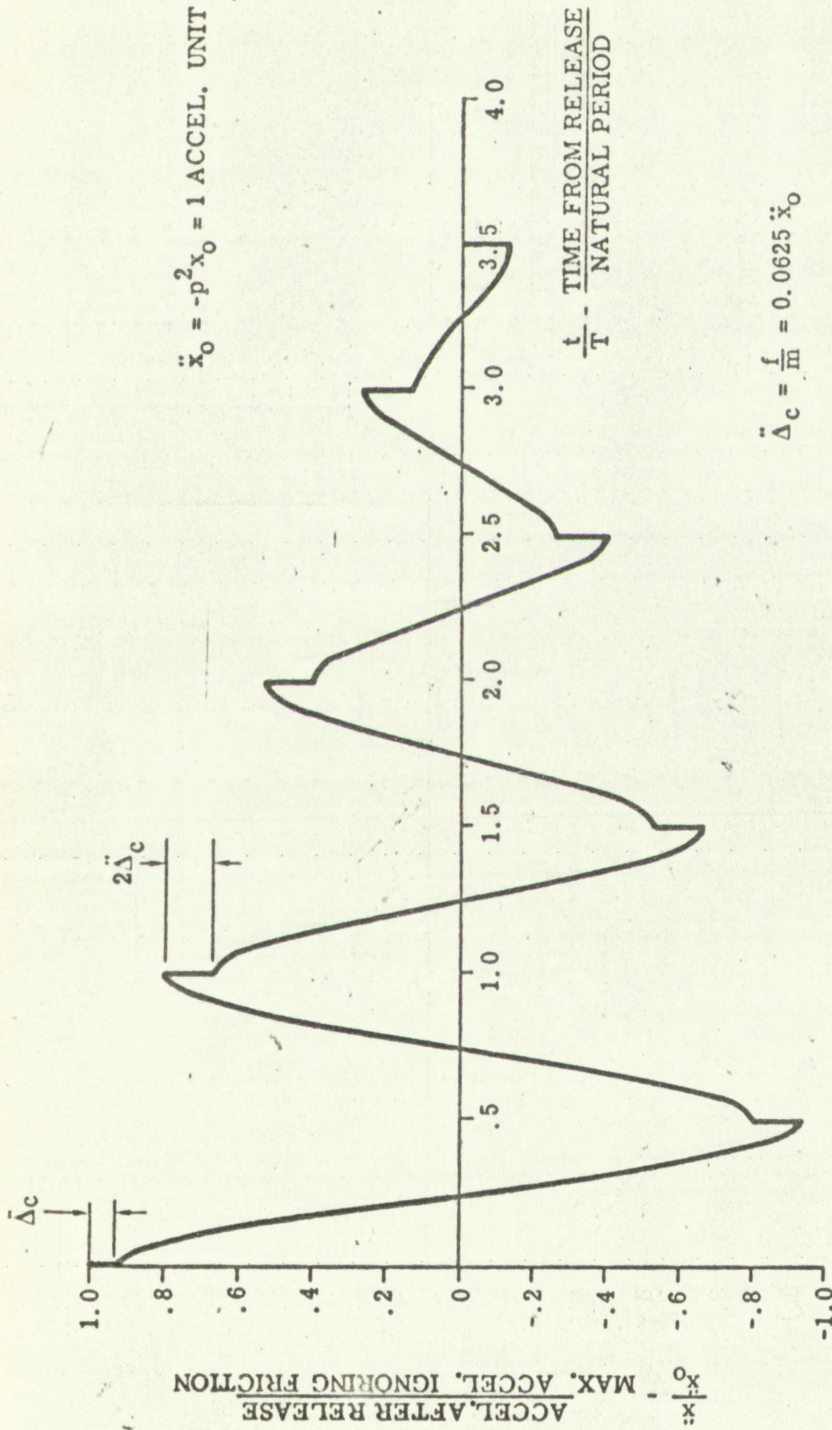


Figure 11 Dry Friction Damped System (Single Degree - Free Vibration)











At  $t = t_1 = \frac{\pi}{p}$ ,  $p^2 \Delta_c$  would instantaneously be zero so response would decrease in magnitude by an amount  $|p^2 \Delta_c|$ . At  $t = \frac{\pi}{p} + \epsilon$ ,  $p^2 \Delta_c$  has become negative, which further decreases  $\ddot{x}_2$  at the start of the second half cycle. The acceleration motion of  $\ddot{x}_2$  will continue about  $\ddot{\lambda}_1$  in free vibration until  $t \rightarrow \frac{2\pi}{p}$  (at which time another discontinuity occurs) or until the level of  $\ddot{\lambda}_1$  changes. Fig. 12 depicts what happens to a coulomb-damped single-degree system when the support has different input acceleration levels that change at times when  $\frac{\ddot{x}}{p} \neq 0$ . Fortunately, one need not be concerned with the magnitudes of  $(\dot{\lambda} - \dot{x})$  in order to determine whether  $\text{sgn}(\dot{\lambda} - \dot{x})$  is (+) or (-). The  $\text{sgn}$  term can only change when  $\ddot{x}$  goes through zero on the phase-plane diagram. It makes no difference whether  $\ddot{x}$  is (+) or (-). The  $p^2 \Delta_c$  correction in amplitude at  $\frac{\ddot{x}}{p} = 0$  is always toward the phase-plane center which is the  $\ddot{\lambda}_1$  level. The  $\ddot{\lambda}_1$  magnitude must be greater than  $\ddot{\Delta}_c$ , else the support and mass will respond as though rigidly connected.

Whenever the support excitation is a velocity step, either spring deflection or mass acceleration response can be found easily. It makes no difference whether the support velocity is initially zero or finally zero, the phase-plane diagram is the same as for a free vibration condition. The initial point on the phase plane for spring deflection (as shown in Eq. 16) can be derived from Eq. 12; namely, at  $t = 0$ , for no initial spring deflection

$$\dot{u} = \dot{u}_0; u = 0.$$

(16)





Similarly, the initial point on the phase-plane diagram for acceleration response can be found from the expressions (assuming no spring deflection)

$$\ddot{x}_0 = \ddot{\Delta}_c; \ddot{x}_0 = p^2 |\delta \dot{\lambda}_0| \quad (17)$$

where  $|\delta \dot{\lambda}_0|$  = velocity change of support at  $t = 0$ . Eq. 17 can be found by solving Eq. 9 when  $\lambda(t) = \dot{\lambda}_0 t$ , and then differentiating.

### 3. Viscously Damped Systems

Another predominant type of friction frequently encountered in damped systems is viscous friction. (Actually no system will have a single-type damper, but quite often one type is more pronounced than another type; hence, the use of the word "predominant.")

For vibration problems involving viscous damping, the equation of motion of free vibration of a single-degree system is

$$m\ddot{x} + c\dot{x} + kx = 0 \quad (18)$$

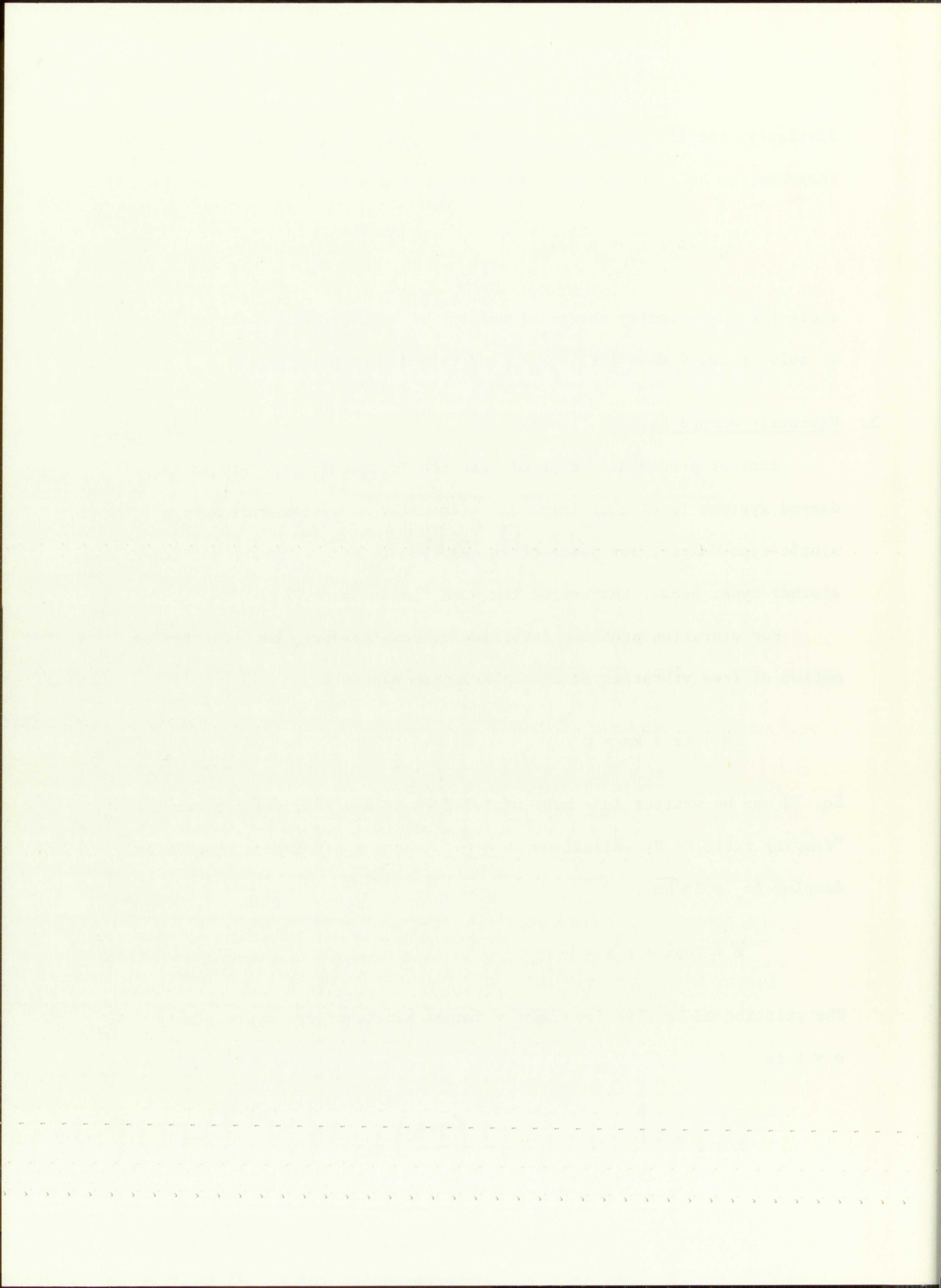
Eq. 18 can be written in a more useful form in Eq. 18a, using a term "damping ratio." By definition,  $\nu = \frac{c}{c_r}$ , where  $c_r$  is amount of critical damping ( $c_r = 2\sqrt{km}$ ).

$$\ddot{x} + 2\nu p\dot{x} + p^2 x = 0 \quad (18a)$$

The solution of Eq. 18a for lightly damped single-degree systems when  $\nu < 1$  is

$$x = e^{-\nu p t} \left[ x_0 \cos p' t + \left( \frac{\dot{x}_0 + \nu p x_0}{p'} \right) \sin p' t \right], \quad (19)$$





where  $p'$  (the damped resonant frequency)  $= p \sqrt{1 - v^2}$ .

Eq. 19 shows that a phase-plane plot for a viscously damped system is a logarithmic spiral in an oblique coordinate system. The development of this type phase-plane plot which follows is from Ref. (5).

Eq. 19 can be written

$$x = e^{-vpt} R \cos (p't - \phi) , \quad (19a)$$

where

$$R = \sqrt{x_0^2 + \left( \frac{\dot{x}_0 + vpx_0}{p'} \right)^2}$$

$$\phi = \tan^{-1} \frac{\left( \frac{\dot{x}_0 + vpx_0}{p'} \right)}{x_0} .$$

Differentiating Eq. 19a,

$$\frac{\dot{x}}{p} = -e^{-vpt} R \left[ \sqrt{1 - v^2} \sin (p't - \phi) + v \cos (p't - \phi) \right] . \quad (20)$$

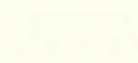
Letting

$$\sqrt{1 - v^2} = \cos \sigma$$

$$v = \sin \sigma$$

$$(p't - \phi) = \psi$$

$$e^{-vpt} R = s ,$$



where  $\theta$  is the angle between the horizontal and the vertical line segment.

It is shown that a point on the line  $\theta = 0$  is a stationary point.

As a Lagrangian multiplier is introduced, the function

is defined. It is shown that the function is stationary at the point  $\theta = 0$ .

It is also shown that

where  $\theta$  is the angle between the horizontal and the vertical line segment. It is shown that the function is stationary at the point  $\theta = 0$ .

$$z = \sqrt{\frac{1}{2} + \frac{1}{2} \cos \theta}$$

$$\frac{1}{z} = \frac{1}{\sqrt{\frac{1}{2} + \frac{1}{2} \cos \theta}}$$

where  $\theta$  is the angle between the horizontal and the vertical line segment.

$$\frac{1}{z} = \frac{1}{\sqrt{\frac{1}{2} + \frac{1}{2} \cos \theta}} \quad (10)$$

where  $\theta$  is the angle between the horizontal and the vertical line segment.

$$\sqrt{\frac{1}{2} + \frac{1}{2} \cos \theta}$$

$$\theta = 0$$

$$\frac{1}{z} = \frac{1}{\sqrt{\frac{1}{2} + \frac{1}{2} \cos \theta}}$$



Eq. 20 becomes

$$\frac{\dot{x}}{p} = -s(\cos \sigma \sin \psi + \sin \sigma \cos \psi) ,$$

or

$$-\frac{\dot{x}}{p'} = s \sin \psi + s \cos \psi \tan \sigma .$$

Finally, from Eq. 19a

$$-\frac{\dot{x}}{p'} = s \sin \psi + x \tan \sigma . \quad (21)$$

The plot of Eqs. 19a and 21 are shown in Fig. 13. These equations represent a line of length "s" rotating counterclockwise with a constant angular speed  $p'$ . The exponential decrease of s with time indicates the trajectory path is a logarithmic spiral. Thus, to make a phase-plane plot, one needs to have a spiral curve or template drawn for each value of  $\psi$  existing in any single-degree system. When an initial point  $x_1$ ,  $\frac{\dot{x}_1}{p'}$  is given on a phase-plane plot and an input of  $\lambda_1$  is known (the damper tied to ground), the center of the spiral can be placed at  $\lambda_1$  on the inclined axis,  $\lambda$ , and the template turned around until the spiral passes over the initial point. Fig. 14 shows how a point representing initial conditions would be located and the spiral trajectory drawn for the first step. The abscissa of the plot can be graduated either in  $\frac{\dot{x}}{p'}$  or  $\frac{\dot{x}}{p}$  by multiplying the former by  $\cos \sigma$ .



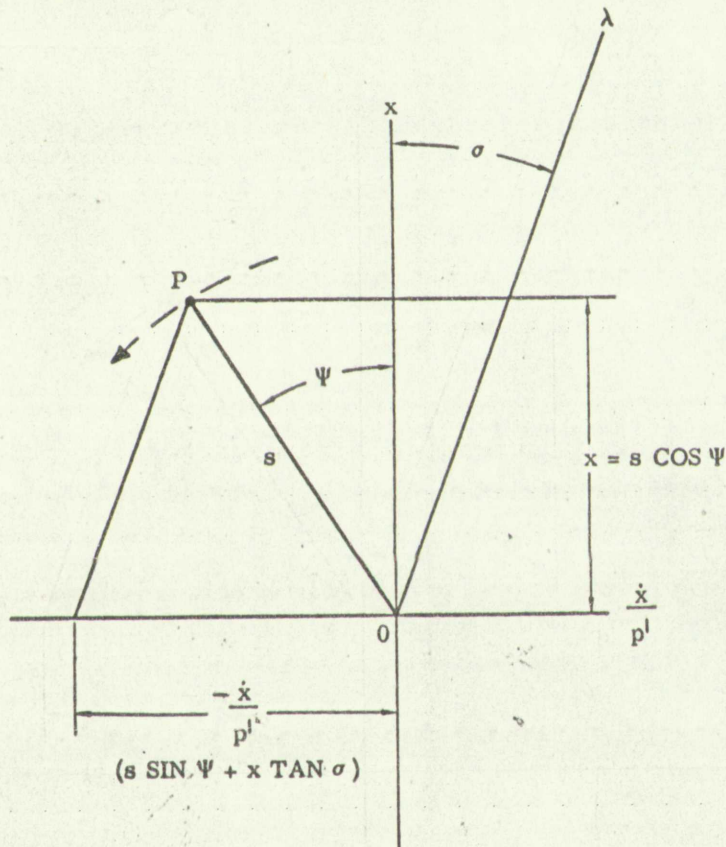


Figure 13 Oblique Axes,  $\lambda$  and  $\frac{\dot{x}}{p^l}$  for Phase-Plane Diagram of Visously Damped Vibration.



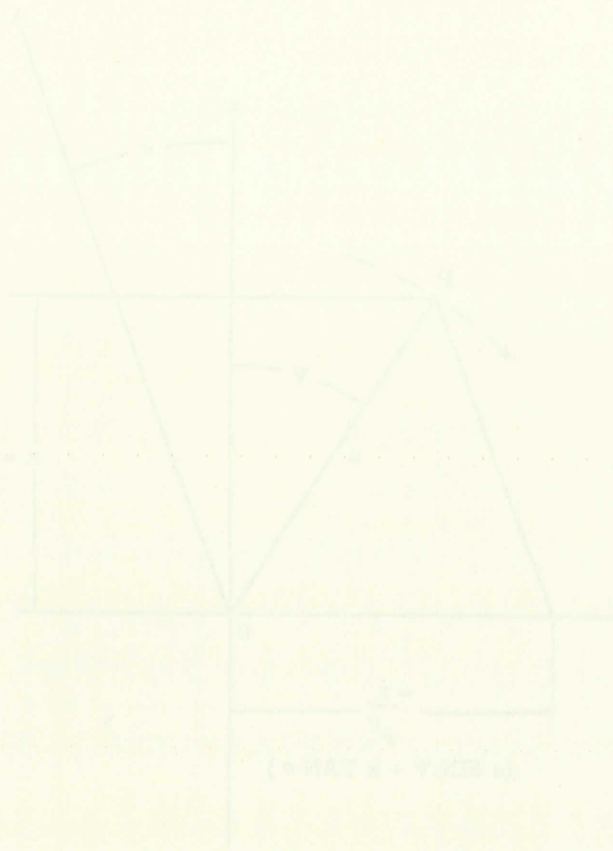


Figure 12. Geometric construction of the  $\alpha$  and  $\beta$  angles for the  $\alpha$ - $\beta$  diagram.

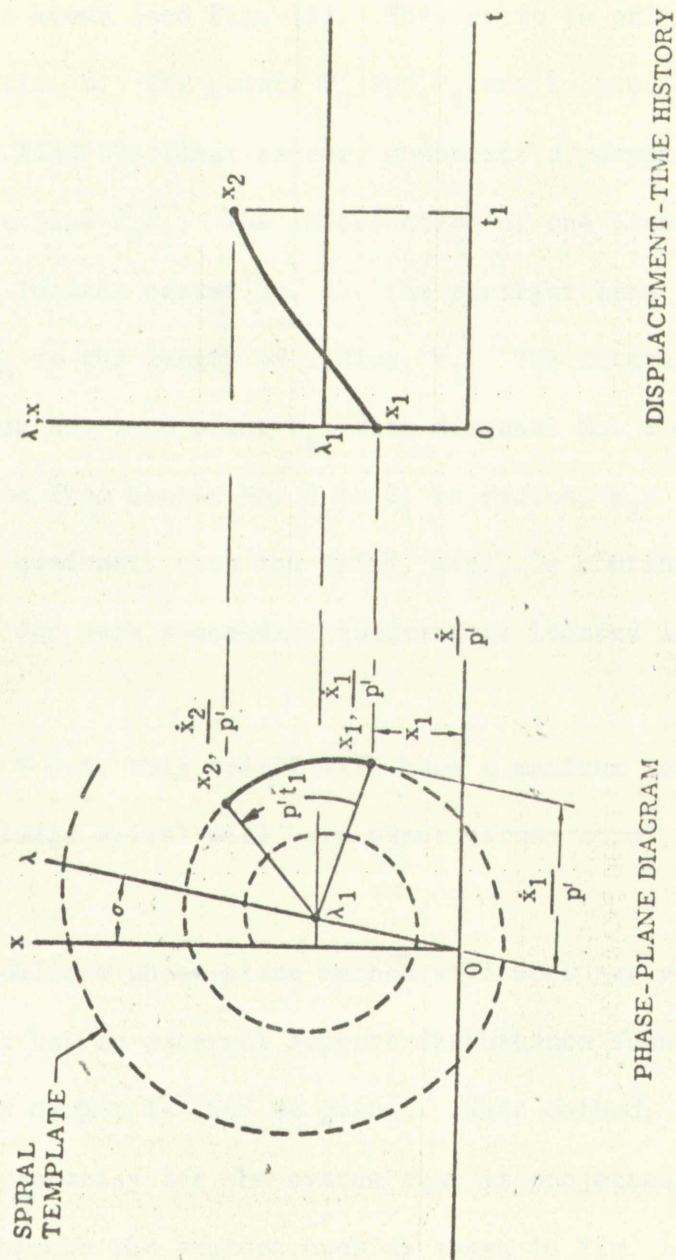


Figure 14 Displacement-Time Response from Spiral Template on Oblique Coordinate  
Phase-Plane Diagram





An approximate spiral can be constructed by using a graphical method explained in Ref. (2). Any size spiral can be drawn once the ratio  $\frac{P_0}{P_1}$  is known (see Fig. 15). This ratio is only dependent upon the damping ratio,  $\nu$ . The points  $P_0$  and  $P_1$  are located on perpendicular lines. To find the first center, construct a perpendicular bisector of straight line  $\overline{P_0P_1}$ . The intersection of the bisector with diagonal line No. 2 locates center No. 1. The straight line from center No. 1 to point  $P_0$  is the length of radius,  $r_1$ . The intersection of radius No. 1 (from center No. 1 to point  $P_1$ ) with diagonal No. 1 determines center No. 2. The distance from center No. 2 to  $P_1$  is radius,  $r_2$ . Then the spiral in the second quadrant, then the third, etc., is continued in sequence since the center for each succeeding quadrant is located in the preceding quadrant.

If  $\nu < 0.5$ , this spiral will have a maximum localized error of  $\pm 2\%$ . The approximate spiral will have exact values at  $0^\circ$ ,  $45^\circ$ ,  $90^\circ$ , etc., from the start.

The oblique phase-plane method will work satisfactorily for a system that has an external support disturbance such as shown in Fig. 16a. The viscous damper is tied to ground. This method, in general, will not work satisfactorily for the system that is subjected to an external disturbance through the support such as shown in Fig. 16b. The viscous damper now is acting similarly to the friction damper of system in Fig. 9 (damper fastened to support), only now the viscous force,  $c$ , is dependent upon the magnitude of the relative velocity as well as the direction.

An approximate spiral can be constructed by using a graphical

method explained in Ref. (2). Any other spiral can be drawn using the

ratio  $\frac{r_0}{r_1}$  is known (see Fig. 1). This ratio is only dependent upon the

choosing ratio,  $r_0$ . The points  $P_0$  and  $P_1$  are located on perpendicular

lines. To find the first center, construct a perpendicular bisector

of straight line  $P_0P_1$ . The intersection of this bisector with diagonal

line No. 2 locates center No. 1. The straight line from center No. 1

to point  $P_0$  is the length of radius  $r_1$ . The intersection of radius No. 1

(from center No. 1 to point  $P_1$ ) with diagonal No. 1 determines center No. 2.

The distance from center No. 2 to  $P_1$  is radius  $r_2$ . Then the spiral is

the second quadrant, then the third, etc., is continued in sequence since

the center for each succeeding quadrant is located in the preceding

quadrant.

If  $\theta > 0.5$ , this spiral will have a maximum localized error of 25%.

The approximate spiral will have exact values at  $0^\circ$ ,  $45^\circ$ ,  $90^\circ$ , etc., from

the start.

The oblique phase-plane method will work satisfactorily for a

system that has an external support disturbance such as shown in Fig. 15a.

The viscous damper is tied to ground. This method, in general, will not

work satisfactorily for the system that is subjected to an external dis-

turbance through the support such as shown in Fig. 15b. The viscous

damper now is acting relatively to the friction damper of system in Fig. 15

(damper fastened to support); only now the viscous force,  $c$ , is dependent

upon the relative motion of the mass and support as well as the direction

$$\text{NAT. LOG.} \left( \frac{P_0}{P_1} \right) = \frac{\pi}{2} \sqrt{\frac{\nu}{1-\nu^2}}$$

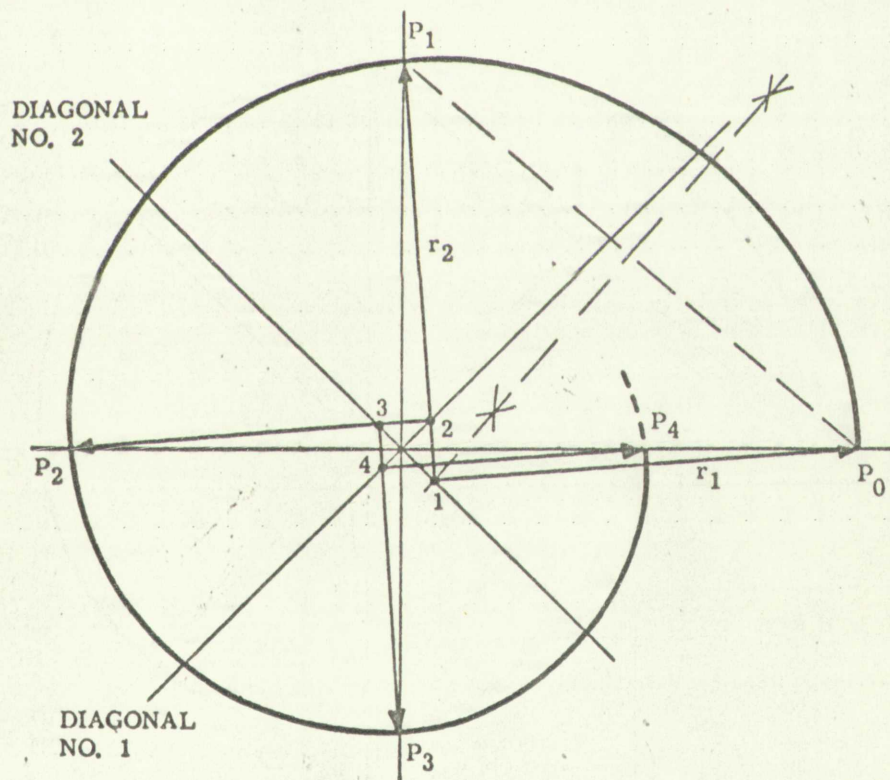


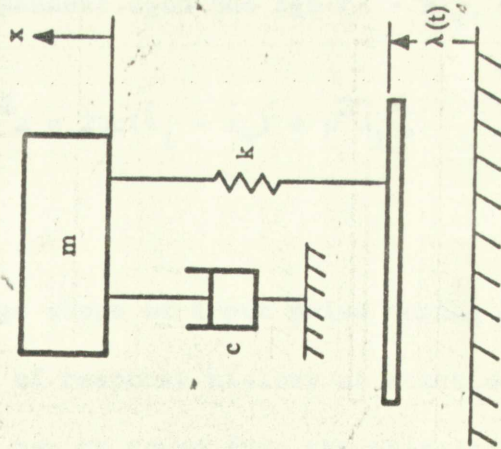
Figure 15 Approximate Circular-Quadrant Construction of Exponential Spiral





Figure 10. Approximate Circular-Function Construction of  $\sqrt{2}$  and  $\sqrt{3}$

(a) SUPPORT EXCITATION  
DAMPER FASTENED TO GROUND



(b) SUPPORT EXCITATION  
DAMPER FASTENED TO SUPPORT

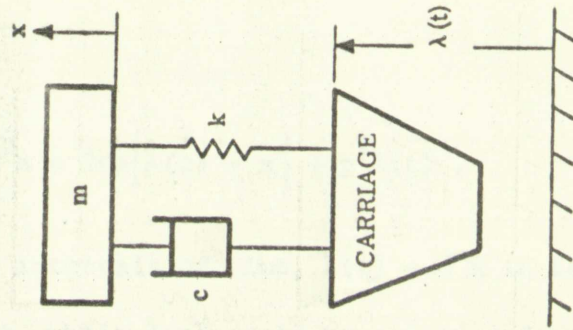


Figure 16 Viscously Damped Systems Subjected to Transient Support Motion





The general differential equation of motion for support excitation where the damper is tied to the support is

$$m\ddot{x} + c\dot{x} + kx = c\dot{\lambda}(t) + k\lambda(t) \quad (22)$$

or

$$\ddot{x} + p^2x = 2vp\left[\dot{\lambda}(t) - \dot{x}\right] + p^2\lambda(t) . \quad (22a)$$

For small intervals of time,  $\dot{\lambda}(t)$  and  $\dot{x}$  in Eq. 22a could be considered constant, while  $\lambda(t)$  could be considered varying linearly with time. The  $\lambda(t)$  for each step in turn could be approximated by the average value of  $\lambda$  during the step  $\lambda_i$ , so that the area under the step is equivalent to the original area under the input displacement curve. Now Eq. 22a is written in format similar to Eq. 9 except the friction force is not dependent upon the  $\text{sgn}(\dot{\lambda} - \dot{x})_i$ , i.e.,

$$\ddot{x} + p^2x = 2vp(\dot{\lambda}_i - \dot{x}_*) + p^2\lambda_i , \quad (22b)$$

where

$\dot{\lambda}_i$  = average slope of input pulse during step

$\dot{x}_*$  = slope of response history at start of the step. (This value can be found from the phase-plane diagram.)

$\lambda_i$  = average value of  $\lambda$  during the step.

The general differential equation of motion for a system is

where the input is  $x(t)$  and the output is  $y(t)$ .

$$m\ddot{y} + c\dot{y} + ky = c\dot{x} + kx \quad (21)$$

or

$$\ddot{y} + 2\zeta\omega_n\dot{y} + \omega_n^2 y = 2\zeta\omega_n\dot{x} + \omega_n^2 x \quad (22)$$

For small intervals of time,  $\dot{x}(t)$  and  $\ddot{x}(t)$  can be con-

sidered constant, while  $\ddot{x}(t)$  could be considered varying linearly with

time. The  $\ddot{x}(t)$  for each step is then could be approximated by the

average value of  $\ddot{x}$  during the step  $\Delta t$ , so that the area under the curve

is equivalent to the original area under the input displacement curve.

Now Eq. (22) is written in form similar to Eq. (21) except the friction

force is not dependent upon the sign of  $\dot{y}$ , i.e.,

$$\ddot{y} + 2\zeta\omega_n\dot{y} + \omega_n^2 y = 2\zeta\omega_n\dot{x} + \omega_n^2 x \quad (23)$$

where

$\bar{\dot{x}} =$  average slope of input pulse during step

$\dot{x}_0 =$  slope of response history at start of the step. (This

value can be found from the phase-plane diagram.)

$\bar{\Delta} =$  average value of  $\Delta$  during the step.



The solution of Eq. 22b is

$$x = x_* \cos pt_i + \frac{\dot{x}_*}{p} \sin pt_i + \left[ \lambda_i + 2v \left( \frac{\dot{\lambda}_i - \dot{x}_*}{p} \right) \right] (1 - \cos pt_i), \quad (23)$$

where  $2v \left( \frac{\dot{\lambda}_i - \dot{x}_*}{p} \right) = \Delta_{vi}$ , the "delta" term used to correct the phase-plane center. Eq. 23 is now similar in format to Eq. 10.

A rectangular coordinate system for constructing the phase-plane diagram is now required. There are no critical points of concern as there were in the coulomb-damped system. The closer  $\dot{\lambda}$  and  $\dot{x}$  become, the less correction is needed for  $\lambda_i$ , the uncorrected center of the circular arc of the step.

Fig. 17 shows the responses of two types of viscously damped specimens to a symmetrical triangle support displacement. The damper in one case is tied to ground, while in the other case the damper is tied to the movable support. A damping ratio of 0.2 was selected. Step intervals of  $\frac{t_i}{T} = 0.10$  were taken. (After the pulse is over any response history could have been found using the oblique phase-plane method entirely.) Comparisons of  $x$  and  $\dot{x}$  of both systems were made with the analytical solutions at  $t = 0.4T$  and  $t = 0.8T$ . The results are shown in Table II.



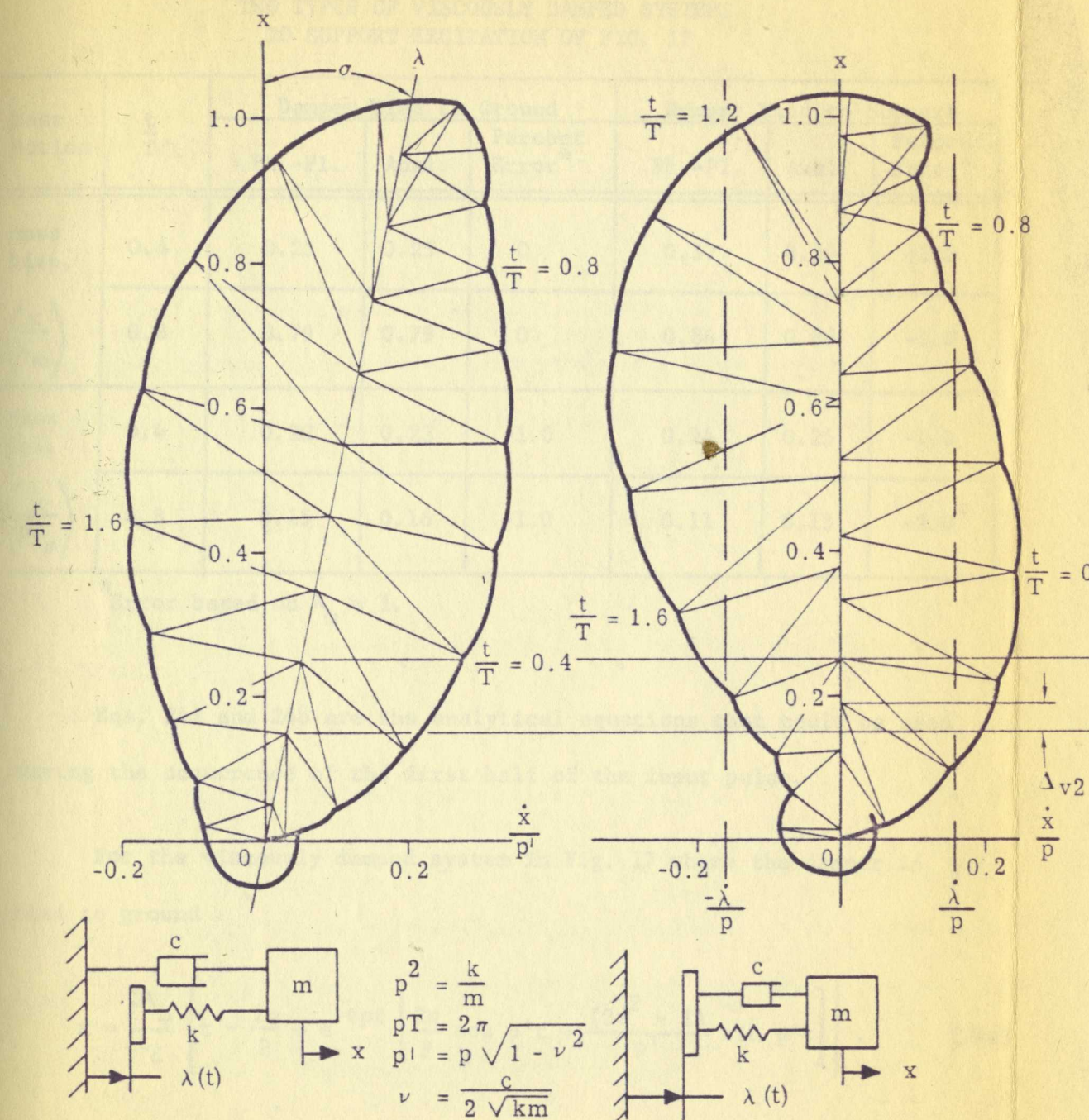




## PHASE-PLANE DIAGRAMS

(DAMPER TIED TO GROUND)

(DAMPER TIED TO SUPPORT)



## DISPLACEMENT-TIME HISTORIES

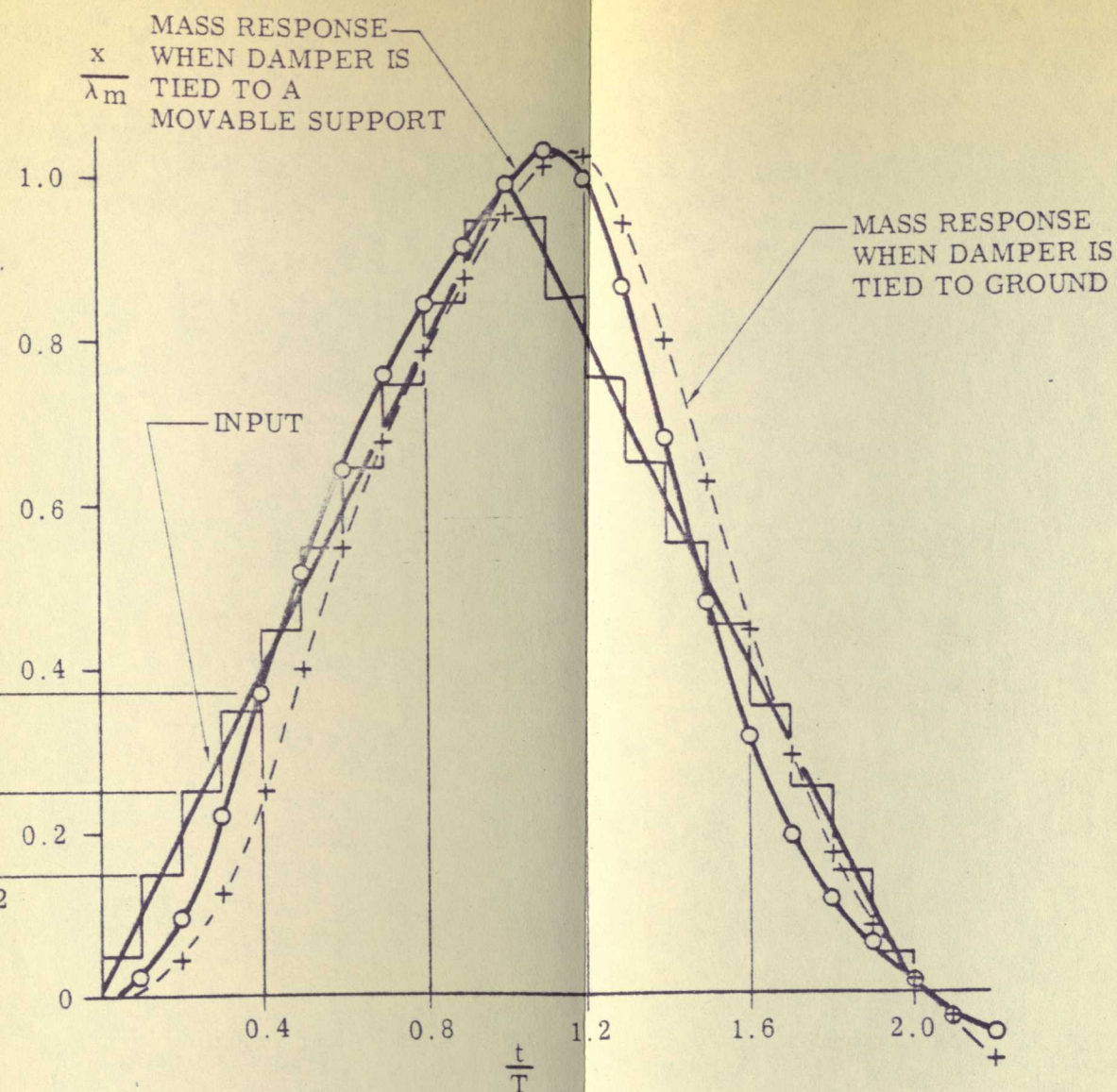


Figure 17 Responses of Specimen to Transient Input Displacement When Damper is Fastened to Either a Fixed or Movable Support







TABLE II

PHASE-PLANE AND ANALYTICAL RESPONSES OF  
TWO TYPES OF VISCOUSLY DAMPED SYSTEMS  
TO SUPPORT EXCITATION OF FIG. 17

Mass Motion	$\frac{t}{T}$	Damper Tied to Ground			Damper Tied to Support		
		Ph.-Pl.	Anal.	Percent Error*	Ph.-Pl.	Anal.	Percent Error*
Mass Disp.	0.4	0.25	0.25	0	0.37	0.34	+3.0
$\left(\frac{x}{\lambda_m}\right)$	0.8	0.79	0.79	0	0.84	0.86	-1.0
Mass Vel.	0.4	0.22	0.23	-1.0	0.24	0.25	-1.0
$\left(\frac{\dot{x}}{p\lambda_m}\right)$	0.8	0.15	0.16	-1.0	0.11	0.13	-2.0

\*Error based on  $\lambda_m = 1$ .

Eqs. 24a and 24b are the analytical equations that could be used during the occurrence of the first half of the input pulse.

For the viscously damped system in Fig. 17 where the damper is tied to ground

$$x = \frac{2\lambda_m}{t_d} \left\{ t - \frac{2v}{p} + e^{-vpt} \left[ \frac{2v}{p} \cos p't + \frac{(2v^2 - 1)}{p'} \sin p't \right] \right\}. \quad (24a)$$





For the viscously damped system in Fig. 17 where the damper is tied to the movable support

$$x = \frac{2\lambda_m}{t_d} \left[ t - \frac{1}{p'} e^{-vpt} \sin p't \right], \quad (24b)$$

where  $p' = p \sqrt{1 - v^2}$ . The  $\dot{x}$ 's of Table II were found by differentiating Eqs. 24a and 24b.

For problems involving response in terms of spring deflection of a viscously damped system when the support has a known acceleration input applied, the phase-plane diagram can be drawn using the oblique coordinate system. The differential equation of motion is

$$\ddot{x} + 2vp\dot{x} + p^2x = 2vp\dot{\lambda}(t) + p^2\lambda(t). \quad (25)$$

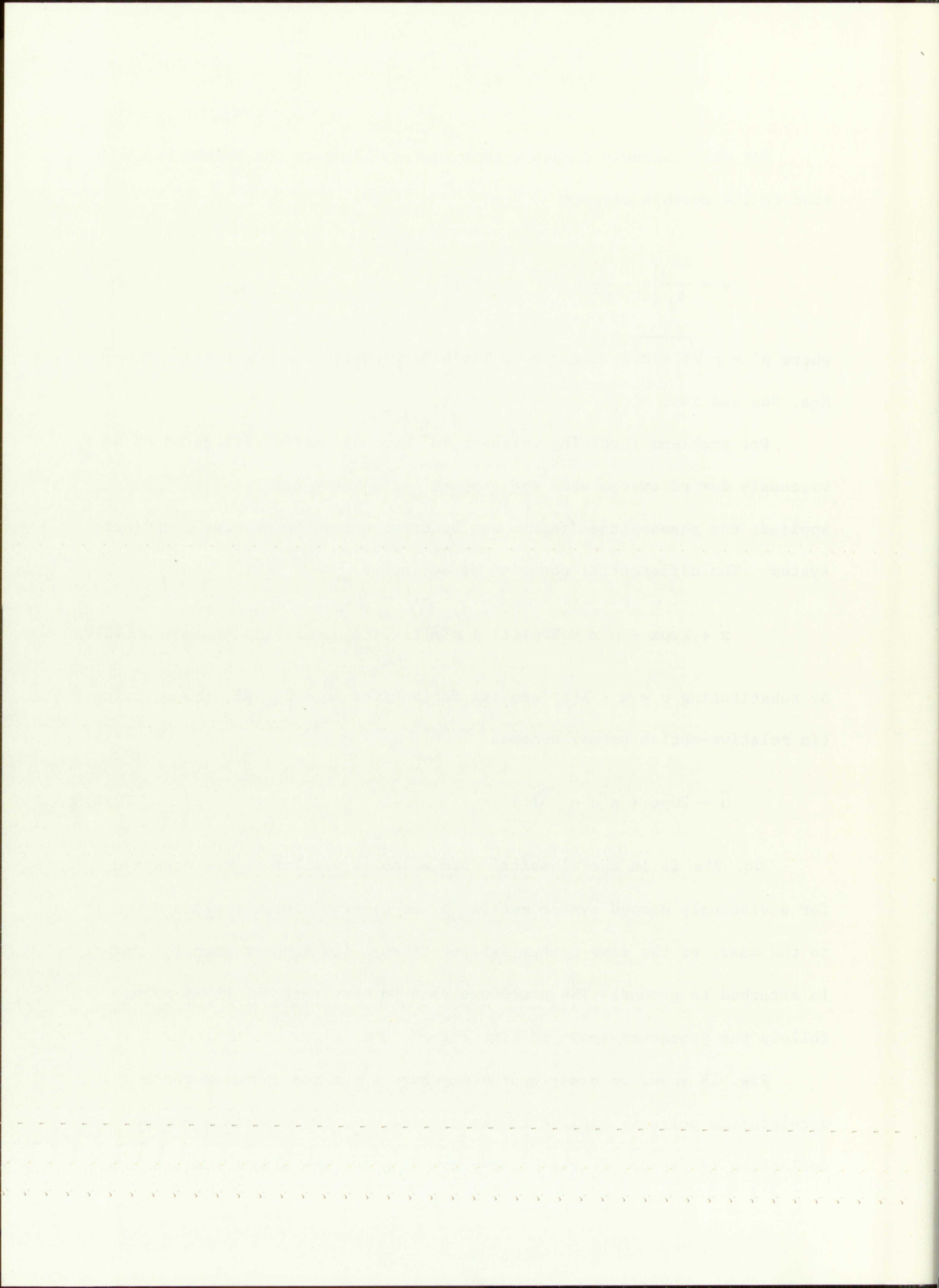
By substituting  $u = x - \lambda(t)$  and its derivatives into Eq. 25, the equation (in relative-motion terms) becomes

$$\ddot{u} + 2vp\dot{u} + p^2u = -\ddot{\lambda}(t). \quad (25a)$$

Eq. 25a is in the classical form which is similar to the equation for a viscously damped system excited by an external force applied directly to the mass, or the same system excited through its support when the damper is attached to ground. The procedure used to construct the phase plane follows the procedure shown in Fig. 14.

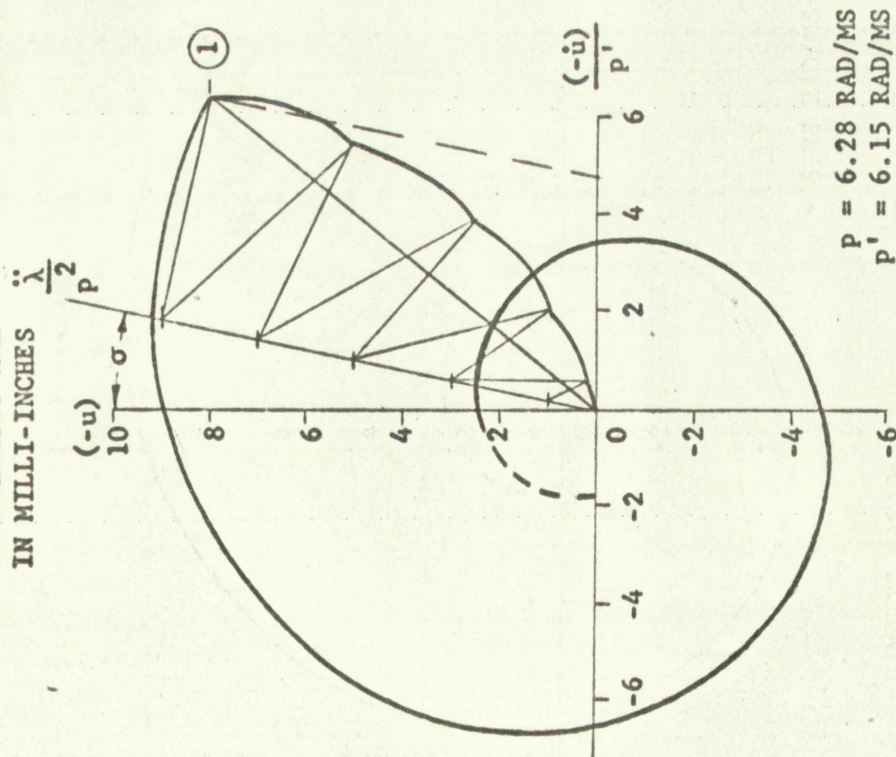
Fig. 18 shows an example problem where a terminal peak sawtooth acceleration pulse is applied to the support, and the resulting spring deflection is found. In the phase-plane diagram, the slanted dotted line





# PHASE-PLANE DIAGRAM

COORDINATES ARE  
IN MILLI-INCHES



# DEFLECTION-TIME HISTORY

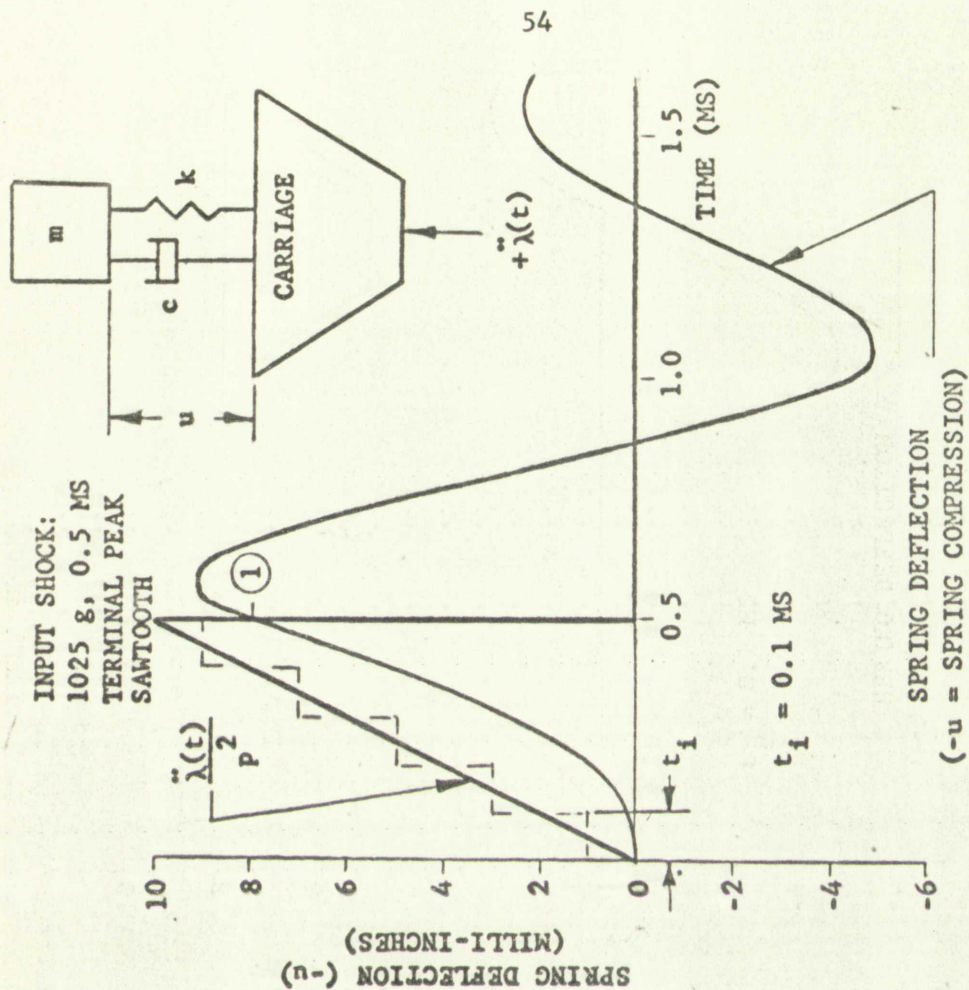


Figure 18 Example Problem Showing Responsive Deflection-Time History of Spring When Specimen Is Subjected to Sawtooth Acceleration Pulse

Figure 1. The effect of the concentration of the reactants on the rate of the reaction.

Figure 2. The effect of the temperature on the rate of the reaction.

Figure 3. The effect of the catalyst on the rate of the reaction.



Figure 4. The effect of the catalyst on the rate of the reaction.

Figure 5. The effect of the temperature on the rate of the reaction.

Figure 6. The effect of the concentration of the reactants on the rate of the reaction.



extending from point ① to the abscissa represents the rate of change of spring compression at the end of the pulse.

For single-degree, viscously damped systems the procedure applied to displacements also applies to acceleration phase-plane diagrams. This is because the second derivatives of the differential equation of motion can be made to look similar to the original equation. Compare

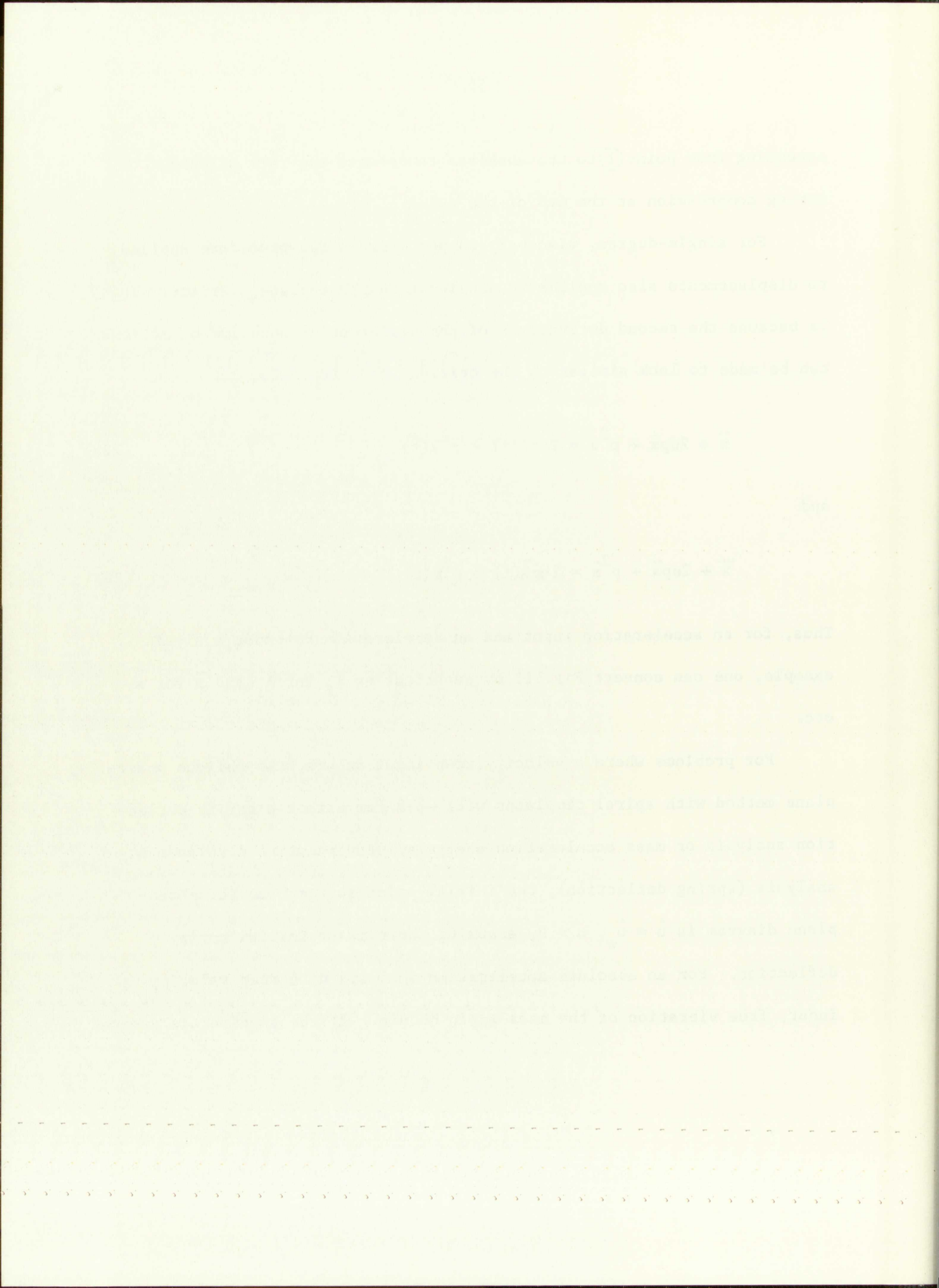
$$\ddot{x} + 2\zeta p \dot{x} + p^2 x = 2\zeta p \dot{\lambda}(t) + p^2 \lambda(t) \quad (22a)$$

and

$$\ddot{\ddot{x}} + 2\zeta p \ddot{\dot{x}} + p^2 \ddot{x} = 2\zeta p \ddot{\dot{\lambda}}(t) + p^2 \ddot{\lambda}(t) \quad (26)$$

Thus, for an acceleration input and an acceleration response analysis example, one can convert Fig. 17 by substituting  $\ddot{\lambda}_i$  for  $\lambda_i$  and  $\ddot{x}$  for  $x$ , etc.

For problems where a velocity step input occurs, the oblique phase-plane method with spiral templates will work for either a spring deflection analysis or mass acceleration analysis. For relative displacement analysis (spring deflection), the initial point at  $t = 0$  on the phase-plane diagram is  $\dot{u} = \dot{u}_*$ ,  $u = 0$ , assuming there is no initial spring deflection. For an absolute acceleration analysis with step velocity input, free vibration of the mass again occurs. If the specimen is dropped





onto the floor and no relative motion occurs before impact,  $x_0 = 0$  and  $\dot{x} = \dot{x}_0$ , so the initial starting conditions for  $\ddot{x}_0$  and  $\ddot{\ddot{x}}_0$  are

$$\ddot{x}_0 = -2vp\dot{x}_0, \quad (27)$$

$$\ddot{\ddot{x}}_0 = -2vp\ddot{x}_0 - p^2\dot{x}_0, \quad (28)$$

or

$$\ddot{\ddot{x}}_0 = p^2(4v^2 - 1)\dot{x}_0. \quad (28a)$$

Eqs. 27-28a are derived from Eq. 22 for  $\lambda(t) = 0$ .

If the specimen is initially at rest and the support receives a sudden change in velocity,  $\dot{\lambda}_0$ , then on the phase-plane diagram the initial points for  $\ddot{x}_0$  and  $\ddot{\ddot{x}}_0$  are

$$\ddot{x}_0 = 2vp\dot{\lambda}_0 \quad (29)$$

and

$$\ddot{\ddot{x}}_0 = -p^2(4v^2 - 1)\dot{\lambda}_0. \quad (30)$$

Eqs. 29 and 30 are derived from Eq. 22 for  $\dot{\lambda}(t) = \dot{\lambda}_0$ .

A single-degree system that has both viscous and coulomb damping combined can be solved by the two methods shown above. The only requirement is to know how much  $v$  and  $\Delta_c$  are present. If one could vibrate a



(13)

(14)

(15)

(16)

test item at resonance and suddenly reduce the input amplitude to zero and observe the type of decay, some insight as to values of  $\nu$  and  $\Delta_c$  might be gained. Generally speaking, viscous friction is more pronounced during the first few swings of the responsive motion while dry friction is more prevalent during the latter swings.





## V. PHASE-PLANE ANALYSIS - MULTIDEGREE SYSTEMS

### 1. Undamped Systems

Fortunately the method utilizing displacement inputs and displacement responses is suitable for multidegree system adaptation. The method requires the use of principal coordinates, however. For a general two-degree undamped system arrangement such as shown in Fig. 1, the differential equations of motion are (in rectangular coordinates)

$$m_1 \ddot{x} = k_1 [\lambda(t) - x] + k_2 [y - x] \quad (31a)$$

$$m_2 \ddot{y} = k_3 [\lambda(t) - y] + k_2 [x - y] . \quad (31b)$$

By the proper selection of coordinates, Eqs. 31a and 31b can be rewritten in a form in which they are independent of each other. Instead of indicating the configuration of an undamped system in Fig. 1 by use of coordinates  $x$  and  $y$ , the configuration can be described in principal coordinates by two principal modes of vibration,  $\theta_I$ , and  $\theta_{II}$ . During either principal mode of vibration, the two coordinates  $x$  and  $y$  are represented by harmonic functions of the same period and phase and have amplitudes in a certain constant ratio. To show this, consider a free vibration of system in Fig. 1, no damping. Eq. 31 would become

$$m_1 \ddot{x} + (k_1 + k_2)x - k_2 y = 0 \quad (32a)$$

# 2. ANALYTICAL SOLUTION OF THE PROBLEM

## 2.1. Generalized coordinates

Consequently, the method of generalized coordinates and displacement is suitable for solving the problem. The method requires the use of generalized coordinates, however, for a general two-degree-of-freedom system, such as shown in Fig. 1, the differential equations of motion are (for rectangular coordinates)

$$m_1 \ddot{x}_1 + k_1(x_1 - x_2) + k_2(x_1 - y) = 0 \quad (2.1)$$

$$m_2 \ddot{x}_2 + k_1(x_2 - x_1) + k_2(x_2 - y) = 0 \quad (2.2)$$

By the proper selection of coordinates, Eqs. 2.1 and 2.2 can be written in a form in which they are independent of each other. Instead of indicating the configuration of an undamped system in Fig. 1 by use of

coordinates  $x$  and  $y$ , the configuration can be described in terms of coordinates  $q_1$  and  $q_2$ , the generalized coordinates. During motion, the generalized coordinates  $q_1$  and  $q_2$  are related to the coordinates  $x$  and  $y$  by the relations  $q_1 = x$  and  $q_2 = x - y$ . The coordinates  $q_1$  and  $q_2$  are independent of each other. To show this, consider a free vibration of system in Fig. 1, as depicted. Let  $q_1$  and  $q_2$  be the

$$m_1 \ddot{q}_1 + k_1(q_1 - q_2) + k_2(q_1 - y) = 0 \quad (2.3)$$



$$m_2 \ddot{y} + (k_2 + k_3)y - k_2 x = 0 . \quad (32b)$$

A possible solution for Eq. 32 is

$$x = X \cos pt \quad (33a)$$

$$y = Y \cos pt , \quad (33b)$$

which is one of the conditions necessary to describe motion in principal coordinates.

Differentiation of Eq. 33 and substitution into Eq. 32 shows that

$$-p^2 X m_1 + (k_1 + k_2)X - k_2 Y = 0 \quad (34a)$$

$$-p^2 Y m_2 + (k_2 + k_3)Y - k_2 X = 0 , \quad (34b)$$

from which it must follow that

$$\frac{Y}{X} = \alpha = \frac{k_1 + k_2 - m_1 p^2}{k_2} = \frac{k_2}{k_2 + k_3 - m_2 p^2} . \quad (35)$$

Eq. 35 shows the constant amplitude ratio for harmonic functions of Eq. 33. Thus, a second condition for principal coordinates is satisfied.





Solving for  $p^2$  from Eq. 35,

$$p^2 = \frac{1}{2} \left\{ \left( \frac{k_1 + k_2}{m_1} + \frac{k_2 + k_3}{m_2} \right) \pm \left[ \left( \frac{k_1 + k_2}{m_1} + \frac{k_2 + k_3}{m_2} \right)^2 - 4 \left( \frac{k_1 k_2 + k_1 k_3 + k_2 k_3}{m_1 m_2} \right) \right]^{1/2} \right\}. \quad (36)$$

There are thus two solutions for  $p^2$ . For lower root (lower mode),  $p^2 = p_I^2$ , and therefore  $\alpha = \alpha_I$ . For the higher root (higher mode),  $p^2 = p_{II}^2$  and  $\alpha = \alpha_{II}$ . Therefore, from Eqs. 35 and 33, it can be said that  $x_I = \theta_I$  for lowest mode and  $x_{II} = \theta_{II}$  for second mode;  $y_I = \alpha_I \theta_I$  for lowest mode and  $y_{II} = \alpha_{II} \theta_{II}$  for second mode where  $\theta_I$  and  $\theta_{II}$  are independent principal coordinates.

Substituting  $x_I = \theta_I$ ,  $y_I = \alpha_I \theta_I$  and their derivatives into either Eq. 32a or Eq. 32b produces the following equation

$$\ddot{\theta}_I + p_I^2 \theta_I = 0 \quad (\text{lower mode}). \quad (37a)$$

In the substitution

$$\alpha_I = \frac{k_1 + k_2 - m_1 p_I^2}{k_2}$$

which was found from Eq. 35. In similar fashion, it can be shown that

$$\ddot{\theta}_{II} + p_{II}^2 \theta_{II} = 0 \quad (\text{higher mode}) \quad (37b)$$





when  $x_{II} = \theta_{II}$ ,  $y_{II} = a_{II} \theta_{II}$  and their derivatives are substituted into either Eq. 32a or Eq. 32b, where

$$a_{II} = \frac{k_2}{k_2 + k_3 - m_2 p_{II}^2}.$$

Eq. 37 is in the form which indicates that a graphical solution by phase-plane techniques is possible. Each mode is independent of the other.

The question now arises as to how the principal coordinates can be converted to, say, rectangular coordinates or vice versa in order to utilize the phase plane. By superposing  $\theta$ 's, the principal coordinates for the general case of linear systems, it can be said that

$$x = \theta_I + \theta_{II} \quad (38a)$$

$$y = a_I \theta_I + a_{II} \theta_{II}. \quad (38b)$$

Phase planes normally would be constructed in principal coordinates.

The relationship that exists between principal and rectangular coordinates of an external excitation depends upon the physical setup of the specimen. The general theoretical solution of Eq. 31 expressed in the form of Eq. 38 when there is support excitation is

$$x = \left[ A_I \cos p_I t + B_I \sin p_I t + H_I \xi(t) \right] \\ + \left[ A_{II} \cos p_{II} t + B_{II} \sin p_{II} t + H_{II} \eta(t) \right] \quad (39a)$$





$$y = a_I \left[ A_I \cos p_I t + B_I \sin p_I t + H_I \xi(t) \right] + a_{II} \left[ A_{II} \cos p_{II} t + B_{II} \sin p_{II} t + H_{II} \eta(t) \right], \quad (39b)$$

where  $A_I$ ,  $A_{II}$ ,  $B_I$ ,  $B_{II}$  are undetermined modal constants involving initial conditions,

$H_I$ ,  $H_{II}$  = constants dependent upon the system configuration to describe external excitation in principal coordinates,

$\xi(t)$ ,  $\eta(t)$  = expressions of the response of each mass in each mode due entirely to the type excitation of the support.

In a single-degree system the equivalence of  $\xi(t)$  and  $\eta(t)$  would be  $\gamma'(t)$ , from which the phase-plane gets its input information, e.g.,

$$\gamma'(t) = \lambda_i \left[ 1 - \cos p t_i \right]. \quad (40)$$

From Eq. 31, assume  $\lambda_i$  is applied to a system at rest and is constant during interval  $t_1$ . In a two-degree system  $\xi(t)_1$  during the step describes the responsive motion of the lowest mode in rectangular coordinates, while  $\eta(t)_1$  describes the motion of the second mode in rectangular coordinates.



$$\left. \begin{aligned} \dot{x}_1 &= A_{11}x_1 + A_{12}x_2 + B_1u \\ \dot{x}_2 &= A_{21}x_1 + A_{22}x_2 + B_2u \end{aligned} \right\}$$

where  $A_{11}, A_{12}, A_{21}, A_{22}$  are system matrices and  $B_1, B_2$  are input matrices.

conditions

$$A_{11}, A_{21} = \text{constant dependent upon the system configuration}$$

to describe external excitation is periodic

continuous

$\dot{x}_1, \dot{x}_2$  a representation of the response of each mode in each

mode due entirely to the type excitation of the

system

In a single-degree system the equivalent of  $\dot{x}_1$  and  $\dot{x}_2$  would be

$\dot{x}_1(t)$ , from which the phase-plane plot is also obtained, e.g.,

(40)

$$\dot{x}_1(t) = A_1 \dot{x}_1 + \cos \omega t$$

From Fig. 11, assume  $A_1$  is applied to a system at rest and is

constant during interval  $t_1$ . In a two-degree system  $\dot{x}_1(t)$ , during the

same interval the response of the lowest mode is sinusoidal

oscillations, while the response of the second mode is

transient oscillations.

During the first step, then,

$$\xi(t)_1 = \lambda_1(1 - \cos p_I t_1) \quad (41a)$$

$$\eta(t)_1 = \lambda_1(1 - \cos p_{II} t_1) . \quad (41b)$$

From the initial conditions of the system at rest

$$A_I = A_{II} = B_I = B_{II} = 0 .$$

During the second step interval,  $t_2$ , where  $\lambda_2$  is applied, the  $\xi(t)$  and  $\eta(t)$  terms of Eq. 39 become

$$\xi(t)_2 = \lambda_2 [1 - \cos p_I t_2] \quad (42a)$$

$$\eta(t)_2 = \lambda_2 [1 - \cos p_{II} t_2] . \quad (42b)$$

The constants  $A_I$ ,  $A_{II}$ ,  $B_I$ ,  $B_{II}$  are no longer zero, but represent the conditions of each mode at the end of the previous step. Note that in Eq. 39 each mode is similar in appearance to a single-degree general solution, e.g.,

$$\theta_I = A_I \cos p_I t_2 + B_I \sin p_I t_2 + H_I \xi(t)_2$$

$$x = x_* \cos p t_2 + \frac{\dot{x}_*}{p} \sin p t_2 + \gamma'(t)_2 , \quad (2a)$$

where  $\gamma'(t)_2 = \lambda_2(1 - \cos p t_2)$  for the single-degree system.





Before the similarity is complete, the values of  $H_I$  and  $H_{II}$  must be evaluated. This can only be done by considering the physical structure of the two-degree system. Since it is known that  $A_I = A_{II} = B_I = B_{II} = 0$  at the beginning of the problem, Eq. 39 finally can be reduced to.

$$x = H_I \lambda_1 (1 - \cos p_I t_1) + H_{II} \lambda_1 (1 - \cos p_{II} t_1) \quad (43a)$$

$$y = \alpha_{II} H_I \lambda_1 (1 - \cos p_I t_1) + \alpha_{II} H_{II} \lambda_1 (1 - \cos p_{II} t_1) \quad (43b)$$

during the first step.

Differentiating Eq. 43 twice and substituting into Eq. 31 and reducing for an arbitrary time selection of  $t = 0$ ,

$$m_1 (H_I p_I^2 + H_{II} p_{II}^2) = k_1 \quad (44a)$$

$$m_2 (\alpha_I H_I p_I^2 + \alpha_{II} H_{II} p_{II}^2) = k_3 \quad (44b)$$

Solving for  $H_I$  and  $H_{II}$

$$H_I = \frac{\frac{k_3}{m_2} - \alpha_{II} \frac{k_1}{m_1}}{p_I^2 (\alpha_I - \alpha_{II})} \quad (45a)$$

$$H_{II} = \frac{\alpha_I \frac{k_1}{m_1} - \frac{k_3}{m_2}}{p_{II}^2 (\alpha_I - \alpha_{II})} \quad (45b)$$





These constants will hold true for any step. Now Eq. 39 can be expressed for the step interval as

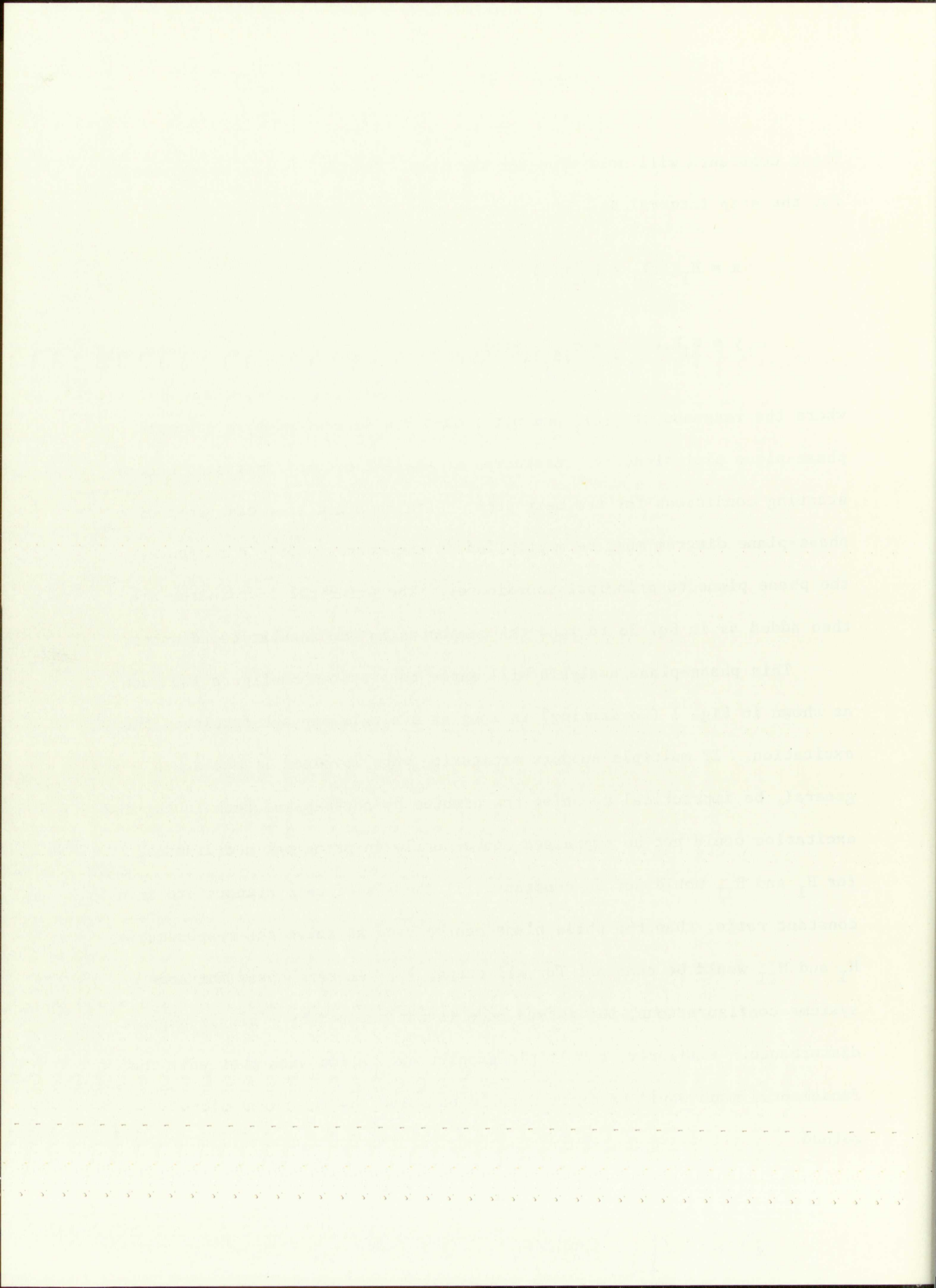
$$x = H_I \xi(t)_1 + H_{II} \eta(t)_1 \quad (46a)$$

$$y = \alpha_I H_I \xi(t)_I + \alpha_{II} H_{II} \eta(t)_I, \quad (46b)$$

where the response of  $\xi(t)_1$  and  $\eta(t)_1$  each are determined by a separate phase-plane plot directly. Responses at the end of the first step become starting conditions for the next step. Data obtained from each step of a phase-plane diagram must be multiplied by the corresponding  $H$  to convert the phase plane to principal coordinates. The principal coordinates are then added as in Eq. 38 to find the responses in rectangular coordinates.

This phase-plane analysis will apply to a system configuration such as shown in Fig. 1 (no damping) as long as a single support furnishes the excitation. If multiple support excitation were involved it would, in general, be impractical to solve the problem by phase-plane techniques; the excitation could not be expressed conveniently in principal coordinates, for  $H_I$  and  $H_{II}$  would not be constant. If the  $\lambda$ 's of each support are in a constant ratio, then the phase plane can be used to solve the responses;  $H_I$  and  $H_{II}$  would be constant for all steps,  $\lambda_1$ . In rare cases for some systems configurations, the second mode is not excited by a single support disturbance. Similarly, a multiple support excitation such that only the fundamental mode would be excited could be solved by the phase-plane method.





Finding any spring deflection when the support has a known input acceleration cannot be done directly in multidegree systems. For the two-degree system of Fig. 1, let spring  $k_1$  deflection be  $u_1$ , spring  $k_2$  deflection be  $u_2$ , and spring  $k_3$  deflection be  $u_3$ .

Now

$$x - \lambda = u_1 \quad (47a)$$

$$y - \lambda = u_3 \quad (47b)$$

$$x - y = u_2 \quad (47c)$$

Differentiating Eq. 47, substituting into Eq. 31, and rearranging terms,

$$m_1 \ddot{u}_1 + k_1 u_1 - k_2 u_2 = -m_1 \ddot{\lambda}(t) \quad (48a)$$

$$m_2 \ddot{u}_3 + k_3 u_3 - k_2 u_2 = -m_2 \ddot{\lambda}(t) \quad (48b)$$

Eq. 48 is not suitable for a phase-plane representation because of the three variables involved.

When the support is subjected to an acceleration input, the acceleration responses of each mass can be solved by a simple extension of the displacement phase-plane analysis. All values of displacement are replaced by acceleration values, i.e.,  $\lambda_1$  by  $\ddot{\lambda}_1$ ;  $x_1$  by  $\ddot{x}_1$ , etc. An example problem illustrates the method to solve the acceleration response of each mass of a two-degree undamped system when the support of the system has a known acceleration-time input.

(A7a)

$$x = z + u$$

(A7b)

$$y = z + u$$

(A7c)

$$x = z + u$$

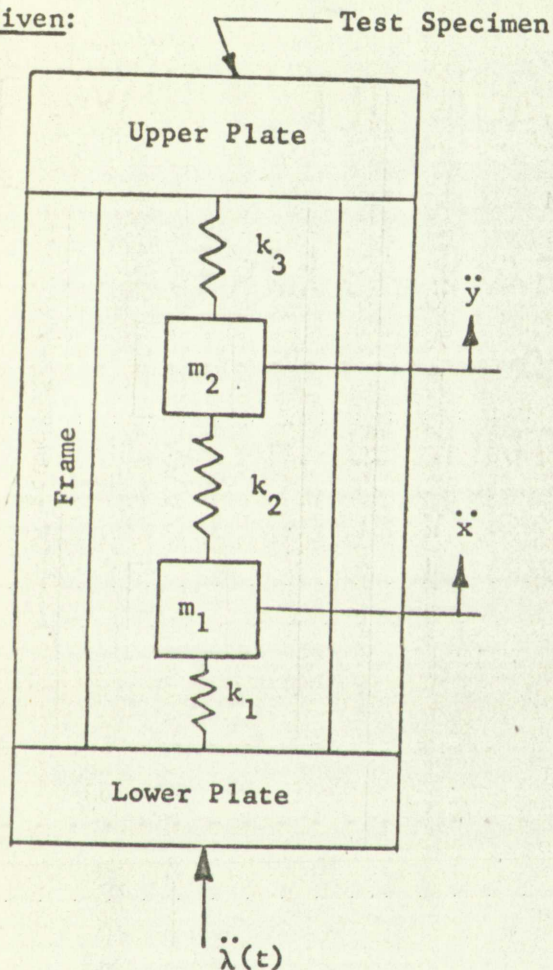
(A8a)

$$u_1 \ddot{x}_1 + k_1 u_1 = -u_1 \ddot{x}_1$$

(A8b)

$$u_2 \ddot{x}_2 + k_2 u_2 = -u_2 \ddot{x}_2$$



Example ProblemGiven:

$$\ddot{\lambda}(t) = \text{half sine pulse}$$

Maximum  
amplitude = 100 g

Duration  
at base = 8 ms

$$k_1 = 96 \text{ lbs/inch}$$

$$k_2 = 96 \text{ lbs/inch}$$

$$k_3 = 192 \text{ lbs/inch}$$

$$m_1 = 5.1 \times 10^{-4} \text{ lb-sec}^2/\text{inch}$$

$$m_2 = 2.55 \times 10^{-4} \text{ lb-sec}^2/\text{inch}$$

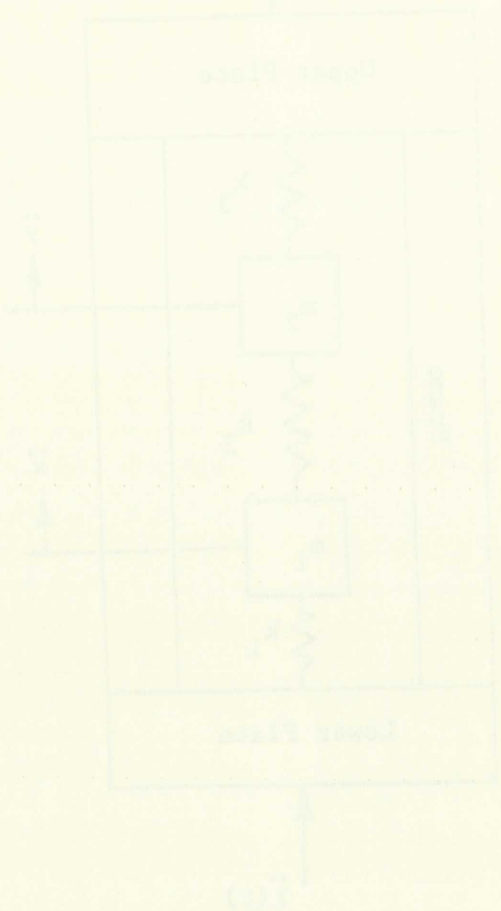
Initial acceleration and jerk of  
each mass is zero at start of  
shock pulse.

Problem: Determine, respectively, the acceleration-time history  $\ddot{x}$  and  $\ddot{y}$  of  $m_1$  and  $m_2$  for a period of 24 ms.

Solution: To draw the phase-plane diagrams for each mode and to convert data to rectangular coordinates, the following constants must be evaluated:

$p_I$  and  $p_{II}$  = two principal modes of vibration (two natural frequencies)

Figure 1. Test Specimen



$\dot{x}(t) = \text{half sine pulse}$

Maximum  
amplitude = 100 g

Duration  
at base = 8 ms

$\dot{x}_1 = 55 \text{ in/sec}$

$\dot{x}_2 = 55 \text{ in/sec}$

$\dot{x}_3 = 155 \text{ in/sec}$

$\dot{x}_4 = 5.1 \times 10^{-4} \text{ in-sec}^2/\text{in}$

$\dot{x}_5 = 1.55 \times 10^{-4} \text{ in-sec}^2/\text{in}$

Initial acceleration and jerk of

each mass is zero at start of

shock pulse.

Following description, respectively, the acceleration-time history  $\ddot{x}$  and  $\dot{x}$

of  $\dot{x}_1$  and  $\dot{x}_2$  for a period of 25 ms

Following the data the phase-plane diagrams for each mode and to construct

data to rectangular coordinates, the following constants must

be evaluated:

$\ddot{x}_1$  and  $\ddot{x}_2$  = the principal modes of vibration (two natural

frequencies)



$\alpha_I$  and  $\alpha_{II}$  = amplitude ratio of the two masses at the two natural frequencies.

$H_I$  and  $H_{II}$  = conversion factors to describe rectangular coordinates of excitation into principal coordinates for system shown.

From Eq. 36,

$$\left. \begin{matrix} p_I^2 \\ p_{II}^2 \end{matrix} \right\} = \frac{1}{2} \left\{ \left( \frac{k_1 + k_2}{m_1} + \frac{k_2 + k_3}{m_2} \right) \pm \left[ \left( \frac{k_1 + k_2}{m_1} + \frac{k_2 + k_3}{m_2} \right)^2 - 4 \left( \frac{k_1 k_2 + k_2 k_3 + k_1 k_3}{m_1 m_2} \right) \right]^{1/2} \right\}. \quad (36a)$$

For convenience let  $m_2 = \frac{1}{2} m_1 = m$ ;  $k_1 = k_2 = \frac{1}{2} k_3 = k$ .

Eq. 36a becomes

$$\left. \begin{matrix} p_I^2 \\ p_{II}^2 \end{matrix} \right\} = \frac{1}{2} \left\{ \left( \frac{2k}{2m} + \frac{3k}{m} \right) \pm \left[ \left( \frac{4k}{m} \right)^2 - 4 \left( \frac{5k^2}{2m^2} \right) \right]^{1/2} \right\} \quad (49)$$

$$= \frac{(0.775)k}{(3.225)m}.$$

By substituting  $k = 96$  lbs/in;  $m = 2.55 \times 10^{-4}$  lb-sec<sup>2</sup>/inch,

$$p_I = 0.54 \text{ rad/ms}$$

$$p_{II} = 1.10 \text{ rad/ms.}$$



From Eq. 10,

$$\left[ \begin{array}{c} \frac{z}{p_I} \\ \frac{z}{p_{II}} \end{array} \right] = -\frac{1}{2} \left( \frac{1 + \frac{z}{p_I} + \frac{z}{p_{II}}}{\frac{z}{p_I}} \right)$$

$$\left( \frac{1 + \frac{z}{p_I} + \frac{z}{p_{II}}}{\frac{z}{p_I}} \right)$$

Eq. 10 becomes

$$\left[ \begin{array}{c} \frac{z}{p_I} \\ \frac{z}{p_{II}} \end{array} \right] = -\frac{1}{2} \left( \frac{1 + \frac{z}{p_I} + \frac{z}{p_{II}}}{\frac{z}{p_I}} \right)$$

$$= \left( \frac{0.735}{1.025} \right)$$

h. Constructing  $k = 95$  lb/in.

$$p_I = 0.34 \text{ inches}$$

$$p_{II} = 1.10 \text{ inches}$$

From Eq. 35,

$$\alpha_I = \frac{k}{3k - m(0.775) \frac{k}{m}} = 0.449$$

$$\alpha_{II} = \frac{k}{3k - m(3.225) \frac{k}{m}} = -4.44 .$$

From Eq. 45,

$$H_I = \frac{\frac{2k}{m} - \alpha_{II} \frac{k}{2m}}{0.775 \left( \frac{k}{m} \right) (\alpha_I - \alpha_{II})} = 1.115$$

$$H_{II} = \frac{\alpha_I \frac{k}{2m} - \frac{2k}{m}}{3.225 \left( \frac{k}{m} \right) (\alpha_I - \alpha_{II})} = -0.113 .$$

It is interesting to note that the exact values of the  $k$ 's and  $m$ 's are not needed to find the constants  $\alpha$  and  $H$ ; only their ratios are needed. This fact permits a model to be studied instead of an actual system.

Eq. 46 now appears,

$$\ddot{x} = 1.115\ddot{\xi}(t) - 0.113\ddot{\eta}(t)$$

$$\ddot{y} = 0.50\ddot{\xi}(t) + 0.501\ddot{\eta}(t) .$$

(50)

From the two phase-plane diagrams,  $\ddot{\xi}(t)$  and  $\ddot{\eta}(t)$  values are found first; values of  $\ddot{x}$  and  $\ddot{y}$  must then be calculated.





The natural period of each mode,  $T_I$  and  $T_{II}$ , can be found from the equations

$$T_I = \frac{2\pi}{P_I} \text{ and } T_{II} = \frac{2\pi}{P_{II}} .$$

Therefore,

$$T_I = 11.6 \text{ ms}$$

and

$$T_{II} = 5.7 \text{ ms.}$$

If the input pulse duration,  $t_d$ , is 8 ms, then

$$\frac{t_d}{T_I} = 0.69$$

and

$$\frac{t_d}{T_{II}} = 1.4 .$$

These ratios are in the range where the maximum response condition of each mode is approached. Therefore, as previously mentioned for single-degree undamped systems, the size of each step required for each phase-plane diagram is dependent upon the input pulse shape and accuracy desired. For the ratios of  $\frac{t_d}{T_I}$  and  $\frac{t_d}{T_{II}}$  found for this problem, a step

The natural period  $T_n$  and  $T_d$  are found from the

equations

$$T_n = \frac{2\pi}{\omega_n} \text{ and } T_d = \frac{2\pi}{\omega_d}$$

Therefore,

$$T_n = 11.6 \text{ ms}$$

and

$$T_d = 1.7 \text{ ms}$$

If the input pulse duration,  $t_p$ , is 5 ms, then

$$\frac{t_p}{T_n} = 0.69$$

and

$$\frac{t_p}{T_d} = 2.94$$

These ratios are in the range where the maximum response condition of

each mode is approached. Therefore, as previously mentioned for single

degree undamped systems, the aim of each step repeated for each

plane diagram is dependent upon the input pulse shape and frequency

desired. For the ratios of  $\frac{t_p}{T_n}$  and  $\frac{t_p}{T_d}$  found for this problem, a



interval approximately equal to 1/10 of each mode natural period was considered satisfactory. Therefore, for mode I, equal step intervals,  $t_i$ , of 1.0 ms were selected; for mode II, equal step intervals of 0.5 ms were selected. Since the angle for each step of the phase-plane diagram is  $p t_i$ , mode I angle was

$$p_I t_i = 0.54(1.0) = 0.54 \text{ rad} = 31.0 \text{ degrees.}$$

For mode II, each angle was

$$p_{II} t_i = 1.10(0.5) = 0.55 \text{ rad} = 31.5 \text{ degrees.}$$

In Fig. 19, the half-sine input pulse of the support and the equivalent step amplitudes for determining the various phase-plane centers are shown.

The phase-plane constructions for both modes are shown in Fig. 20. Values of  $\ddot{\xi}(t)_i$  and  $\ddot{\eta}(t)_i$  at 1-ms intervals were taken and  $\ddot{x}$  and  $\ddot{y}$  calculated in Table III using Eq. 50.

The accuracy of the phase-plane diagram of each mode was checked against the half-sine normalized shock spectra for a single-degree system shown in Ref. (11), page 59. This could be done since each mode separately of a two-degree system behaves just as a single-degree system. (Refer to Eqs. 1 and 37.) The primary spectra shown in Ref. (11) indicated the maximum response of both mode I and mode II that could be expected during



## 2 - DEG. SYSTEM

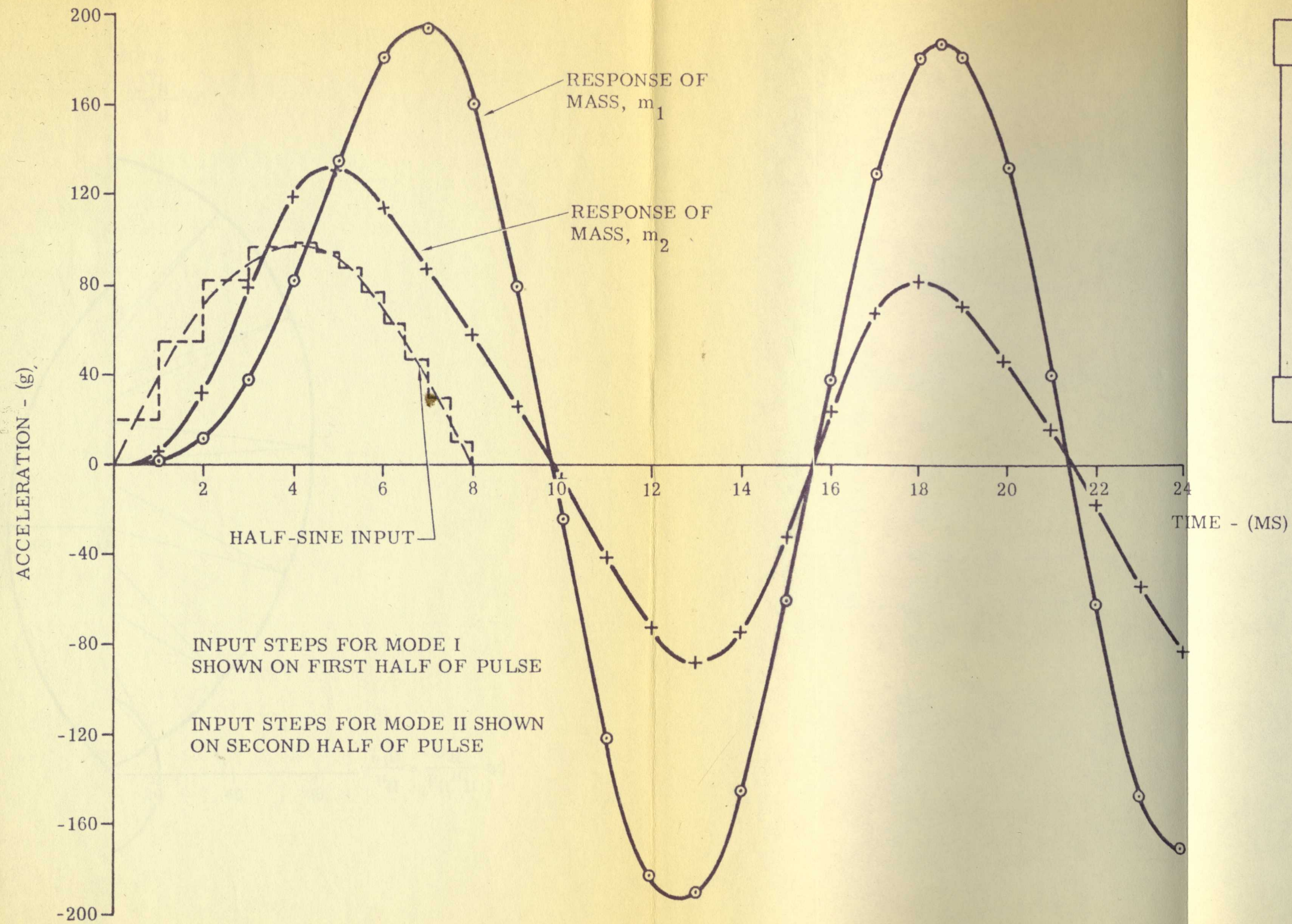
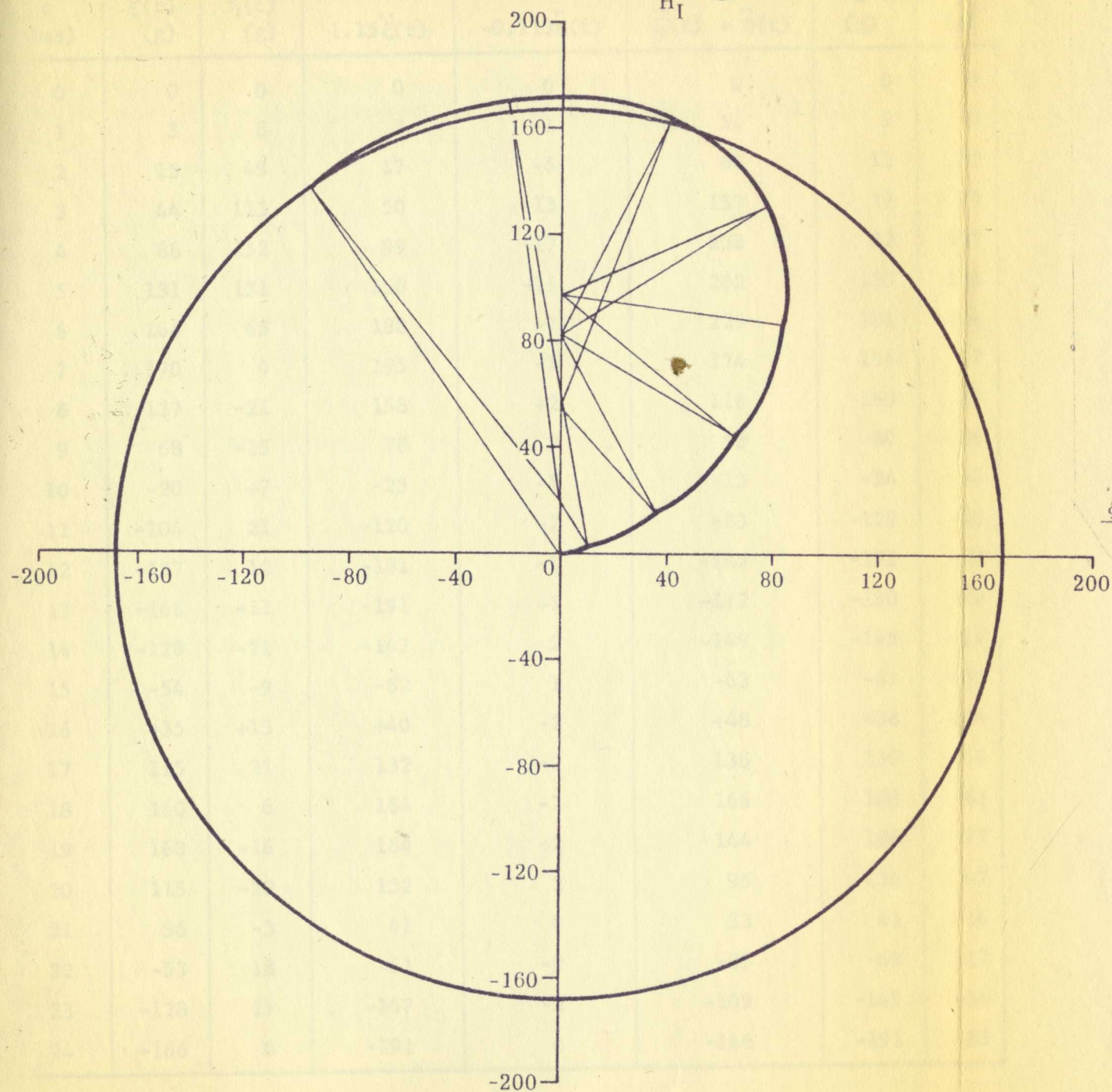


Figure 19 Acceleration-Time Response of Each Mass of an Undamped Two-Degree System to a Half-Sine Shock Pulse, 100g, 8 MS



PHASE PLANE - MODE I

$$\ddot{\xi}(t) = \frac{\ddot{\theta}_I}{H_I} \text{ (g)}$$



PHASE PLANE - MODE II

$$\ddot{\eta}(t) = \frac{\ddot{\theta}_{II}}{H_{II}} \text{ (g)}$$

$$\frac{\ddot{\xi}(t)}{p_I} = \frac{\ddot{\theta}_I}{p_I H_I} \text{ (g)}$$

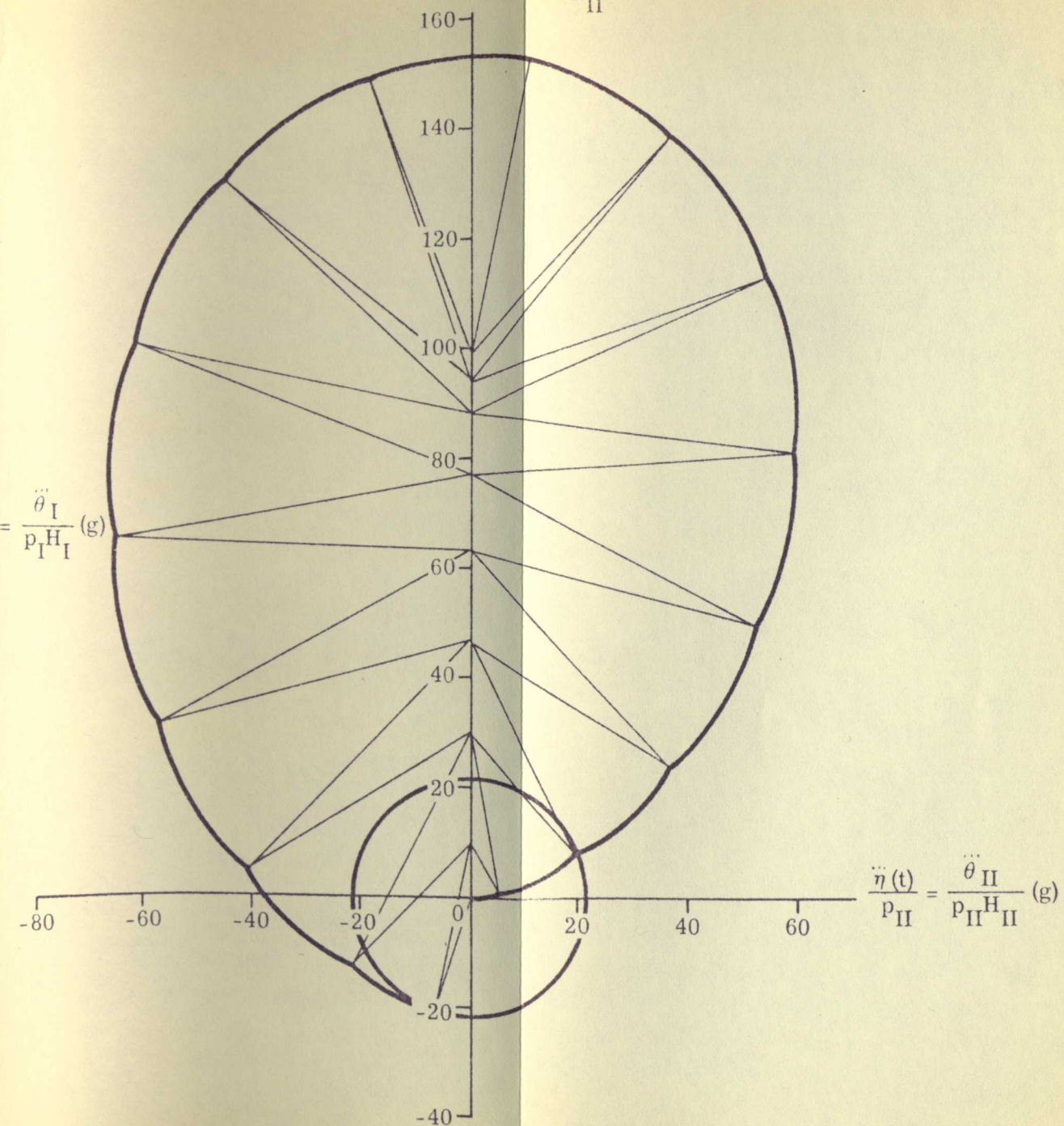


Figure 20 Phase-Plane Diagrams for Two-Degree Undamped System Having Support Excitation







TABLE III

DETERMINATION OF  $\ddot{x}$  AND  $\ddot{y}$ 

$t$ (ms)	$\ddot{\xi}(t)$ (g)	$\ddot{\eta}(t)$ (g)	$1.15\ddot{\xi}(t)$	$-0.113\ddot{\eta}(t)$	$\ddot{\xi}(t) + \ddot{\eta}(t)$	$\ddot{x}$ (g)	$\ddot{y}$ (g)
0	0	0	0	0	0	0	0
1	3	8	3	-1	11	2	6
2	15	49	17	-6	64	11	32
3	44	113	50	-13	157	37	79
4	86	152	99	-17	238	82	119
5	131	131	150	-15	262	135	131
6	164	65	188	-7	229	181	114
7	170	4	195	-1	174	194	87
8	137	-21	158	+2	116	160	58
9	68	-15	78	2	53	80	26
10	-20	+7	-23	-1	-13	-24	-6
11	-104	21	-120	-2	-83	-122	-42
12	-157	12	-181	-1	-145	-182	-72
13	-166	-11	-191	+1	-177	-190	-88
14	-128	-21	-147	2	-149	-145	-74
15	-54	-9	-62	1	-63	-61	-31
16	+35	+13	+40	-2	+48	+38	+24
17	115	21	132	-2	136	130	68
18	160	6	184	-1	166	183	83
19	160	-16	184	+2	144	186	72
20	115	-20	132	2	95	134	47
21	36	-3	41	0	33	41	16
22	-53	18	-61	-2	-35	-63	-17
23	-128	19	-147	-2	-109	-149	-54
24	-166	0	-191	0	-166	-191	-83





the time of the input pulse; the residual spectra indicated the maximum response to be expected of either mode after the half-sine pulse was over. Very good agreement was found between each mode and the shock spectra.

The response histories of  $m_1$  and  $m_2$  are shown in Fig. 19. They were checked at three points against an analytical solution presented in Ref. (2), page 344. The analytical solution as presented therein had to be modified slightly. The following substitutions were made:

$$F_1 = k_1 \lambda \sin \omega t \text{ and } F_2 = k_3 \lambda \sin \omega t ,$$

where  $F$ 's were forcing functions applied to each mass, and

$$\omega = \frac{\pi}{t_d} \text{ for } 0 \leq t \leq \frac{\pi}{\omega} .$$

The analytical solution for the example problem became after differentiating twice,

$$\begin{aligned} \ddot{x} &= -173 \sin 0.54t + 4.6 \sin 1.1t + 225 \sin 0.393t \\ \ddot{y} &= -77.7 \sin 0.54t - 20.4 \sin 1.1t + 164 \sin 0.393t . \end{aligned} \tag{51}$$



The aim of the present work is to study the properties of the

response of the system to various inputs and to the effect of

various parameters on the response. The results are presented in

figures.

The response curves of  $\eta$  and  $\alpha$  are shown in Fig. 1. They

were obtained by numerical solution of the equations presented

in Ref. (2), page 36. The analytical solution as presented therein

had to be modified slightly. The following substitutions were made

$$M_1 = 1.5 \text{ cm wt and } M_2 = 1.5 \text{ cm wt}$$

where  $M_1$  was the limiting function applied to each case, and

$$\alpha = \frac{h}{b} \text{ for } 0 \leq \alpha \leq \frac{\pi}{2}$$

The analytical solution for the simple problem became after all

the following:

$$\eta = 1.12 \sin 0.205 + 0.14 \sin 1.11 + 0.32 \sin 0.393$$

(2)

$$\alpha = 1.71 \sin 0.141 + 0.14 \sin 1.11 + 1.04 \sin 0.393$$

Comparisons of  $\ddot{x}$  and  $\ddot{y}$  were made at  $t = 3, 6, 8$  ms;  $\ddot{\ddot{x}}$  and  $\ddot{\ddot{y}}$  at  $t = 8$  ms. The results are shown below

Time (ms)	Phase-Plane		Analytical	
	$\ddot{x}$ (g)	$\ddot{y}$ (g)	$\ddot{x}$ (g)	$\ddot{y}$ (g)
3	37	79	34	78
6	181	114	177	117
8	160	58	162	60
<hr/>				
	$\ddot{\ddot{x}}$ (g/ms)	$\ddot{\ddot{y}}$ (g/ms)	$\ddot{\ddot{x}}$ (g/ms)	$\ddot{\ddot{y}}$ (g/ms)
8	-57	-29	-56	-30

After  $t = 8$  ms, the phase-plane center of each mode stays at 0, so there should be no great error occurring after that time. (END OF EXAMPLE PROBLEM)

In solving for acceleration responses,  $\ddot{x}$  and  $\ddot{y}$ , of each mass when the support has a sudden velocity change, the initial starting point of each phase-plane diagram is not at the origin. At  $t = 0$ , the acceleration of each mass is zero, but the jerk is not.

Assume the condition where a two-degree system is moving at constant velocity,  $V_1$ , and the support is suddenly brought to rest. At  $t = 0$ ,

$$x_0 = y_0 = 0; \dot{x}_0 = \dot{y}_0 = -|V_1|.$$





If  $x_0$  and  $y_0$  represent the equilibrium point of the system, then  $\ddot{x}_0 = \ddot{y}_0 = 0$  at  $t = 0$ . Therefore, the phase-plane trajectories must start on the jerk axes,  $\ddot{\theta}_I/p_I$  and  $\ddot{\theta}_{II}/p_{II}$ .

Eqs. 39 must be used to solve for  $\text{jerk}_I (\ddot{\theta}_I)$  and  $\text{jerk}_{II} (\ddot{\theta}_{II})$ .

For this problem, Eq. 39 becomes

$$x = B_I \sin p_I t + B_{II} \sin p_{II} t \quad (39c)$$

$$y = \alpha_I B_I \sin p_I t + \alpha_{II} B_{II} \sin p_{II} t, \quad (39d)$$

where

$$p_I B_I = \frac{\dot{y}_0 - \alpha_{II} \dot{x}_0}{\alpha_I - \alpha_{II}}; \quad p_{II} B_{II} = \frac{\alpha_I \dot{x}_0 - \dot{y}_0}{\alpha_I - \alpha_{II}}.$$

$(p_I B_I)$  and  $(p_{II} B_{II})$ , respectively, are the starting velocities of each mode ( $\dot{\theta}_I$  and  $\dot{\theta}_{II}$ ) of the displacement phase-plane diagrams  $(\theta_I, \dot{\theta}_I/p_I)$  and  $(\theta_{II}, \dot{\theta}_{II}/p_{II})$  of the system. Since each mode acts as a single-degree system, it can be said that  $(-p_I^3 B_I)$  is the starting jerk ( $\ddot{\theta}_I$ ) for the lower mode phase plane, while  $(-p_{II}^3 B_{II})$  is the starting jerk ( $\ddot{\theta}_{II}$ ) for the upper mode phase plane.

Thus,

$$-p_I^3 B_I = -p_I^2 \left( \frac{\dot{y}_0 - \alpha_{II} \dot{x}_0}{\alpha_I - \alpha_{II}} \right) = \ddot{\theta}_I \quad (52a)$$

$$-p_{II}^3 B_{II} = -p_{II}^2 \left( \frac{\alpha_I \dot{x}_0 - \dot{y}_0}{\alpha_I - \alpha_{II}} \right) = \ddot{\theta}_{II}, \quad (52b)$$





or for the example assumed where

$$\dot{x}_0 = \dot{y}_0 = -|V_1| \text{ at } t = 0 ,$$

$$\ddot{\theta}_I = p_I^2 |V_1| \left( \frac{1 - \alpha_{II}}{\alpha_I - \alpha_{II}} \right) \quad (52c)$$

$$\ddot{\theta}_{II} = p_{II}^2 |V_1| \left( \frac{\alpha_I - 1}{\alpha_I - \alpha_{II}} \right) . \quad (52d)$$

To convert acceleration values from the phase planes principal coordinates during free vibration, namely

$$\left( \ddot{\theta}_I, \frac{\ddot{\theta}_I}{p_I} \text{ and } \ddot{\theta}_{II}, \frac{\ddot{\theta}_{II}}{p_{II}} \right)$$

to rectangular coordinates,  $\ddot{x}$  and  $\ddot{y}$ , the relationships

$$\ddot{x} = \ddot{\theta}_I + \ddot{\theta}_{II} \quad (38c)$$

$$\ddot{y} = \alpha_I \ddot{\theta}_I + \alpha_{II} \ddot{\theta}_{II} \quad (38d)$$

are used. Eqs. 38c and 38d were obtained by differentiating Eqs. 38a and 38b twice.

As an example of how to locate the starting point on each phase-plane diagram, refer to the example problem on page 67. Assume the test specimen is dropped from a height of 1 foot onto a hard concrete



(32a)

$$\vec{v}_1 = \frac{1}{\sqrt{2}} \begin{pmatrix} 1 \\ 1 \end{pmatrix}$$

(32b)

$$\vec{v}_2 = \frac{1}{\sqrt{2}} \begin{pmatrix} 1 \\ -1 \end{pmatrix}$$

To convert acceleration values from the phase principal

coordinates during free vibration, namely

$$\begin{pmatrix} \ddot{x} \\ \ddot{y} \end{pmatrix} = \frac{1}{\sqrt{2}} \begin{pmatrix} \ddot{u} \\ \ddot{v} \end{pmatrix}$$

to rectangular coordinates,  $\ddot{x}$  and  $\ddot{y}$ , the relationships

(33a)

$$\ddot{x} = \frac{1}{\sqrt{2}} (\ddot{u} + \ddot{v})$$

(33b)

$$\ddot{y} = \frac{1}{\sqrt{2}} (\ddot{u} - \ddot{v})$$

are used. Eqs. 33a and 33b were obtained by differentiating Eqs. 32a

and 32b twice.

As an example of how to locate the starting point on each phase

plane diagram, refer to the example problem on page 64. Assume the

test specimen is dropped from a height of 1 foot onto a hard concrete

surface which the lower plate hits square. Assume a coordinate system where accelerations, velocities, and displacements are positive upward. The velocity of impact,  $V_i = -8$  ft/sec. Knowing the values of the springs and masses,  $\alpha_I$ ,  $\alpha_{II}$ ,  $p_I$ , and  $p_{II}$  can be found from Eqs. 35 and 36. These values are the same as shown in the example; namely,

$$\alpha_I = 0.449; \alpha_{II} = -4.44$$

$$p_I = 0.54 \text{ rad/ms}; p_{II} = 1.10 \text{ rad/ms.}$$

Substituting these values into Eq. 52c and observing correct units,

$$\begin{aligned} \ddot{\theta}_I &= p_I^2 |V_i| \left( \frac{1 - \alpha_{II}}{\alpha_I - \alpha_{II}} \right) \\ &= 10^6 (0.54)^2 (8) \left( \frac{1 + 4.44}{0.449 + 4.44} \right) \end{aligned}$$

$$\ddot{\theta}_I = 2.60 \times 10^6 \text{ ft/sec}^3 .$$

Similarly, from Eq. 52d it can be shown that

$$\ddot{\theta}_{II} = -1.09 \times 10^6 \text{ ft/sec}^3 .$$





To put  $\ddot{\theta}_I$  at time  $t = 0$  on a mode I phase-plane diagram having coordinate axes  $\ddot{\theta}_I$  and  $\ddot{\theta}_I/p_I$ ,  $\ddot{\theta}_I$  must be divided by  $p_I$  or

$$\left. \frac{\ddot{\theta}_I}{p_I} \right|_{t=0} = \frac{2.60 \times 10^6}{(0.54)(10^3)} = 4800 \text{ ft/sec}^2$$

or, in units generally associated with shock testing,

$$\left. \frac{\ddot{\theta}_I}{p_I} \right|_{t=0} = 149 \text{ g} .$$

Similarly, to put  $\ddot{\theta}_{II}$  at time  $t = 0$  on a mode II phase-plane diagram having coordinate axes  $\ddot{\theta}_{II}$  and  $\ddot{\theta}_{II}/p_{II}$ ,

$$\left. \frac{\ddot{\theta}_{II}}{p_{II}} \right|_{t=0} = -30.8 \text{ g} .$$

The other phase-plane coordinate points  $\ddot{\theta}_I$  and  $\ddot{\theta}_{II}$  (at  $t = 0$ ) are zero.

Note that for this type problem where only free vibration occurs, the coordinate scales on the mode I phase plane are not divided by  $H_I$  (nor mode II scales by  $H_{II}$ ) as was done in Fig. 20. This is because the  $H$ 's are only used for scale conversion when external disturbances occur during the time of interest.

The method by which the phase-plane construction was used to determine the responsive motion of each mass of a two-degree undamped system can be extended to include a three-degree system such as the one shown in Fig. 21.

The first term in the expansion is the zeroth-order term, which is the average value of the function over the entire domain.

The second term is the first-order term, which is the average value of the function over the domain, weighted by the coordinate  $x$ .

$$f(x) = \frac{1}{2} + \frac{1}{2}x + \frac{1}{2}x^2 + \dots$$

The third term is the second-order term, which is the average value of the function over the domain, weighted by the coordinate  $x^2$ .

$$f(x) = \frac{1}{2} + \frac{1}{2}x + \frac{1}{2}x^2 + \dots$$

Similarly, the third term in the expansion is the average value of the function over the domain, weighted by the coordinate  $x^3$ .

The fourth term is the third-order term, which is the average value of the function over the domain, weighted by the coordinate  $x^3$ .

$$f(x) = \frac{1}{2} + \frac{1}{2}x + \frac{1}{2}x^2 + \dots$$

The fifth term is the fourth-order term, which is the average value of the function over the domain, weighted by the coordinate  $x^4$ .

It is clear that the expansion of the function in terms of the coordinates  $x$  and  $y$  is a power series.

The expansion of the function in terms of the coordinates  $x$  and  $y$  is a power series, and the coefficients are the averages of the function over the domain, weighted by the coordinates.

(The expansion of the function in terms of the coordinates  $x$  and  $y$  is a power series, and the coefficients are the averages of the function over the domain, weighted by the coordinates.)

It is clear that the expansion of the function in terms of the coordinates  $x$  and  $y$  is a power series, and the coefficients are the averages of the function over the domain, weighted by the coordinates.

It is clear that the expansion of the function in terms of the coordinates  $x$  and  $y$  is a power series, and the coefficients are the averages of the function over the domain, weighted by the coordinates.

The method by which the expansion of the function in terms of the coordinates  $x$  and  $y$  is a power series, and the coefficients are the averages of the function over the domain, weighted by the coordinates.

It is clear that the expansion of the function in terms of the coordinates  $x$  and  $y$  is a power series, and the coefficients are the averages of the function over the domain, weighted by the coordinates.

It is clear that the expansion of the function in terms of the coordinates  $x$  and  $y$  is a power series, and the coefficients are the averages of the function over the domain, weighted by the coordinates.



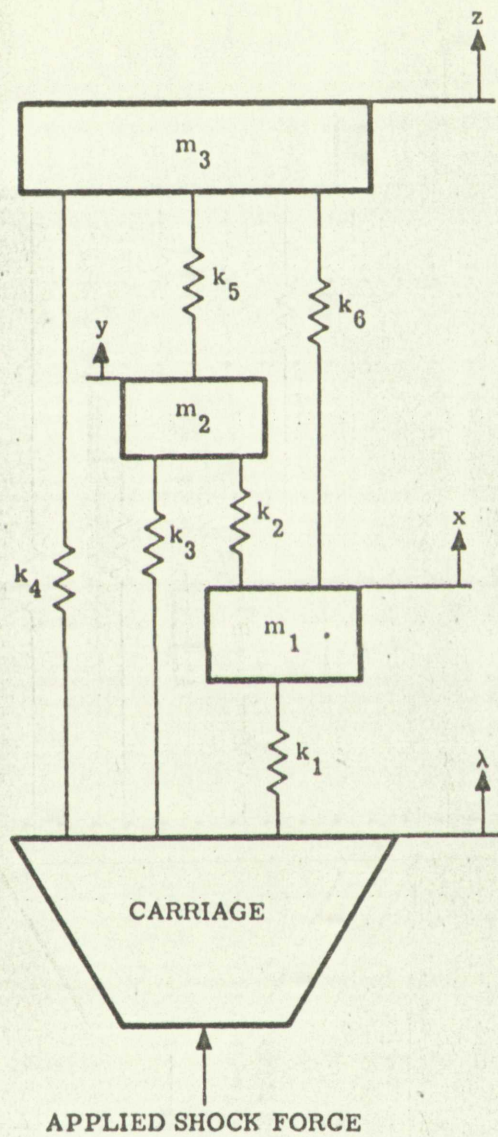


Figure 21 Three-Degree Undamped Spring Mass System with Single Support Excitation





The displacements (accelerations) of each mass must be converted into principal coordinates to describe each mode of vibration to utilize the phase plane. Therefore,

$$x = \theta_I + \theta_{II} + \theta_{III}$$

$$y = \alpha_I \theta_I + \alpha_{II} \theta_{II} + \alpha_{III} \theta_{III} \quad (53)$$

$$z = \beta_I \theta_I + \beta_{II} \theta_{II} + \beta_{III} \theta_{III} ,$$

where  $\theta_I$ ,  $\theta_{II}$ ,  $\theta_{III}$  are coordinates describing the modes of vibration;  $\alpha_I$ ,  $\alpha_{II}$ ,  $\alpha_{III}$ , ratio of amplitude of  $m_2$  to  $m_1$  when vibration in each of the three modes occurs respectively;  $\beta_I$ ,  $\beta_{II}$ ,  $\beta_{III}$ , ratio of amplitude of  $m_3$  to  $m_1$  when vibration occurs in each of the three modes, respectively.

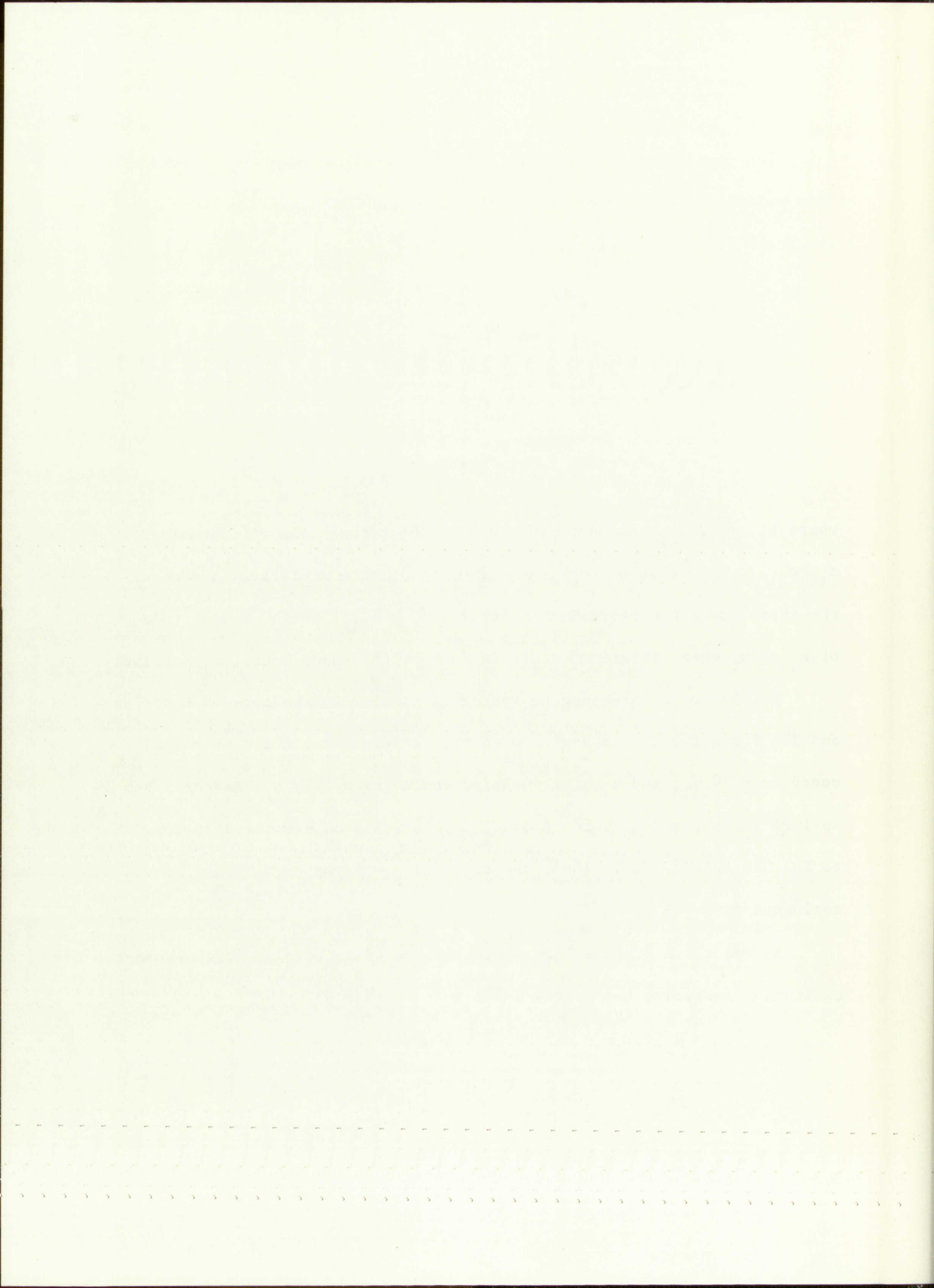
Eq. 53 for a three-degree system is similar to the form of Eqs. 38a and 38b for a two-degree system with the addition of a third principal coordinate,  $\theta_{III}$ , and a third equation involving  $z$ . If  $m_2$  was zero, and springs  $k_2$ ,  $k_3$ , and  $k_5$  were removed, Eq. 53 would be identical in form to Eq. 38a and Eq. 38b. Thus, the ratio of  $\frac{Z}{X} = \beta$  was used, being analogous to  $\frac{Y}{X} = \alpha$  in Eq. 35.

As was shown in Eqs. 38a, 38b, and 46a, 46b, it follows for support excitation (assuming the system is at rest initially)

$$\theta_{I1} = H_I \xi(t)_1$$

$$\theta_{II1} = H_{II} \eta(t)_1 \quad (54)$$

$$\theta_{III1} = H_{III} \zeta(t)_1 ,$$

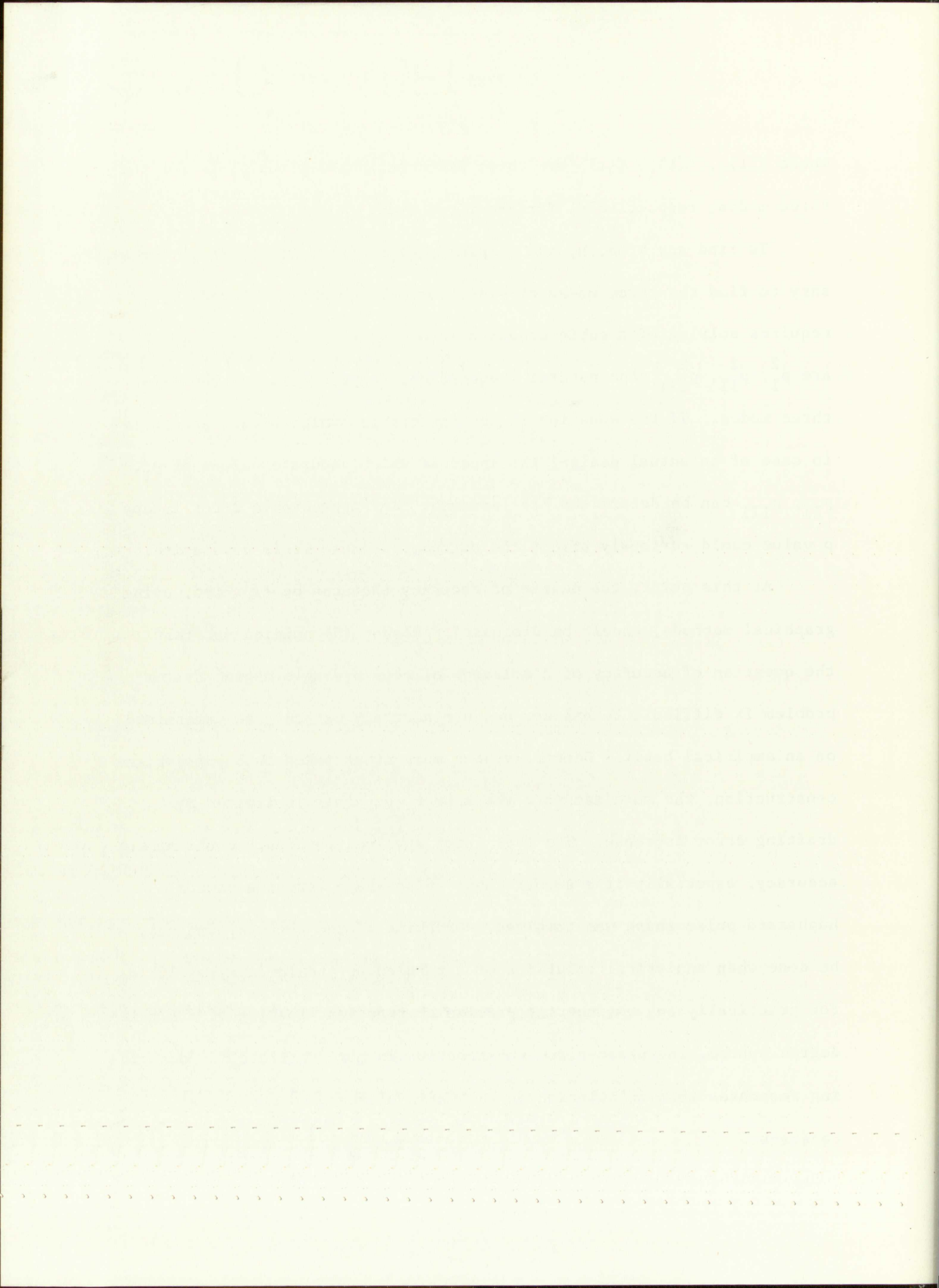




where  $\xi(t)_1$ ,  $\eta(t)_1$ ,  $\zeta(t)_1$  are three different phase-plane plots for the three modes, respectively, for the first step.

To find any  $\alpha$ ,  $\beta$ ,  $H$ , and to plot  $\xi(t)_1$ ,  $\eta(t)_1$ ,  $\zeta(t)_1$ , it is necessary to find the three modes of vibration. To do this analytically requires solving of a cubic equation involving  $p^2$ , the roots of which are  $p_I^2$ ,  $p_{II}^2$ ,  $p_{III}^2$ , the natural frequencies, respectively, of the first three modes. If the equation is not factorable (which occurs generally in case of an actual design) the speed at which accurate values of  $p_I$ ,  $p_{II}$ ,  $p_{III}$  can be determined has lessened. Any appreciable error in any  $p$  value could seriously affect the outcome, because it is cumulative.

At this point, the degree of accuracy that can be expected, using graphical methods, should be discussed. Bishop (5) pointed out that the question of accuracy of a solution of even a single-degree system problem is difficult to answer, because accuracy can only be determined on an empirical basis. Generally, the more steps taken in a phase-plane construction, the more accurate the answer, but this is limited by drafting error increase. The type input involved obviously could affect accuracy, especially if a smooth input pulse shape versus a random haphazard pulse shape was involved. Checking of the accuracy can only be done when analytical solutions of a particular problem are available. For practically any engineering problem of transient loading of a single-degree system, the phase-plane construction is more accurate for describing responses than calculation on the basis of measured mechanical constants.





In multidegree systems, the degree of accuracy decreases while the length of time to solve a problem increases. In any multidegree system the number of phase-plane constructions is proportional to the number of modes of vibration, so the total error is approximately proportioned to the number of modes.

The construction error is somewhat affected by the conversion factor  $H$  and amplitude ratios  $\alpha$  and  $\beta$  by which principal coordinates are changed to rectangular coordinates. For an undamped two-mass, three-spring system similar to that shown in Fig. 1, the maximum value of  $H_I$  found was 1.2 and  $H_{II}$  was 0.4 when several ratios of  $m_1$ ,  $m_2$ ,  $k_1$ ,  $k_2$ , and  $k_3$  were selected. It was found that when the ratio  $k_1/m_1 = k_3/m_2$  that the second mode of vibration would never be excited because  $H_{II} = 0$ .

In one case  $\alpha_{II}$  was found to be -10, but it was compensated by a low value of  $H_{II} = 0.08$ . It would therefore appear that the accuracy obtained for a single-degree undamped system would be approximately twice that for two-degree undamped systems. It would also appear that the accuracy obtained for a single-degree undamped system would be approximately three times the accuracy obtainable for a three-degree system. This statement is qualified to the extent that phase-plane construction follows the guidelines set forth earlier.

The amount of tabular work that needs to be done in converting principal coordinate values to rectangular coordinate values increases



in addition, the degree of freedom of the system is also a function of the number of degrees of freedom of the system. The number of degrees of freedom of the system is also a function of the number of degrees of freedom of the system. The number of degrees of freedom of the system is also a function of the number of degrees of freedom of the system.

The characteristic error is measured by the characteristic error  $H$  and amplitude vector  $\mathbf{h}$  by which the characteristic error is measured. The characteristic error is measured by the characteristic error  $H$  and amplitude vector  $\mathbf{h}$  by which the characteristic error is measured. The characteristic error is measured by the characteristic error  $H$  and amplitude vector  $\mathbf{h}$  by which the characteristic error is measured.

In this case  $H$  was found to be 10, but it was complicated by a low value of  $H$ . It would therefore appear that the accuracy obtained for a single-degree system would be approximately twice that for two-degree system. It would also appear that the accuracy obtained for a single-degree system would be approximately twice that for two-degree system. It would also appear that the accuracy obtained for a single-degree system would be approximately twice that for two-degree system.

directly as the type of degree system. It is therefore estimated that solving a two-degree system problem would take two and one half times as long as a single-degree problem, while a three-degree system problem would take four times as long as a single-degree system problem. Again, this statement is dependent upon the type of phase-plane construction needed for each mode of vibration. It would thus appear that solving a three-degree system problem by graphical techniques would not be too satisfactory a method; computers would be the better way to solve the problem.

## 2. Damped Systems

The addition of damping to a two-degree system is considered in this section. As shown previously, adding damping to a single-degree system produces some difficulties in using the phase-plane technique. In a two-degree system, the difficulties are compounded even more. The main reason is the fact that the coordinate system must be transformed. Two-degree system problems are solved in principal coordinates and then changed to rectangular coordinates. The two principal coordinates used in the undamped two-degree system analysis were independent of each other. Because they were, the phase-plane could be used. Bishop in Ref. (5) summarized the requirements of the equation of motion of multi-degree undamped systems which permit the usage of a phase-plane solution.

elementary as the case of the elementary functions, but the  
analysis of the functions is more complicated. The functions  
as long as a single function is considered, the analysis  
would be the same. The analysis of the functions is the same  
This statement is true. The analysis of the functions is the same  
needed for each function. The analysis of the functions is the same  
Three types of functions are considered. The analysis of the functions is the same  
satisfactorily a set of functions. The analysis of the functions is the same  
problem.

2. Generalization  
The addition of the functions is the same. The analysis of the functions is the same  
this section. At the same time, the analysis of the functions is the same  
system produced. The analysis of the functions is the same  
In a two-dimensional system, the analysis of the functions is the same  
main reason is the fact that the functions are the same. The analysis of the functions is the same  
Two-dimensional systems are the same. The analysis of the functions is the same  
changed to a two-dimensional system. The analysis of the functions is the same  
in the two-dimensional system. The analysis of the functions is the same  
effect. The analysis of the functions is the same  
fact. The analysis of the functions is the same  
degrees of freedom. The analysis of the functions is the same



He states that when normal coordinates are used to define the system configuration, the equations of motion are

$$\begin{aligned}\ddot{q}_I + p_I^2 q_I &= p_I^2 Q_I \\ \ddot{q}_{II} + p_{II}^2 q_{II} &= p_{II}^2 Q_{II} \\ \vdots \quad \quad \quad \vdots \quad \quad \quad \vdots &\end{aligned}$$

$$\ddot{q}_n + p_n^2 q_n = p_n^2 Q_n ,$$

where  $q$ 's are normal coordinates,  $p$ 's are frequencies of free vibration in the  $n$  normal modes, and  $Q_n$ 's are quantities found from the generalized forces (corresponding to each coordinate) which can be expressed in step input form.

If any system has damping and the equation of motion of each mode for a small step can be approximated by the one shown in Eq. 5 or Eq. 22b, a phase-plane solution could work.

In Ref. (6) there is developed the equations of motion of a viscously damped two-degree system in generalized coordinates using Lagrange's equations. Lagrange's general equation is

$$\frac{d}{dt} \frac{\partial T}{\partial \dot{q}_i} - \frac{\partial T}{\partial q_i} + \frac{\partial V}{\partial q_i} + \frac{\partial F}{\partial q_i} = Q_i , \quad (56)$$

It is noted that when normal coordinates are used, the equations of motion are

coupled, and the solution is obtained by the method of variation of parameters.

$$\ddot{q}_1 + \omega_1^2 q_1 = \frac{1}{m_1} \sum_{j=1}^n F_{1j} \cos \omega_j t$$

$$\ddot{q}_2 + \omega_2^2 q_2 = \frac{1}{m_2} \sum_{j=1}^n F_{2j} \cos \omega_j t$$

(18)

$$\ddot{q}_3 + \omega_3^2 q_3 = \frac{1}{m_3} \sum_{j=1}^n F_{3j} \cos \omega_j t$$

where  $q_i$  are normal coordinates,  $\omega_i$  are frequencies of free vibration, in the  $i$ -th normal mode, and  $F_{ij}$  are quantities found from the generalized forces (corresponding to each coordinate) which can be expressed in step

input form

if any system has damping and the equation of motion of each mode

for a small step can be approximated by the one shown in Eq. 5 or Eq. 13b.

A phase-plane solution could work.

In Ref. (8) there is developed the equations of motion of a

viscoelastic damped two-degree system in generalized coordinates using

Lagrange's equations. Lagrange's general equation is

(19)

$$\frac{d}{dt} \left( \frac{\partial L}{\partial \dot{q}_i} \right) - \frac{\partial L}{\partial q_i} = Q_i$$



where  $T$ ,  $V$ ,  $F$  are functions describing, respectively, the kinetic, potential (spring), and dissipated (friction) energy of the given system in each normal coordinate,  $q_i$ , and  $Q_i$  is the generalized external force (which must be found from actual forces).

For small vibrations of the system of Fig. 1 ( $f$ 's = 0)

$$T = \frac{1}{2} (a_{11} \dot{q}_I^2 + a_{22} \dot{q}_{II}^2)$$

$$V = \frac{1}{2} (c_{11} q_I^2 + c_{22} q_{II}^2) \quad (57)$$

$$F = \frac{1}{2} (b_{11} \dot{q}_I^2 + 2b_{12} \dot{q}_I \dot{q}_{II} + b_{22} \dot{q}_{II}^2),$$

where  $a_{11}$ ,  $a_{22}$ ,  $b_{11}$ ,  $b_{12}$ ,  $b_{22}$ ,  $c_{11}$ , and  $c_{22}$  are constants dependent upon the magnitudes of the masses, dampers, and springs, respectively, and also the configuration of the system.

Substituting Eq. 57 into Eq. 56 and assuming for the moment a free vibration condition, ( $Q_i = 0$ ),

$$a_{11} \ddot{q}_I + c_{11} q_I + b_{11} \dot{q}_I + b_{12} \dot{q}_{II} = 0$$

$$a_{22} \ddot{q}_{II} + c_{22} q_{II} + b_{12} \dot{q}_I + b_{22} \dot{q}_{II} = 0. \quad (58)$$

When no damping exists, Eq. 58 becomes Eq. 55 when  $Q_i$  is zero. When damping is present, the two parts of Eq. 58 are generally not independent.





The only way they could be independent is for either  $b_{12}$  or  $q_{II}$  (second mode) = 0. (In an actual system,  $b_{12}$  would rarely be zero; it would be zero when the dampers are in the same ratio as the springs; e.g.,  $\frac{k_3}{k_1} = \frac{c_3}{c_1}$ ). When both parts of Eq. 58 are not independent, the phase-plane technique cannot be used; whenever they are independent the phase plane can be used.

Eq. 58 describes a two-degree system where only viscous damping is present. How would Eq. 58 appear if only coulomb damping were present? For small intervals where the  $\text{sgn } f$  did not change, the friction force could be considered combined with the generalized force,  $Q_1$  (provided the external forces are independent of the normal coordinates  $q_I$  and  $q_{II}$ ).

Fig. 22 shows how an undamped two-degree system would appear in forced vibration. (This example is similar to a coulomb-damped system for the interval when the friction does not change.)

The differential equation of motion is

$$m_1 \ddot{x} + (k_1 + k_2)x - k_2 y = F_1 \quad (59a)$$

$$m_2 \ddot{y} + (k_2 + k_3)y - k_2 x = F_2, \quad (59b)$$

where  $F_1$  and  $F_2$  are external excitation forces on each mass, respectively.

Eqs. 59 are independent of each other when written in normal coordinate form. If at  $t = 0$

$$x_0 = \dot{x}_0 = y_0 = \dot{y}_0 = 0,$$

The only way they could be independent is for either  $\omega_1$  or  $\omega_2$  to be zero. (In an actual system,  $\omega_1$  would rarely be zero; it would be

zero when the dampers are in the same ratio as the springs; viz.,

$$\frac{b_1}{k_1} = \frac{b_2}{k_2} \quad (2.11)$$

When both parts of Eq. 2.8 are not independent, the phase-angle

technique cannot be used; whenever they are independent the phase plane

can be used.

Fig. 2.8 describes a two-degree system where only viscous damping

is present. Then would Fig. 2.8 appear if only Coulomb damping were present?

For small intervals where the sign  $\dot{x}$  did not change, the friction force

could be considered combined with the generalized force,  $Q_1$  (or  $Q_2$ ).

the external forces are independent of the normal coordinates  $x_1$  and  $x_2$ .

Fig. 2.9 shows how an undamped two-degree system would appear in

forced vibration. (This example is similar to a Coulomb-damped system

for the interval when the friction does not change.)

The differential equation of motion is

$$m_1 \ddot{x}_1 + (k_1 + k_2)x_1 - k_2 x_2 = F_1 \cos \omega t \quad (2.12)$$

$$m_2 \ddot{x}_2 + (k_2 + k_3)x_2 - k_2 x_1 = F_2 \cos \omega t \quad (2.13)$$

where  $F_1$  and  $F_2$  are external excitation forces on each mass, respectively.

Eq. 2.9 are independent of each other when written in normal

coordinates form. If at  $t = 0$

$$x_1 = x_2 = \dot{x}_1 = \dot{x}_2 = 0$$



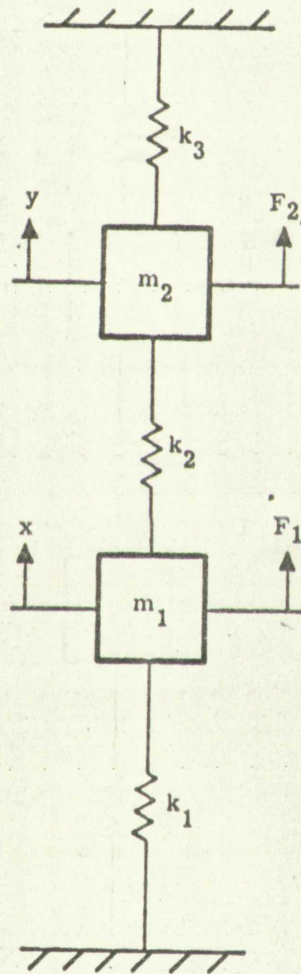


Figure 22 A Two-Degree Undamped System Under Force Excitation



Figure 12. A Two-Degree-of-Freedom System with Spring Supports



then the solution is

$$x = H_I \xi(t) + H_{II} \eta(t)$$

(60)

$$y = \alpha_I H_I \xi(t) + \alpha_{II} H_{II} \eta(t) .$$

Here  $\xi(t)$  represents a function of the generalized force,  $Q_I$ , while  $\eta(t)$  represents the generalized force,  $Q_{II}$ . If  $F_1$  and  $F_2$  are constant for a step interval, then

$$\xi(t)_i = \lambda^* (1 - \cos p_I t_i)$$

(61)

$$\eta(t)_i = \lambda^* (1 - \cos p_{II} t_i) ,$$

where  $\lambda^*$  is a quantity representing an equivalent support motion that has to stay constant during the step and is related in some fashion to  $F_1$  and  $F_2$  for the step. The relationship must stay constant for all steps in order that  $H_I$  and  $H_{II}$  (the conversion from rectangular to normal coordinates) will stay constant. Varying  $H_I$  and  $H_{II}$  with each step would be impractical for phase-planes. ( $H_I$  and  $H_{II}$  are found by substituting Eq. 61 into Eq. 60, differentiating Eq. 60, and substituting into Eq. 59.) Arbitrarily, let  $F_1 = m_I p_I^2 \lambda_1^*$  in Eq. 59. Then to find  $H_I$  and  $H_{II}$ , it is necessary to know the relationship between  $F_1$  and  $F_2$ . For the step, then, let the ratio of  $\frac{F_2}{F_1} = \gamma_1$  (a known constant).





Then, in Eq. 59,

$$F_2 = \gamma_1 F_1 = \gamma_1 m_1 k_1 \lambda_1^* . \quad (62)$$

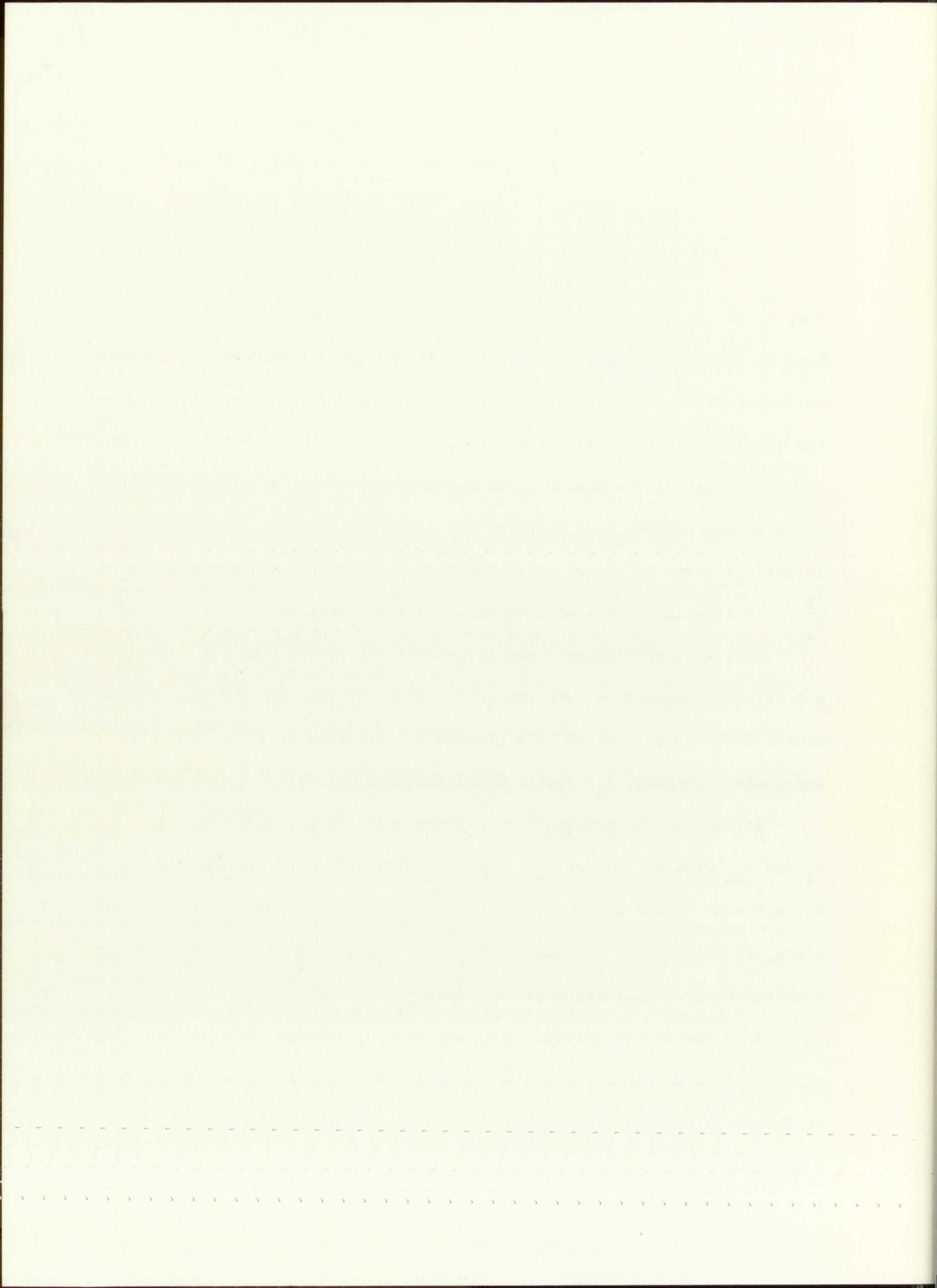
Now,  $H_I$  and  $H_{II}$  can be evaluated by the simultaneous solution of both Eqs. 59. Thus, the ratio  $\gamma_1$  must be held constant throughout the entire motion study. It has been shown in Ref. (2) that, if  $\gamma_1 = \frac{m_2}{m_1} \alpha_I$ , only the single lower mode will be excited.

In general, the preceding analysis will hold for a coulomb friction force acting between each mass and its support. However, the coulomb forces will have to change signs simultaneously in order for the ratio of  $\frac{f_2}{f_1}$ , the friction forces on each mass, to stay constant.

This will only happen when the masses are moving 0 or 180 degrees out of phase; therefore, for the system shown in Fig. 22, only the fundamental mode can be excited if a phase-plane solution is to be used with any coulomb damping,  $f_1$ ,  $f_2$ , or  $f_3$  as shown in Fig. 1.

If the support motion from a common point occurs as in Fig. 1,  $H_I$  and  $H_{II}$  will not be constant for each step unless the friction force on each mass is the same. Also, only the fundamental mode can be excited, since, if this is not the case, the sgn of  $f_1$ ,  $f_2$ , and  $f_3$  will not change simultaneously. This requires the ratio  $\frac{m_2}{m_1} \alpha_I = 1.0$ .

In a two-degree system, if  $k_3$  spring = 0, coulomb friction can occur only on mass  $m_1$ . The  $(\lambda + \Delta_c)$  will exist in every term of the differential equation, so  $H_I$  and  $H_{II}$  are independent of excitation.





In trying to adapt viscous damping to the phase-plane-delta technique, trouble occurs in that the magnitude of the  $\Delta_v$  term varies from step to step, which means  $H_I$  and  $H_{II}$  will not be constant. A phase-plane construction would be too tedious to construct.

From the foregoing it appears that damped multidegree systems must be excluded from the list of problems that can be easily solved by graphical techniques.

In order to make systems subject to the phase-plant  
technique, suitable means to find the eigenvalues of the  $A$  matrix  
from eq. (1), which means  $\lambda$  and  $\lambda^*$  will not be available. A  
phase-plant construction would be too tedious to construct.  
From the foregoing it appears that shaped multivariable systems  
must be excluded from the list of problems that can be easily solved  
by classical techniques.



## VI. EXPERIMENTAL INVESTIGATION

Three different single-degree system models were designed and subjected to mechanical shock pulses similar to the pulses that would be generated in mechanical shock testing in industry. The three models were: (1) undamped, (2) coulomb damped, and (3) viscously damped. Results of the monitored and the phase-plane acceleration-time histories of each model are compared.

### 1. Single-Degree System Designs

A view of the undamped model is shown in Fig. 23. The design of the model consisted of a single concentrated mass suspended between two sets of four helical coil springs (total of eight springs), each having the same spring rate. One end of each set of springs was held rigid within a very stiff framework. The mass was constrained to move only in either direction of the longitudinal axis by Teflon bushings riding upon four guide rods. The lower plate was fastened to a shock machine carriage during all shock tests. The input shock to each model was monitored by a piezoelectric accelerometer mounted on top of the framework which was the specimen fixture. The responsive accelerations were monitored by an identical piezoelectric accelerometer mounted directly upon the suspended mass. The instrumentation circuitry used is shown in Fig. 24.





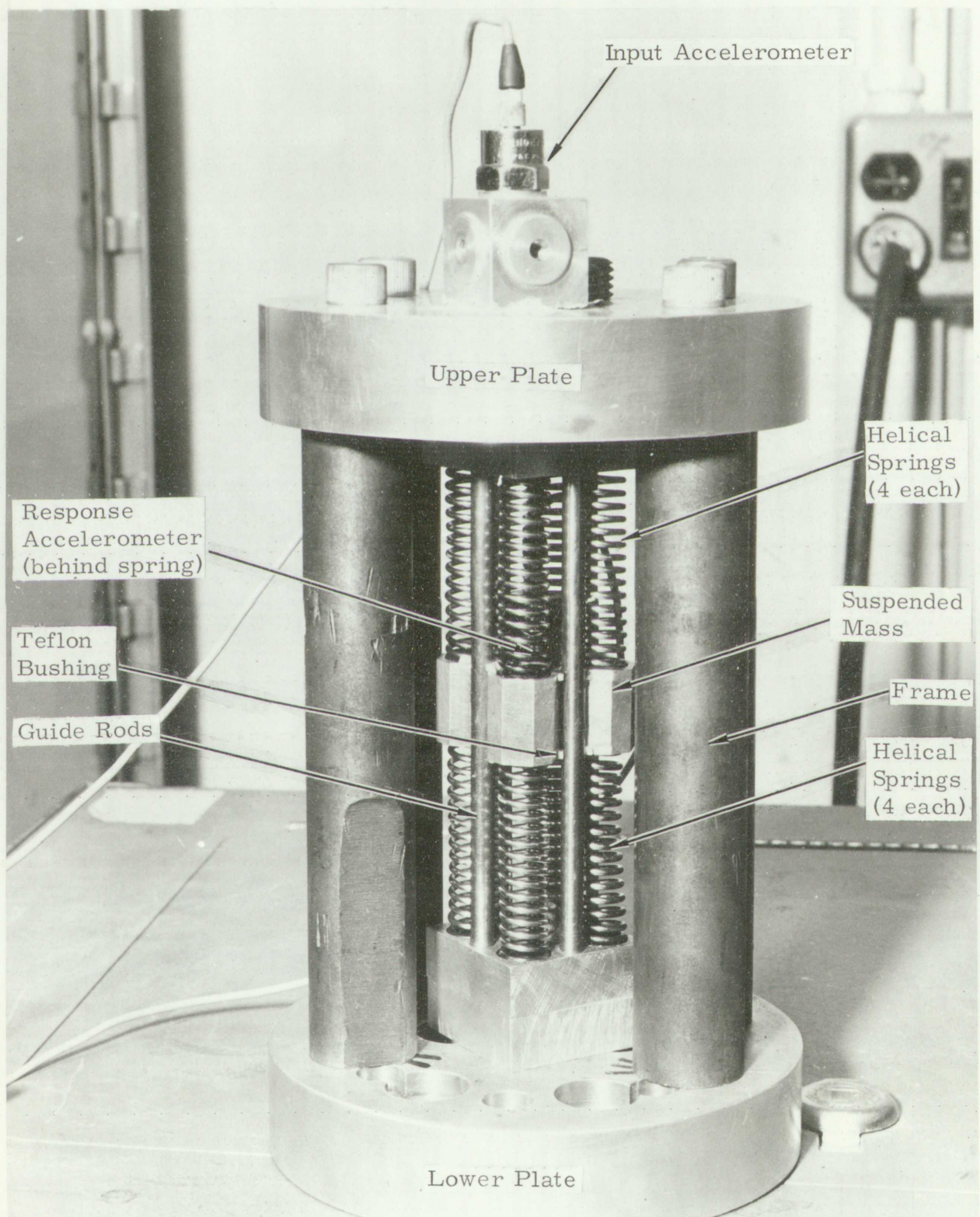


Figure 23. Model for Experimental Investigation

1-3

LIMBAUGH ENGINEERING & AERIAL SURVEYS, INC.  
3125 CARLISLE BLVD., N.E.  
ALBUQUERQUE, NEW MEXICO



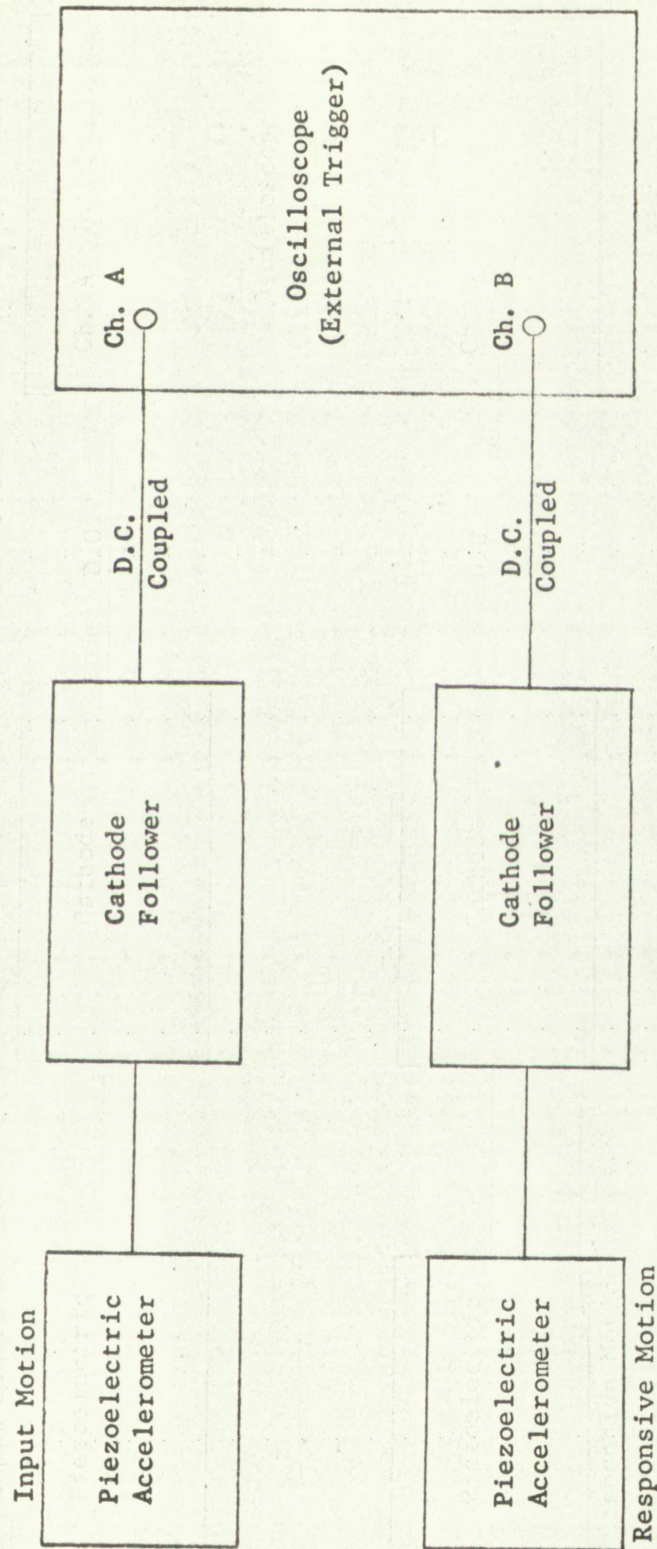
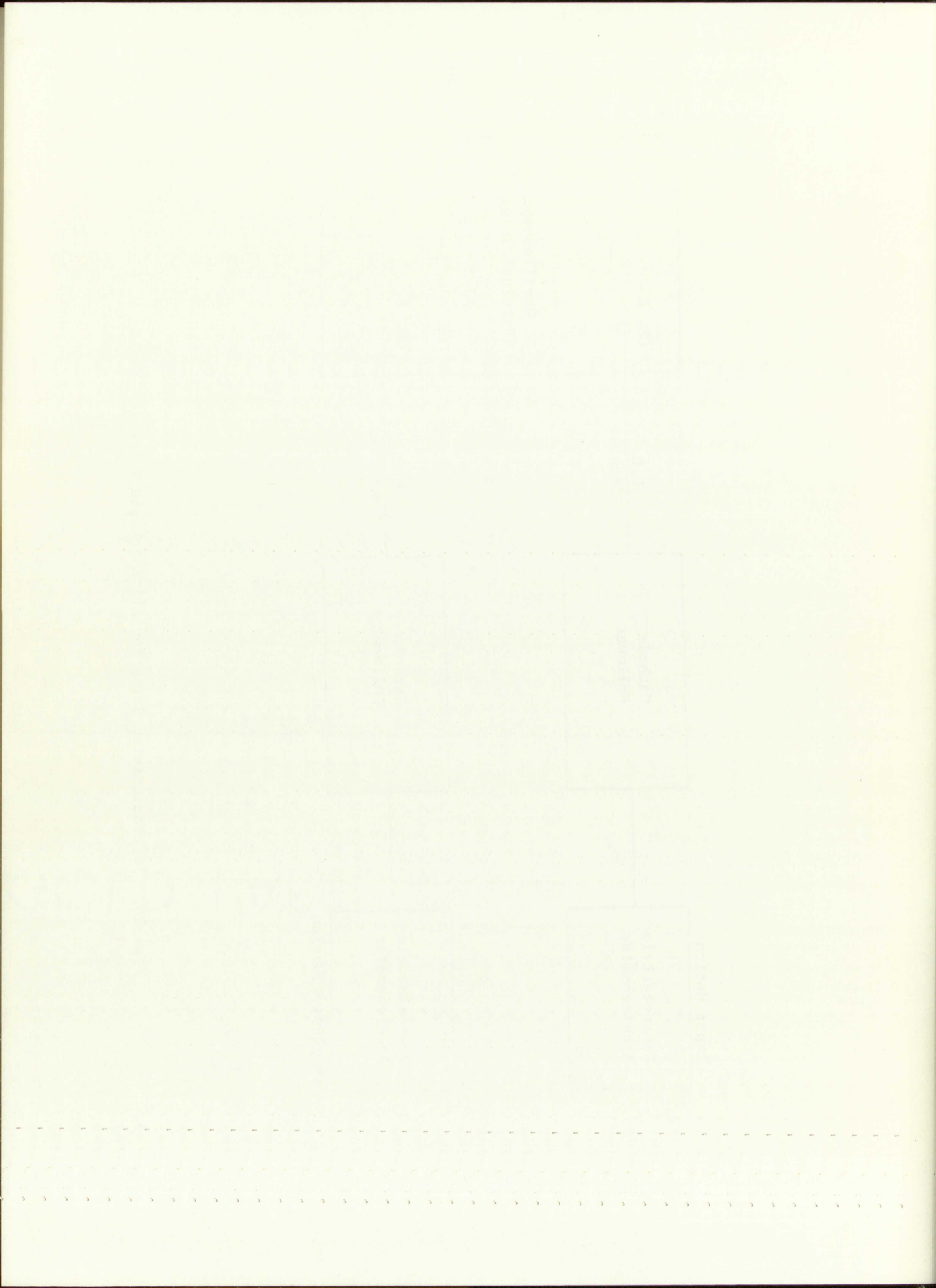


Fig. 24. Instrumentation Setup for All Shock and Vibration Tests





A sketch showing the actual idealized spring-mass configuration is shown in Fig. 25a. The mass,  $m$ , is very light with respect to the supports, so feedback of the mass during shock could be neglected. Fig. 25a shows that the model had two different inputs,  $\ddot{\lambda}_1(t)$  and  $\ddot{\lambda}_2(t)$ , applied at either support. In reality  $\ddot{\lambda}_2(t)$  lags behind  $\ddot{\lambda}_1(t)$  in time of occurrence and is slightly different in appearance because of its transmission through the frame. However, since the frame was quite rigid in comparison with the helical springs, the phase shift and shape difference were negligible. Thus, it was assumed that  $\ddot{\lambda}_1(t) = \ddot{\lambda}_2(t)$  for all practical purposes. All the sets of four springs on opposite sides of the mass were in parallel. For a linear system, then, they were assumed to be all on one side as shown in Fig. 25b. Similarly, since both supports were receiving the same input, they could be represented as one support. Thus, Fig. 25b is shown as a special case of Fig. 1 for which portions of this thesis were developed.

Actually, an undamped model never occurs in reality. However, sometimes the amount of damping is so small that for a few cycles of vibration the amplitude loss is very small. By careful alignment and greasing of the guide rods and by use of a very small contact area between bushings and guide rods, a very lightly damped model (essentially undamped for the time interval of interest during shock) was obtained.

The coulomb-damped model was similar in design to the undamped model shown in Fig. 23. Coulomb friction was introduced by increasing



A system having the same characteristics as the

is shown in Fig. 1. The system is shown in Fig. 1.

Figure 1 shows the system in the case of the

applied to the system. The system is shown in Fig. 1.

of the system is shown in Fig. 1. The system is shown in Fig. 1.

is shown in Fig. 1. The system is shown in Fig. 1. The system is shown in Fig. 1.

is shown in Fig. 1. The system is shown in Fig. 1. The system is shown in Fig. 1.

is shown in Fig. 1. The system is shown in Fig. 1. The system is shown in Fig. 1.

is shown in Fig. 1. The system is shown in Fig. 1. The system is shown in Fig. 1.

is shown in Fig. 1. The system is shown in Fig. 1. The system is shown in Fig. 1.

is shown in Fig. 1. The system is shown in Fig. 1. The system is shown in Fig. 1.

is shown in Fig. 1. The system is shown in Fig. 1. The system is shown in Fig. 1.

is shown in Fig. 1. The system is shown in Fig. 1. The system is shown in Fig. 1.

is shown in Fig. 1. The system is shown in Fig. 1. The system is shown in Fig. 1.

is shown in Fig. 1. The system is shown in Fig. 1. The system is shown in Fig. 1.

is shown in Fig. 1. The system is shown in Fig. 1. The system is shown in Fig. 1.

is shown in Fig. 1. The system is shown in Fig. 1. The system is shown in Fig. 1.

is shown in Fig. 1. The system is shown in Fig. 1. The system is shown in Fig. 1.

is shown in Fig. 1. The system is shown in Fig. 1. The system is shown in Fig. 1.

is shown in Fig. 1. The system is shown in Fig. 1. The system is shown in Fig. 1.

is shown in Fig. 1. The system is shown in Fig. 1. The system is shown in Fig. 1.

is shown in Fig. 1. The system is shown in Fig. 1. The system is shown in Fig. 1.

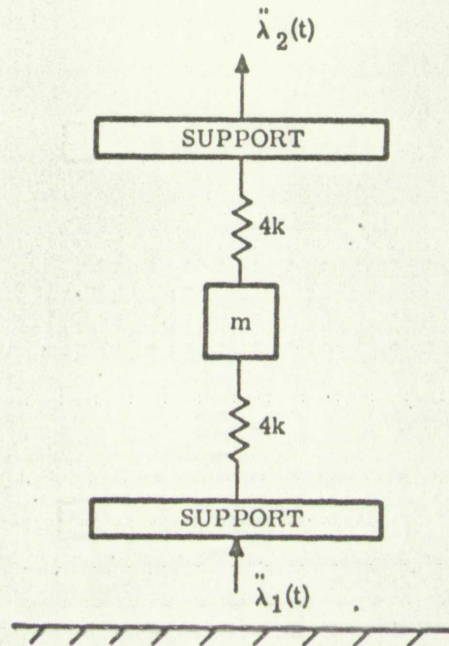


Figure 25a Actual Idealized Model

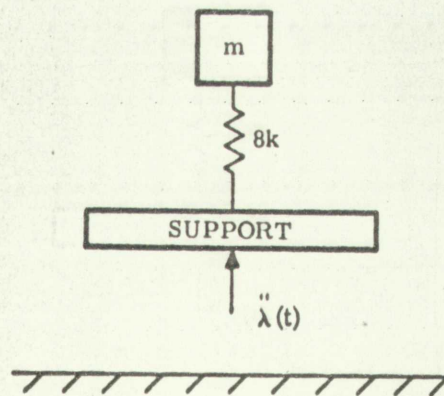


Figure 25b Equivalent Ideal Model



Figure 25a Active Isolation Model

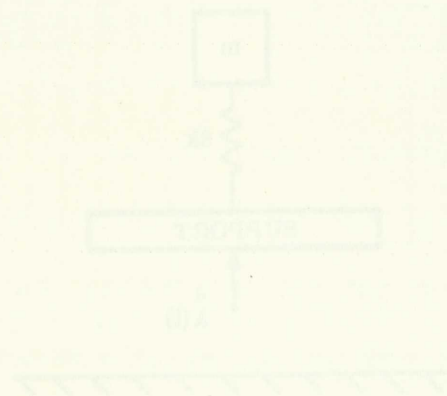


Figure 25b Repassive Isolation Model



the normal pressure between the bushings and the dry guide rods. The contact area between the bushings and guide rods was increased to reduce wear during vibration testing of the model. The friction damper thus appeared fastened to the support and to the mass of the model.

The viscously damped model design was similar to the model of Fig. 23 with a viscous damper added. The construction and positioning of the damper was in the same manner as shown by  $c_1$  in Fig. 1. A 5/8-inch piston was fastened to the mass; a 2-1/2-inch-long cylinder was fastened to the support. The piston had four 1/8-inch-diameter holes through which 10-W motor oil was metered whenever the piston moved relative to the cylinder. A suitable damping ratio was achieved, so no fine adjustment was incorporated into the design.

Details of each model, such as spring rates, weight of suspended mass, magnitude of dry friction, and viscous forces, could have been measured and then the natural and resonant frequencies of the system calculated. Instead, all parameters needed to solve a transient response problem were found by subjecting each model to a vibration test. A resonant search was conducted to determine the natural frequency for the undamped and coulomb-damped models and the resonant frequency for the viscously damped model. (For a damping ratio of 0.2, the resonant frequency is only 2% lower than the natural frequency.) Once the natural or

The normal pressure between the bushings and the key guide rails, the contact with the bushings and guide rails was increased to reduce wear during vibration testing of the model. The friction damper was appeared fastened to the support and to the mass of the model.

The viscously damped model design was similar to the model of Fig. 22 with a viscous damper added. The connecting and positioning of the damper was in the same manner as shown by c in Fig. 1. A 3/8-inch piston was fastened to the mass; a 2-1/2-inch-long cylinder was fastened to the support. The piston had four 1/8-inch-diameter holes through which 10-W motor oil was injected whenever the piston moved relative to the cylinder. A suitable damping ratio was achieved, so no fine adjustment was incorporated into the design.

Details of each model, such as spring rates, weight of suspended mass, magnitude of dry friction, and viscous forces, could have been measured and then the natural and resonant frequencies of the system calculated. Instead, all parameters needed to solve a transient response problem were found by subjecting each model to a vibration test. A

transient search was conducted to determine the natural frequency for the undamped and Coulomb-damped models and the resonant frequency for the viscously damped model. For a damping ratio of 0.2, the resonant frequency is only 12 lower than the natural frequency. Thus the natural ex

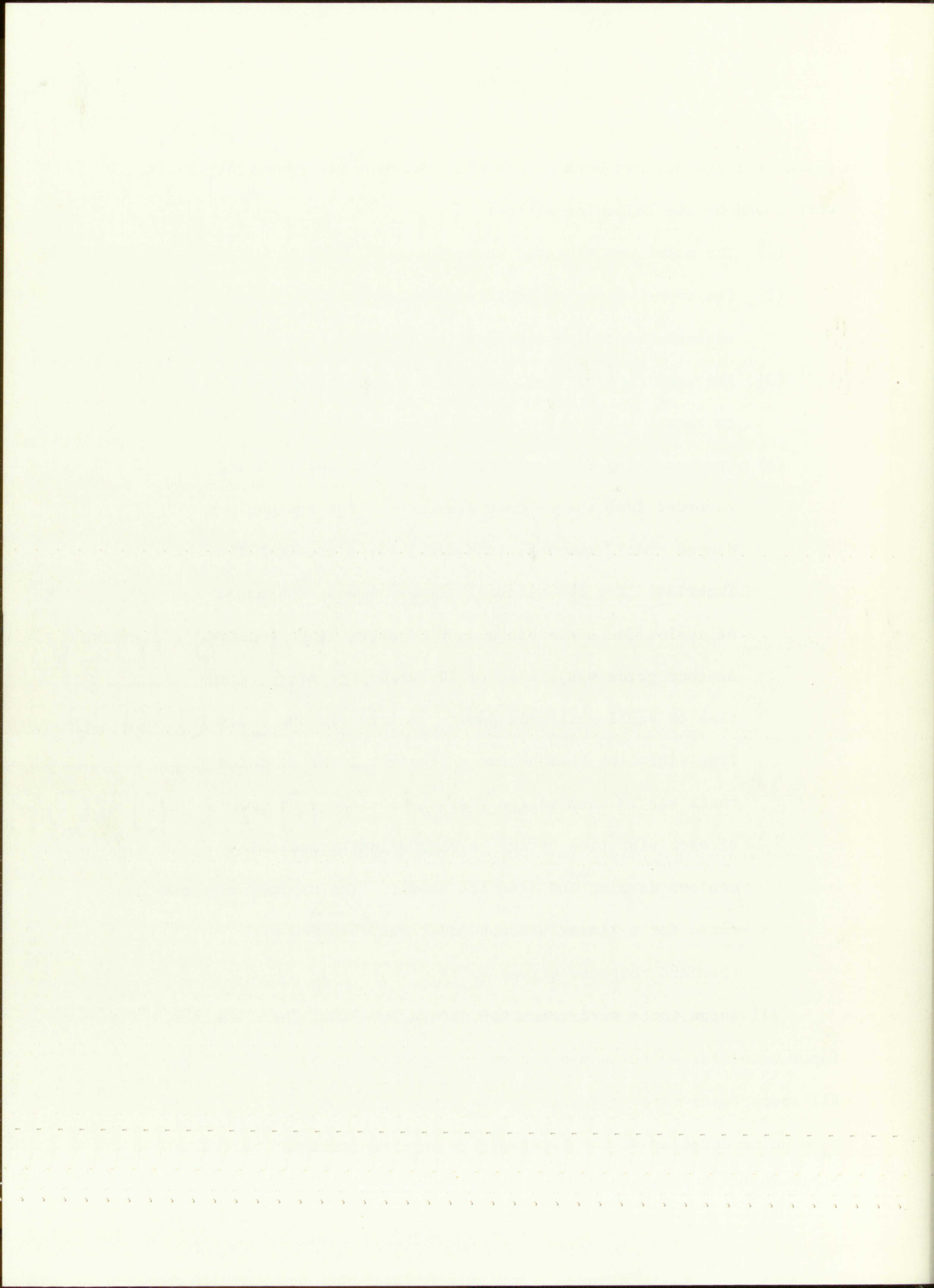


resonant frequency had been determined, the type and amount of damping were found by the following method:

- (1) The model was vibrated at resonance;
- (2) The input vibration amplitude was adjusted to give a maximum responsive acceleration level;
- (3) The amplitude of input vibration suddenly was brought to zero;
- (4) The resulting decay of the response was observed and recorded from the readout equipment. For the coulomb-damped model, the amplitude decay was a straight line function. For the viscously damped model, the number of cycles for a certain amount of decay was one guide. Another guide was a plot of the amplitude decay versus time on semilogarithmic paper. A true viscous decay in free vibration thus became a straight line. A third check was to observe the characteristics of the peak of each vibration cycle. A discontinuity indicated coulomb damping and also its amount. The maximum response ratio for a linear viscous model was compared with standard response curves.

All shock tests were conducted upon a free-fall shock machine. The input acceleration pulse was shaped by impacting upon Butyl rubber pads. All shock tests were conducted in the range of  $0.5 < \frac{t_d}{T} < 2.0$ , where  $t_d$  = pulse duration at the base and  $T$  = specimen undamped natural period.



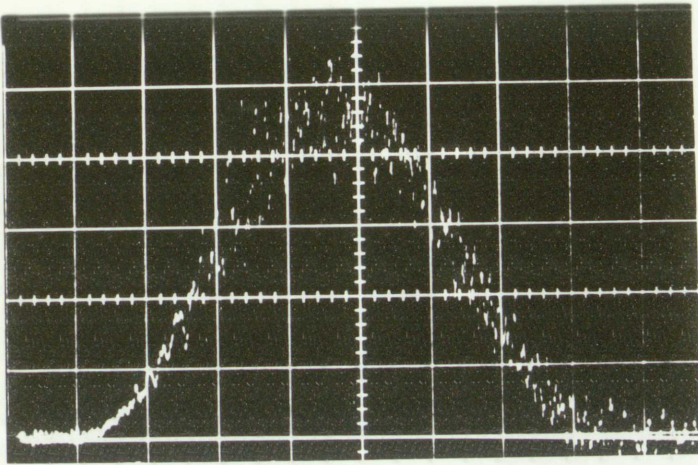


## 2. Test Results

Fig. 26 shows, during shock, actual acceleration-time histories for a system that could be considered undamped for a few cycles. From the vibration test the undamped natural period of the specimen was found to be 10.6 ms. When the input vibration amplitude at resonance was suddenly decreased to zero, the responsive amplitude decayed as shown in Fig. 27. The type of decay indicated the structure damping of the springs approximated viscous damping equivalent to a damping ratio of 0.0008. For a few cycles of responsive vibration under consideration during the shock test, the system only showed minute changes in amplitude so damping was neglected. Fig. 28 shows a comparison of the undamped systems response (determined both by measurement and graphically) to an input acceleration pulse of 46 g, 15 ms (measured at the zero line). The pulse shape approximated a haversine. Steps of 1-ms intervals were used to plot the phase-plane diagram. One can see in Fig. 28 that the peak of the measured response was 81 g while the peak of the phase-plane response was 73 g. From the shock spectra for a pure haversine pulse, Ref. (11), the phase-plane solution is in good agreement. However, the measured peak response is higher than that theoretically possible for a linear undamped spring-mass system subjected to input shape shown, or even for a half-sine shape of same amplitude and duration. It thus appears that the model must be slightly nonlinear



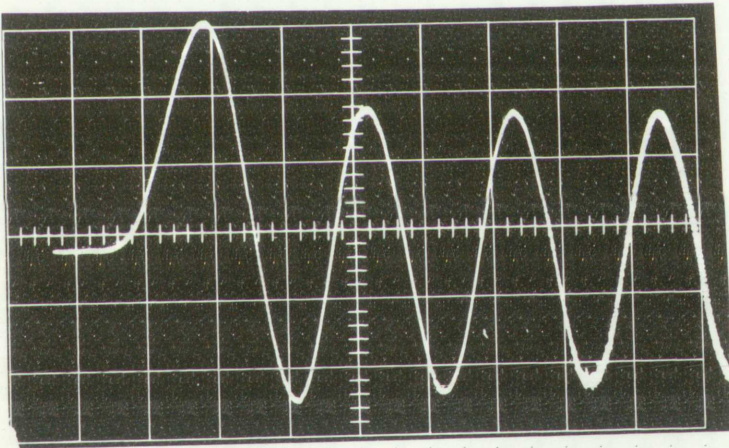




Input Pulse

10 g/cm

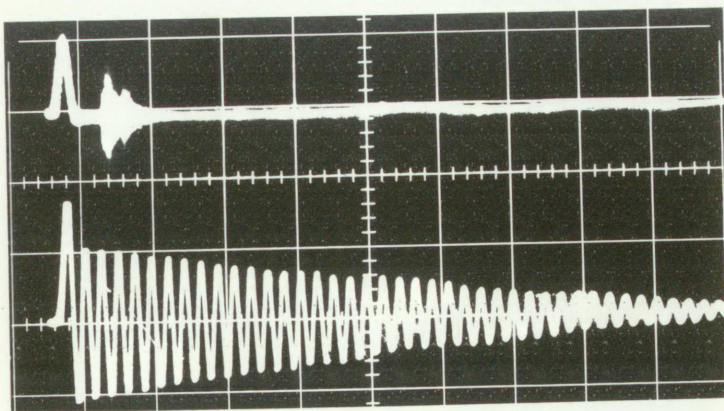
2 ms/cm



Mass Response

25 g/cm

5 ms/cm



Input and Response  
to Same Time Base

50 g/cm

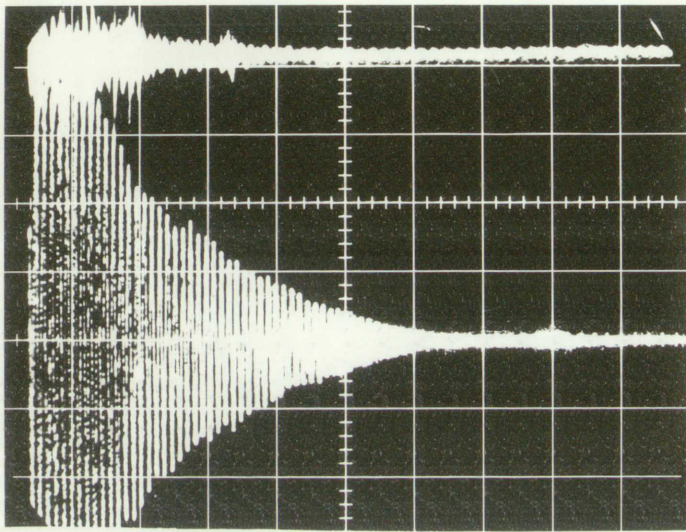
50 ms/cm

Figure 26. Acceleration-Time History of an Undamped Single-Degree System Under Shock

BAUGH ENGINEERING & AERIAL SURVEYS, INC.  
3125 CARLISLE BLVD., N.E.  
ALBUQUERQUE, NEW MEXICO

3-4

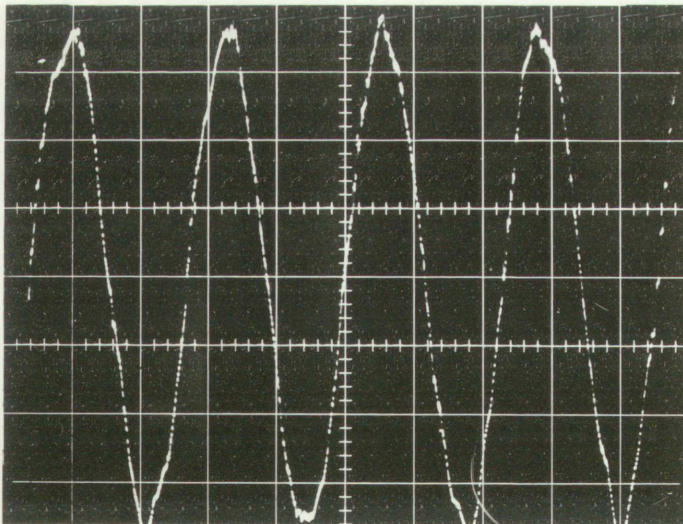




Amplitude Decay During  
Vibration Test

25 g/cm  
100 ms/cm

Response Ratio at Resonance = 65/1



Waveform of Mass at a  
Responsive Amplitude of  
 $\pm 85$  g

25 g/cm

Figure 27. Responsive Motions During Vibration Tests



3-5

LIMBAUGH ENGINEERING & AERIAL SURVEYS, INC.  
3125 CARLISLE BLVD., N.E.  
ALBUQUERQUE, NEW MEXICO

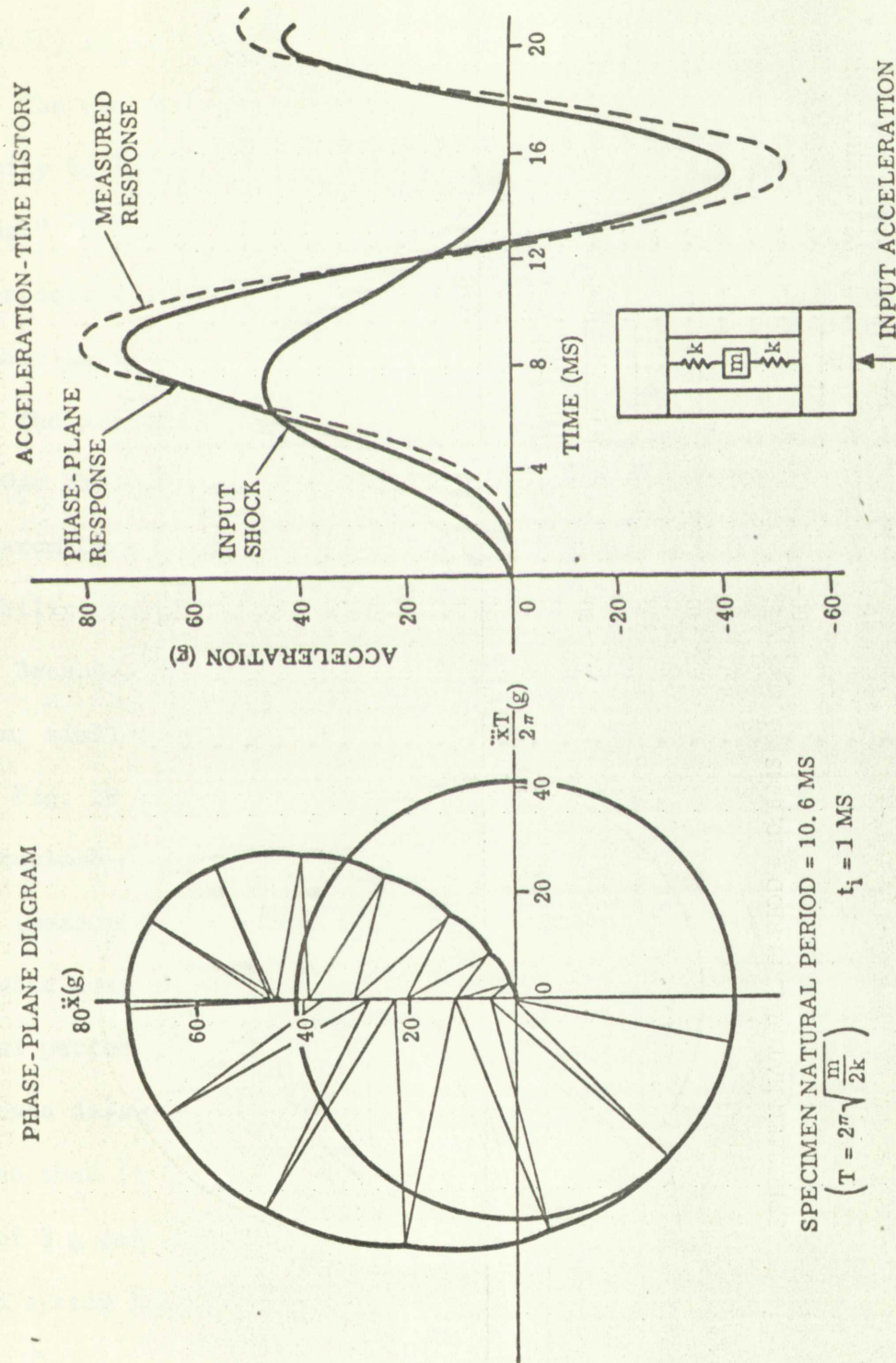


Figure 28 Comparison of Phase-Plane and Measured Response of a Linear System (Damping Neglected) to an Applied Shock Pulse





in its motion. Observation of the responsive motion under vibration at approximately the same amplitude ( $\pm 85$  g) Fig. 27, shows that some non-linearity of waveform is present.

The waveform does not appear harmonic nor sinusoidal in the vicinity of the peaks. The sharp peaks are indicative of a "stiffening spring." A "stiffened" spring at a particular deflection will cause a higher acceleration at that deflection than the acceleration caused by a linear spring.

The possibility that the accelerometers were not in good calibration was checked. When the test was repeated with the location of the accelerometers reversed, the same type of response was observed. This possibility was therefore ruled out.

Because of the amount of nonlinearity observed in the undamped system, similar nonlinearities might be expected in the damped systems.

Fig. 29 shows, during shock, the actual acceleration-time history of a coulomb-damped model in response to an input shock pulse of 58 g, 12 ms (measured at the zero line). The input shock approximated a parabolic cusp shape. As shown in the vibration test, the undamped natural period of the model was 8.4 ms. The characteristics of the amplitude decay from resonance are shown in Fig. 30. It can readily be seen that it is a linear decay. The amplitude decay indicated a loss of 8 g per cycle. Also, in Fig. 30, it is shown how a coulomb-damped system behaves under sustained vibration. A discontinuity occurs

in the present. Examination of the temperature records for the

experimentally the same results were obtained.

Intensity of vibration is given by

The waveform does not appear to be a simple sine wave in the

velocity of the motion. The shape of the waveform is a

complex. A "beat" phenomenon is observed. The beat is caused by

higher acceleration at that instant. The acceleration is caused by

a linear spring.

The possibility that the measurements were not in good condition

was checked. When the test was repeated with the same equipment

and the same waveform was obtained. The same type of waveform was

possibility was therefore ruled out.

Because of the amount of motion observed in the undamped

system, similar motion might be expected in the damped system.

Fig. 28 shows during shock the actual acceleration-time history

of a single-degree model in response to an input shock pulse of 18 g

12 ms (duration of the test pulse). The peak value of the response is

approximately 20 g. As shown in the figure, the response is

oscillatory. The period of the motion was 0.2 ms. The amplitude of the

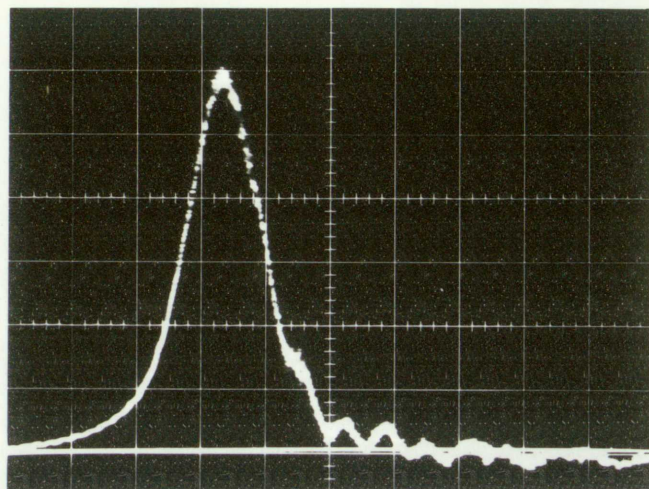
oscillations decay from response and shown in Fig. 29. It was found

that the decay is a linear decay. The waveform after 10 cycles is

shown in Fig. 30. Also, in Fig. 30, it is shown for a constant

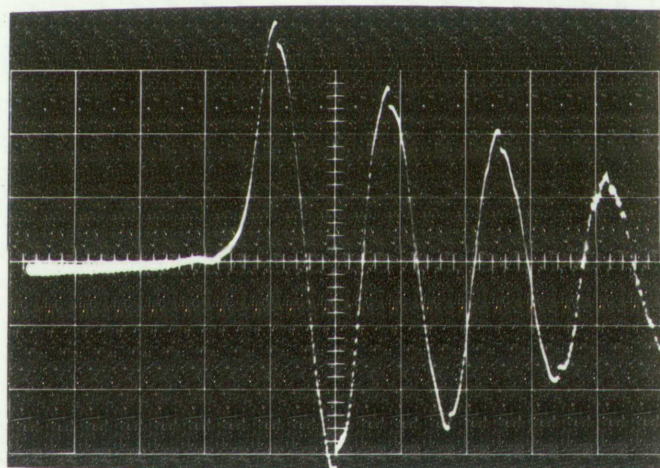
input a series of curves which show the response of the system for



Input Pulse

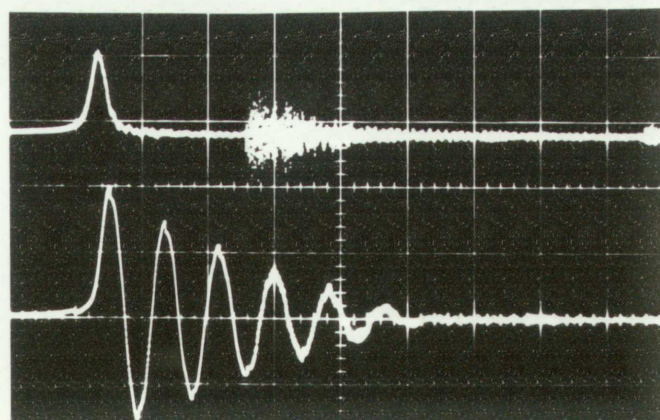
10 g/cm

2 ms/cm

Mass Response

25 g/cm

5 ms/cm

Input and Response  
to Same Time Base

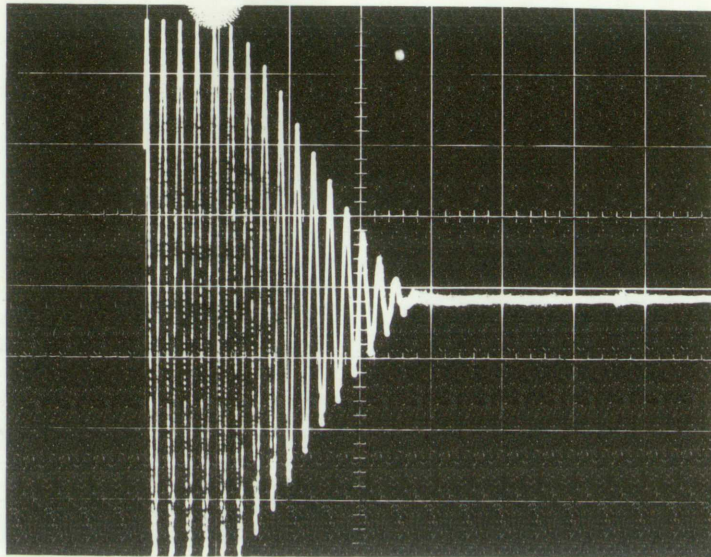
50 g/cm

10 ms/cm

Figure 29. Acceleration-Time History of a Coulomb-Damped Single-Degree System During a Shock Test



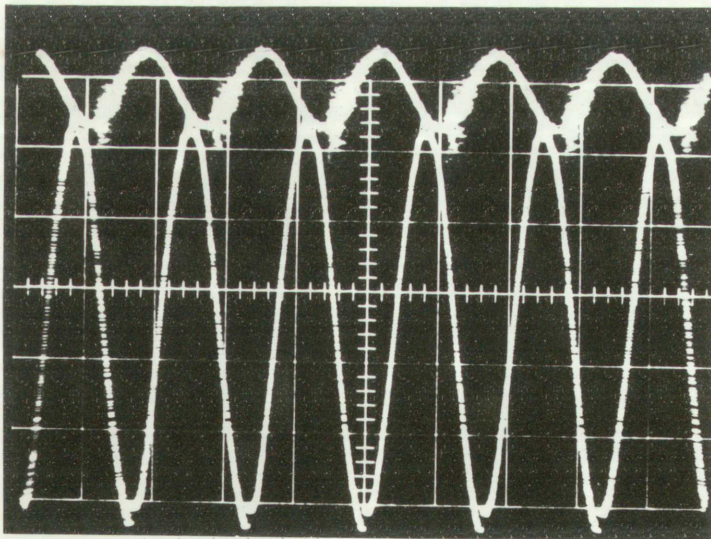
B-1



Amplitude Decay During  
Vibration Test

25 g/cm

50 ms/cm



Input and Responsive Wave-  
form During Vibration Test

Input - 10 g/cm

Response - 25 g/cm

5 ms/cm

Figure 30. Model Response During Vibration Testing

3-4

LIMBAUGH ENGINEERING & AERIAL SURVEYS, INC.  
3125 CARLISLE BLVD., N.E.  
ALBUQUERQUE, NEW MEXICO



at the peak acceleration of each cycle corresponding to the time the friction force changes direction. The amplitude of the response peaks is limited by hysteretic damping in the springs.

Fig. 31 shows the comparison of the phase-plane response and the measured response to the shock pulse mentioned above. Steps of 0.5-ms intervals were taken to plot the phase-plane diagram.

The peak measured response was considerably higher than the phase-plane response. At first glance the 15 g difference appears prohibitive. However, considering the fact that the undamped system response was approximately 8 g higher than theoretical, the difference does not seem too great. The peak responses occur at the same time and the rates of decay are similar for the two responses. It is interesting to note how the mass responds directly with the input pulse until static friction is overcome, at which time relative motion between the mass and support can occur. The phase plane was constructed assuming that static and sliding friction were identical. This assumption did not affect the peak response significantly.

Fig. 32 shows, during shock, the actual acceleration-time history of the viscously damped model in response to an input shock of 36 g, 11 ms (measured at the zero line). The input shock approximated a haversine pulse shape.

The damping ratio of the model was found to be 0.040 during the vibration test while the natural period was 11.3 ms. Fig. 33a shows





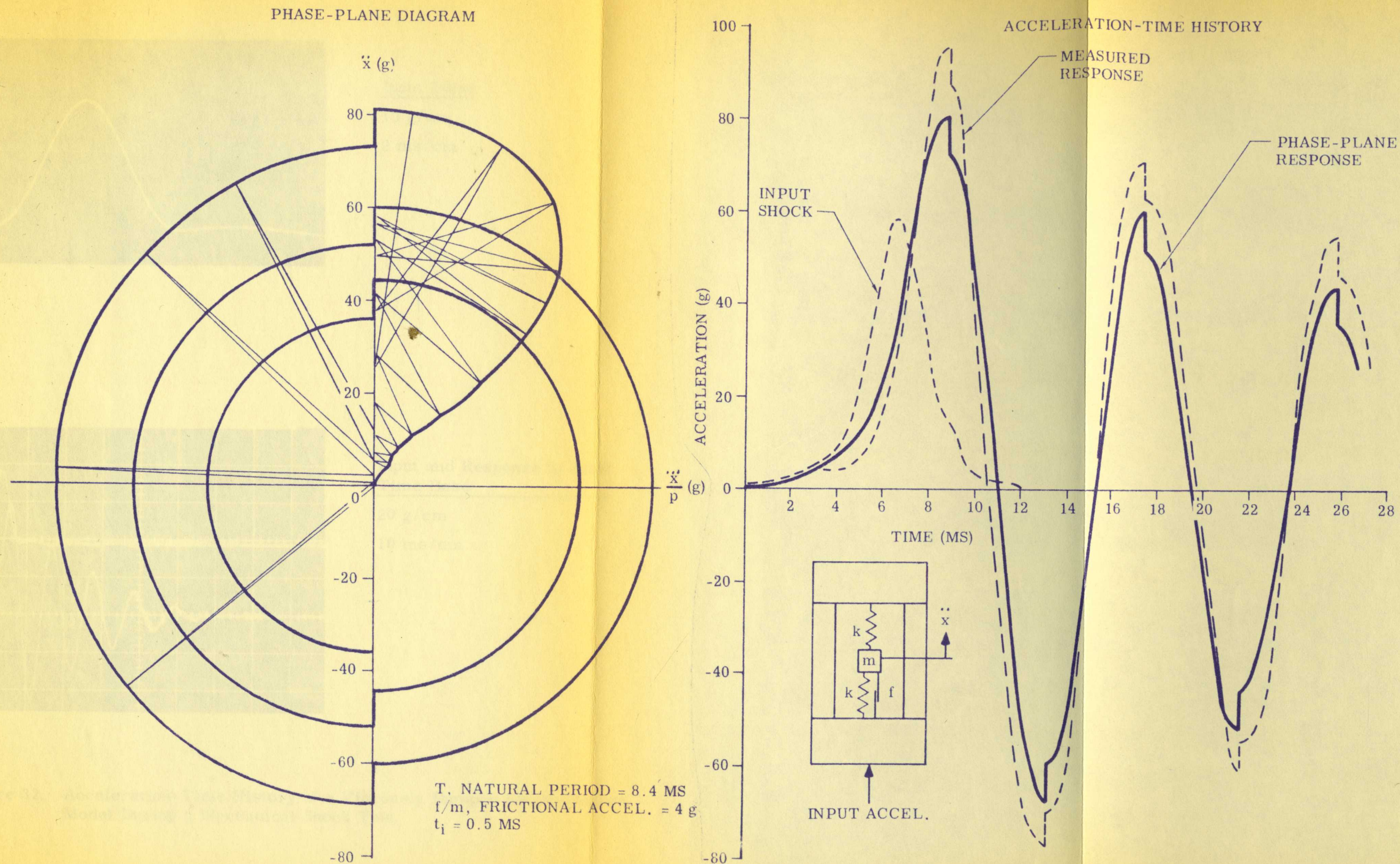
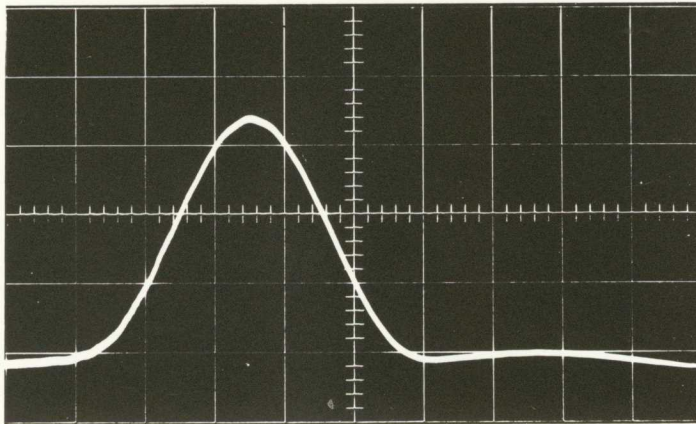


Figure 31 Comparison of Phase-Plane and Measured Response of a Coulomb Damped Single-Degree System to an Applied Acceleration Shock Pulse



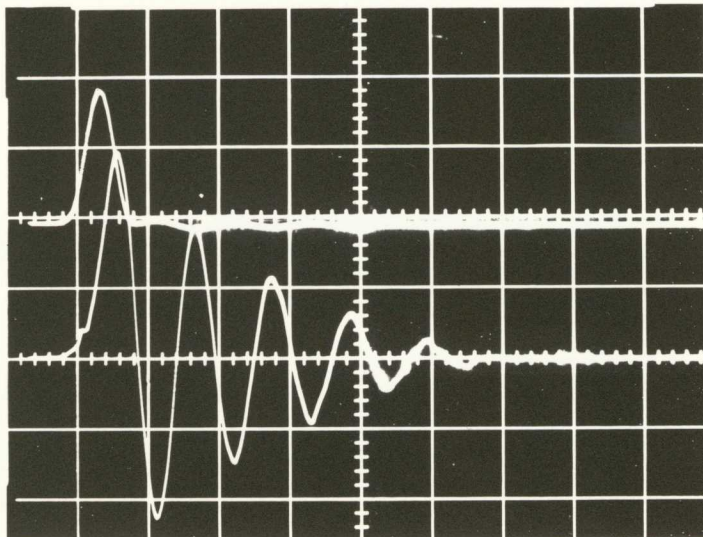




Input Pulse

10 g/cm

2 ms/cm



Input and Response to Same  
Time Base

20 g/cm

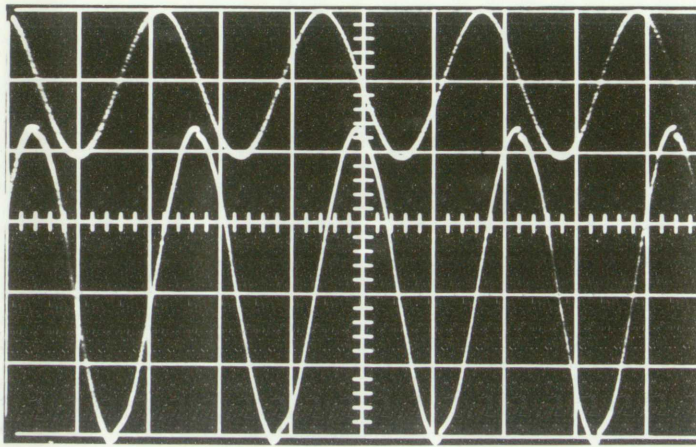
10 ms/cm

Figure 32. Acceleration-Time History of a Viscously Damped Single-Degree Model During a Mechanical Shock Test

3-3

LIMBAUGH ENGINEERING & AERIAL SURVEYS, INC.  
3125 CARLISLE BLVD., N.E.  
ALBUQUERQUE, NEW MEXICO





Input and Responsive Waveform  
During Vibration Test at  
Resonance

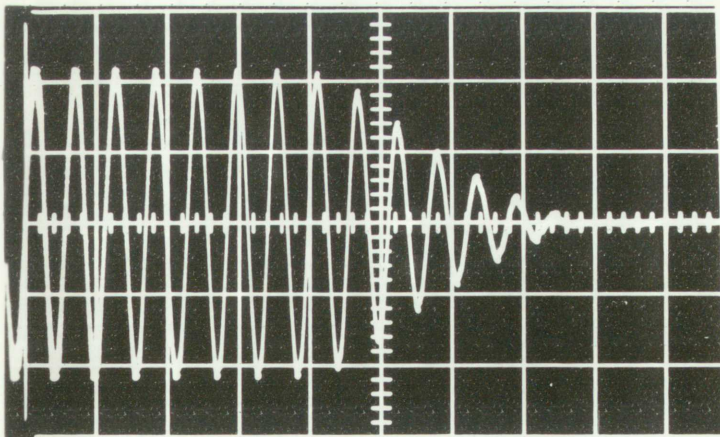
---

Input - 5 g/cm

Response - 30 g/cm

Sweep - 5 ms/cm

(a)



Amplitude Decay During  
Vibration Test

---

30 g/cm

20 ms/cm

(b)

Figure 33. Viscously Damped Model Response During Vibration Testing

3-7

LIMBAUGH ENGINEERING & AERIAL SURVEYS, INC.  
3125 CARLISLE BLVD., N.E.  
ALBUQUERQUE, NEW MEXICO



the model vibrating at resonance, while Fig. 33b shows the transient decay characteristics. Examination of both the steady-state response and transient-decay response indicated good agreement for damping ratio. (The coulomb friction of approximately 1 g was neglected.)

The type of oil used in the damper was 10-W motor oil. The viscosity of this oil was somewhat temperature sensitive. Since the vibration test was conducted at a temperature of 90°F and the shock test at 75°F, a correction to the damping ratio was made, i.e., for shock, it was calculated from temperature-viscosity curves for 10-W oil that  $\nu = 0.064$  at 75°F.

Fig. 34 shows the comparison of the phase-plane response and the measured response to the shock pulse mentioned above. Steps of 0.5-ms intervals were taken to draw the phase-plane diagram. Rectangular coordinates and the  $\Delta_{vi}$  method were used during the time of the shock pulse. Table IV presents data for determining the center of each step. A spiral template was drawn to plot the residual vibration phase-plane in oblique coordinates.

If the phase-plane had been plotted completely in oblique coordinates (assuming the damper was tied to the ground as in Fig. 17), the error in maximum response values would have been greater, but still acceptable. The magnitude of the maximum responsive acceleration in oblique coordinates (not shown in Fig. 34) was 52 g as compared to







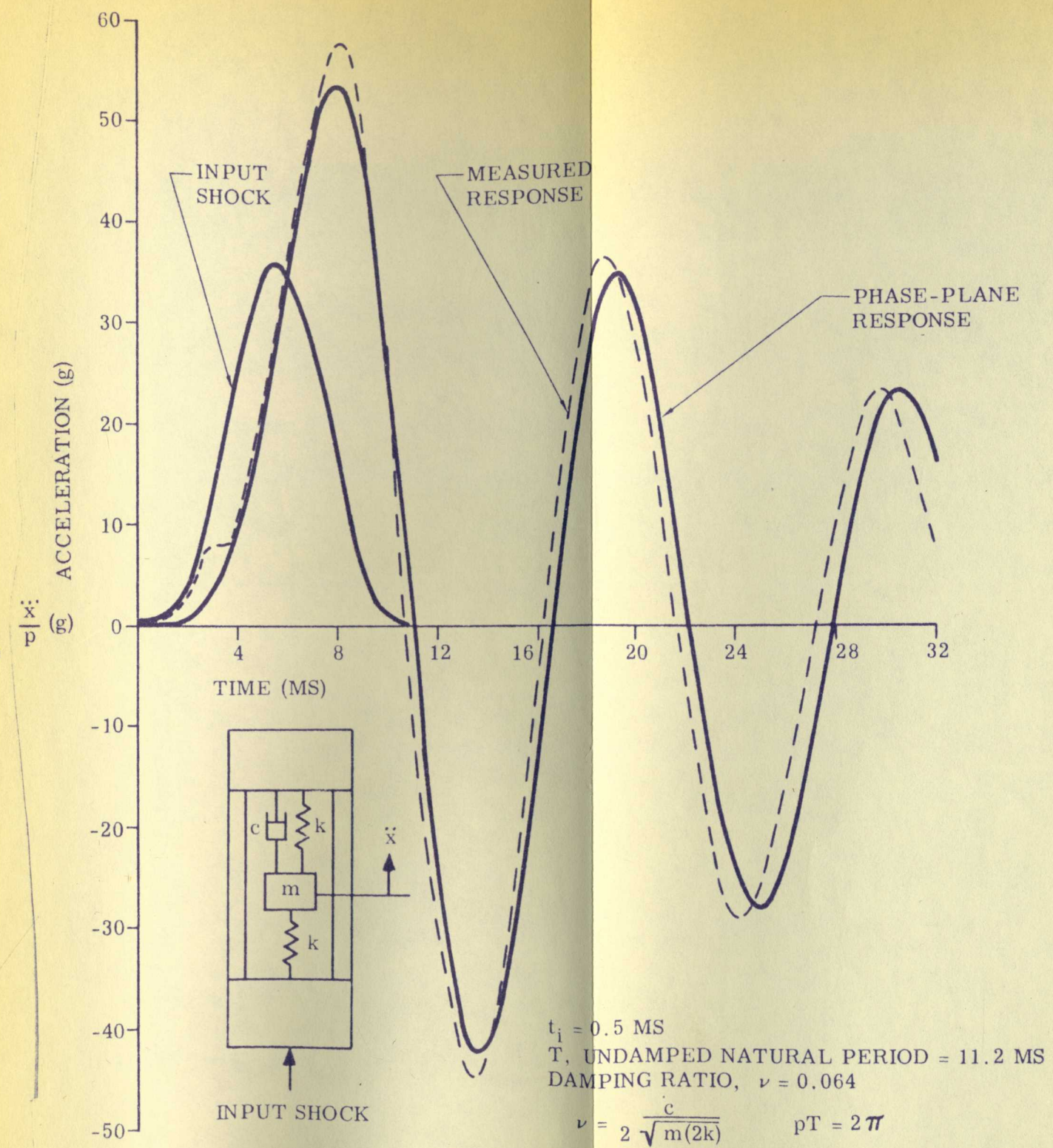
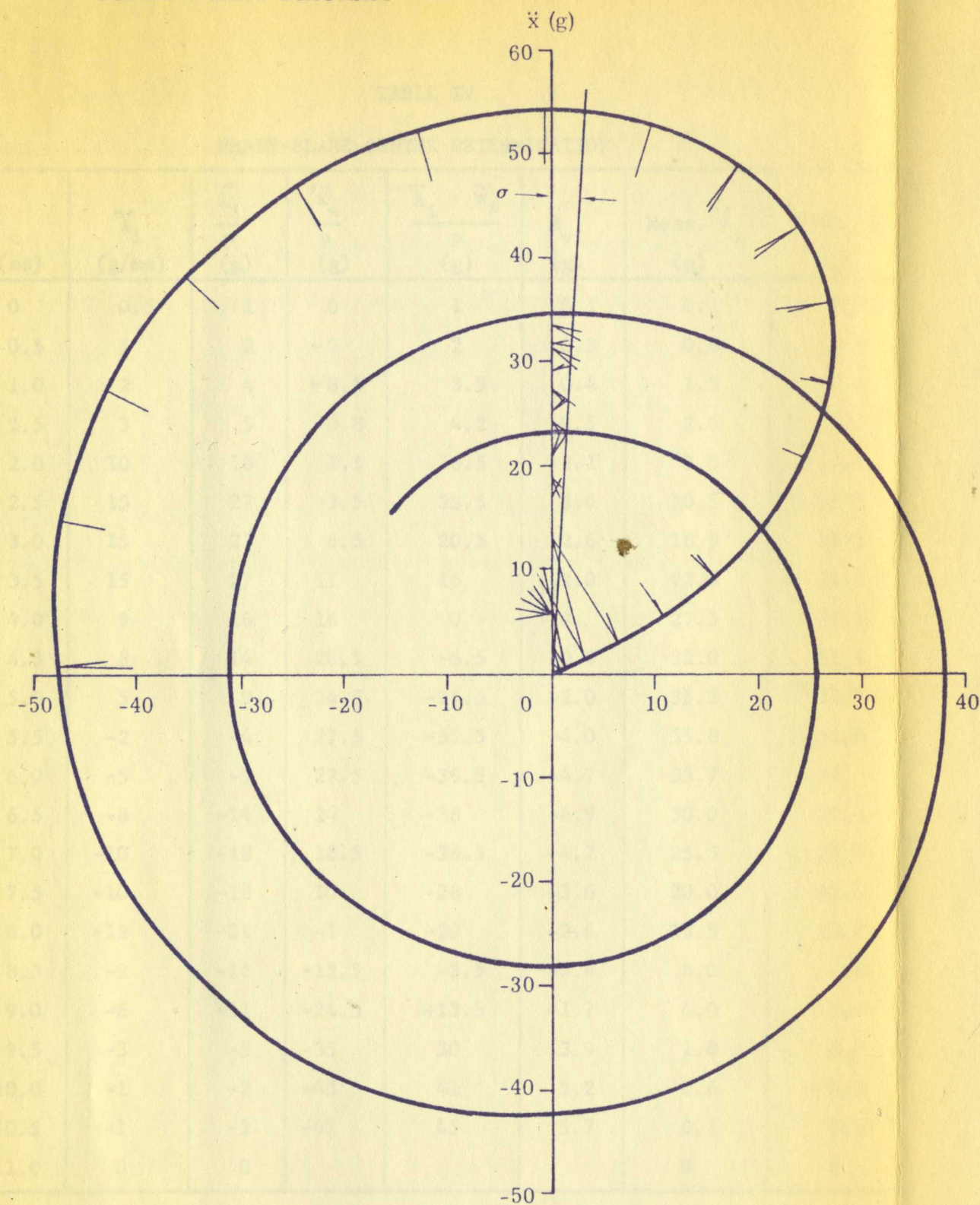


Figure 34 Comparison of Phase-Plane and Measured Response of a Viscously Damped Model Subjected to an Acceleration Shock Pulse







TABLE IV

## PHASE-PLANE CENTER DETERMINATION

t (ms)	$\ddot{\lambda}_i$ (g/ms)	$\frac{\ddot{\lambda}_i}{p}$ (g)	$\frac{\ddot{x}_*}{p}$ (g)	$\frac{\ddot{\lambda}_i - \ddot{x}_*}{p}$ (g)	$\ddot{\Delta}_{vi}$ (g)	Meas. $\ddot{\lambda}_i$ (g)	Corr. $\ddot{\lambda}_i$ (g)
0	0.5	1	0	1	0.1	0.1	0.2
0.5	1	2	~0	2	0.3	0.6	0.9
1.0	2	4	~0.5	3.5	0.4	1.3	1.7
1.5	3	5	0.8	4.2	0.5	2.6	3.1
2.0	10	18	1.5	16.5	2.1	5.5	7.6
2.5	15	27	3.5	23.5	3.0	10.5	13.5
3.0	15	27	6.5	20.5	2.6	16.5	19.1
3.5	15	27	11	16	2.0	22.5	24.5
4.0	9	16	16	0	0	27.5	27.5
4.5	8	14	20.5	-6.5	-0.8	32.0	31.2
5.0	5	9	24.5	-15.5	-2.0	35.5	33.5
5.5	-2	-4	27.5	-31.5	-4.0	35.8	31.8
6.0	-5	-9	27.5	-36.5	-4.7	33.7	29
6.5	-8	-14	24	-38	-4.9	30.0	25.1
7.0	-10	-18	18.5	-36.5	-4.7	25.5	20.8
7.5	-10	-18	10	-28	-3.6	20.0	16.4
8.0	-12	-21	-1	-20	-2.6	13.5	10.9
8.5	-9	-16	-12.5	-3.5	-0.4	8.0	7.6
9.0	-6	-11	-24.5	+13.5	+1.7	4.0	5.7
9.5	-3	-5	-35	30	3.9	1.8	5.7
10.0	-1	-2	-43	41	5.2	0.6	5.8
10.5	-1	-2	-47	45	5.7	0.1	5.8
11.0	0	0				0	0

Table 1. Summary of data for the 1990-1991 season.

Station	Depth (m)	Temperature (°C)	Salinity (psu)	Density (kg/m³)	Current (cm/s)	Direction (°)	Speed (cm/s)	Direction (°)	Speed (cm/s)
1	0.5	18.5	35.2	1022.5	1.2	135	1.2	135	1.2
2	1.0	18.2	35.1	1022.4	1.1	135	1.1	135	1.1
3	1.5	17.8	35.0	1022.3	1.0	135	1.0	135	1.0
4	2.0	17.5	34.9	1022.2	0.9	135	0.9	135	0.9
5	2.5	17.2	34.8	1022.1	0.8	135	0.8	135	0.8
6	3.0	16.8	34.7	1022.0	0.7	135	0.7	135	0.7
7	3.5	16.5	34.6	1021.9	0.6	135	0.6	135	0.6
8	4.0	16.2	34.5	1021.8	0.5	135	0.5	135	0.5
9	4.5	15.8	34.4	1021.7	0.4	135	0.4	135	0.4
10	5.0	15.5	34.3	1021.6	0.3	135	0.3	135	0.3
11	5.5	15.2	34.2	1021.5	0.2	135	0.2	135	0.2
12	6.0	14.8	34.1	1021.4	0.1	135	0.1	135	0.1
13	6.5	14.5	34.0	1021.3	0.0	135	0.0	135	0.0
14	7.0	14.2	33.9	1021.2	0.0	135	0.0	135	0.0
15	7.5	13.8	33.8	1021.1	0.0	135	0.0	135	0.0
16	8.0	13.5	33.7	1021.0	0.0	135	0.0	135	0.0
17	8.5	13.2	33.6	1020.9	0.0	135	0.0	135	0.0
18	9.0	12.8	33.5	1020.8	0.0	135	0.0	135	0.0
19	9.5	12.5	33.4	1020.7	0.0	135	0.0	135	0.0
20	10.0	12.2	33.3	1020.6	0.0	135	0.0	135	0.0
21	10.5	11.8	33.2	1020.5	0.0	135	0.0	135	0.0
22	11.0	11.5	33.1	1020.4	0.0	135	0.0	135	0.0
23	11.5	11.2	33.0	1020.3	0.0	135	0.0	135	0.0
24	12.0	10.8	32.9	1020.2	0.0	135	0.0	135	0.0
25	12.5	10.5	32.8	1020.1	0.0	135	0.0	135	0.0
26	13.0	10.2	32.7	1020.0	0.0	135	0.0	135	0.0
27	13.5	9.8	32.6	1019.9	0.0	135	0.0	135	0.0
28	14.0	9.5	32.5	1019.8	0.0	135	0.0	135	0.0
29	14.5	9.2	32.4	1019.7	0.0	135	0.0	135	0.0
30	15.0	8.8	32.3	1019.6	0.0	135	0.0	135	0.0
31	15.5	8.5	32.2	1019.5	0.0	135	0.0	135	0.0
32	16.0	8.2	32.1	1019.4	0.0	135	0.0	135	0.0
33	16.5	7.8	32.0	1019.3	0.0	135	0.0	135	0.0
34	17.0	7.5	31.9	1019.2	0.0	135	0.0	135	0.0
35	17.5	7.2	31.8	1019.1	0.0	135	0.0	135	0.0
36	18.0	6.8	31.7	1019.0	0.0	135	0.0	135	0.0
37	18.5	6.5	31.6	1018.9	0.0	135	0.0	135	0.0
38	19.0	6.2	31.5	1018.8	0.0	135	0.0	135	0.0
39	19.5	5.8	31.4	1018.7	0.0	135	0.0	135	0.0
40	20.0	5.5	31.3	1018.6	0.0	135	0.0	135	0.0
41	20.5	5.2	31.2	1018.5	0.0	135	0.0	135	0.0
42	21.0	4.8	31.1	1018.4	0.0	135	0.0	135	0.0
43	21.5	4.5	31.0	1018.3	0.0	135	0.0	135	0.0
44	22.0	4.2	30.9	1018.2	0.0	135	0.0	135	0.0
45	22.5	3.8	30.8	1018.1	0.0	135	0.0	135	0.0
46	23.0	3.5	30.7	1018.0	0.0	135	0.0	135	0.0
47	23.5	3.2	30.6	1017.9	0.0	135	0.0	135	0.0
48	24.0	2.8	30.5	1017.8	0.0	135	0.0	135	0.0
49	24.5	2.5	30.4	1017.7	0.0	135	0.0	135	0.0
50	25.0	2.2	30.3	1017.6	0.0	135	0.0	135	0.0
51	25.5	1.8	30.2	1017.5	0.0	135	0.0	135	0.0
52	26.0	1.5	30.1	1017.4	0.0	135	0.0	135	0.0
53	26.5	1.2	30.0	1017.3	0.0	135	0.0	135	0.0
54	27.0	0.8	29.9	1017.2	0.0	135	0.0	135	0.0
55	27.5	0.5	29.8	1017.1	0.0	135	0.0	135	0.0
56	28.0	0.2	29.7	1017.0	0.0	135	0.0	135	0.0
57	28.5	0.0	29.6	1016.9	0.0	135	0.0	135	0.0
58	29.0	0.0	29.5	1016.8	0.0	135	0.0	135	0.0
59	29.5	0.0	29.4	1016.7	0.0	135	0.0	135	0.0
60	30.0	0.0	29.3	1016.6	0.0	135	0.0	135	0.0
61	30.5	0.0	29.2	1016.5	0.0	135	0.0	135	0.0
62	31.0	0.0	29.1	1016.4	0.0	135	0.0	135	0.0
63	31.5	0.0	29.0	1016.3	0.0	135	0.0	135	0.0
64	32.0	0.0	28.9	1016.2	0.0	135	0.0	135	0.0
65	32.5	0.0	28.8	1016.1	0.0	135	0.0	135	0.0
66	33.0	0.0	28.7	1016.0	0.0	135	0.0	135	0.0
67	33.5	0.0	28.6	1015.9	0.0	135	0.0	135	0.0
68	34.0	0.0	28.5	1015.8	0.0	135	0.0	135	0.0
69	34.5	0.0	28.4	1015.7	0.0	135	0.0	135	0.0
70	35.0	0.0	28.3	1015.6	0.0	135	0.0	135	0.0
71	35.5	0.0	28.2	1015.5	0.0	135	0.0	135	0.0
72	36.0	0.0	28.1	1015.4	0.0	135	0.0	135	0.0
73	36.5	0.0	28.0	1015.3	0.0	135	0.0	135	0.0
74	37.0	0.0	27.9	1015.2	0.0	135	0.0	135	0.0
75	37.5	0.0	27.8	1015.1	0.0	135	0.0	135	0.0
76	38.0	0.0	27.7	1015.0	0.0	135	0.0	135	0.0
77	38.5	0.0	27.6	1014.9	0.0	135	0.0	135	0.0
78	39.0	0.0	27.5	1014.8	0.0	135	0.0	135	0.0
79	39.5	0.0	27.4	1014.7	0.0	135	0.0	135	0.0
80	40.0	0.0	27.3	1014.6	0.0	135	0.0	135	0.0
81	40.5	0.0	27.2	1014.5	0.0	135	0.0	135	0.0
82	41.0	0.0	27.1	1014.4	0.0	135	0.0	135	0.0
83	41.5	0.0	27.0	1014.3	0.0	135	0.0	135	0.0
84	42.0	0.0	26.9	1014.2	0.0	135	0.0	135	0.0
85	42.5	0.0	26.8	1014.1	0.0	135	0.0	135	0.0
86	43.0	0.0	26.7	1014.0	0.0	135	0.0	135	0.0
87	43.5	0.0	26.6	1013.9	0.0	135	0.0	135	0.0
88	44.0	0.0	26.5	1013.8	0.0	135	0.0	135	0.0
89	44.5	0.0	26.4	1013.7	0.0	135	0.0	135	0.0
90	45.0	0.0	26.3	1013.6	0.0	135	0.0	135	0.0
91	45.5	0.0	26.2	1013.5	0.0	135	0.0	135	0.0
92	46.0	0.0	26.1	1013.4	0.0	135	0.0	135	0.0
93	46.5	0.0	26.0	1013.3	0.0	135	0.0	135	0.0
94	47.0	0.0	25.9	1013.2	0.0	135	0.0	135	0.0
95	47.5	0.0	25.8	1013.1	0.0	135	0.0	135	0.0
96	48.0	0.0	25.7	1013.0	0.0	135	0.0	135	0.0
97	48.5	0.0	25.6	1012.9	0.0	135	0.0	135	0.0
98	49.0	0.0	25.5	1012.8	0.0	135	0.0	135	0.0
99	49.5	0.0	25.4	1012.7	0.0	135	0.0	135	0.0
100	50.0	0.0	25.3	1012.6	0.0	135	0.0	135	0.0



54 g determined by the  $\Delta_{v1}$  method. Unfortunately, the error in oblique coordinate plotting always tends to show less response than really occurs.

The two responsive histories show very good agreement in peak amplitude for the first three cycles of vibration. The last few cycles of vibration are distorted (see Fig. 32), which is due partly to coulomb friction being predominant. The discontinuity occurring at the start of the measured response (Fig. 32) is the static friction being overcome. The slight discrepancy between the measured and calculated period of the residual vibration must be due to instrumentation error in recording time. The difference in natural frequency and resonant frequency for  $v = 0.064$  is  $\approx 0.1\%$ .

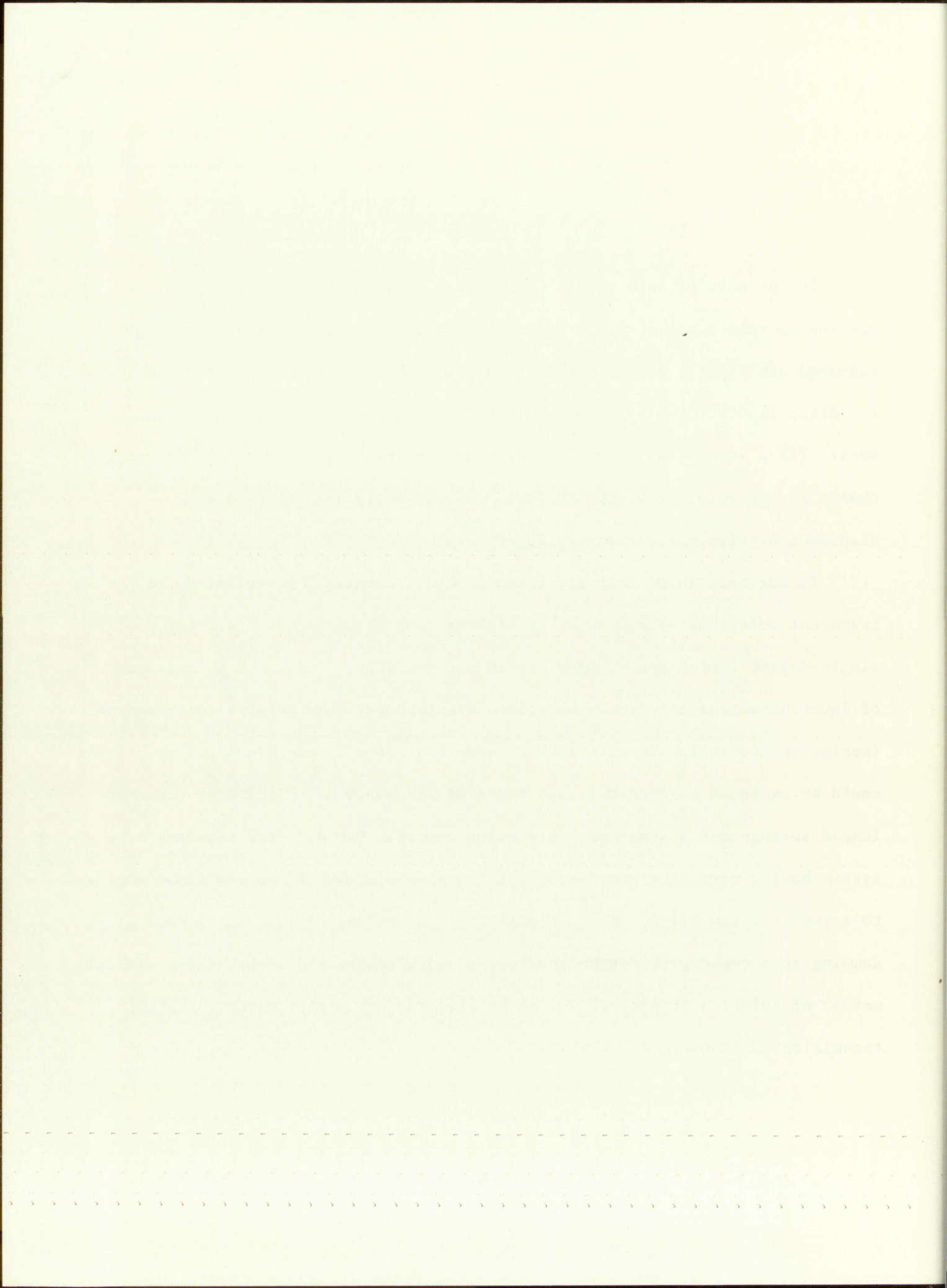




## VII. CONCLUSIONS

The purpose of this thesis has been to explore the possibility of developing relatively simple graphical solutions for the responses of linear undamped and lightly damped lumped spring-mass systems that were subjected to transient inputs. Two types of excitation of primary interest in this thesis were: (1) a controlled known acceleration-time history and (2) a sudden step change in the velocity of the support. Of secondary interest was the displacement-time excitation of the support.

It has been shown that for these types of inputs, phase-plane-delta graphical solutions of responses of lightly coulomb-damped or viscously damped single-degree lumped spring mass are indeed possible. The types of response of interest were acceleration, absolute displacement, and relative displacement (spring deflection). It was further shown that some of the graphical techniques could be extended to find the same types of responses of multidegree undamped lumped spring-mass systems having similar inputs. However, the response of a system having more than two degrees of freedom was found to be too cumbersome to solve in a few hours. Also, the addition of either coulomb or viscous damping to a two-degree system involved so many restrictions that the graphical method of solution in general had to be discarded as a tool which a trained technician could use.





Considering the single-degree systems in detail, it was found that support excitation of a system required consideration of the relative motion between the responding mass and the support. In the literature search conducted, it was found that no author had attempted the problem of determining (by phase-plane techniques) response histories of a damped system where a damper was tied between the responding mass and a movable support. For the single-degree systems, then, input pulses having a shape of either symmetrical triangle or terminal peak sawtooth were selected for ease in comparing the graphical solutions with analytical solutions obtained using Laplace transforms. Three ranges of the ratio of pulse duration to system natural period,  $\frac{t_d}{T}$ , were considered:

$$\frac{t_d}{T} < 0.2 ,$$

$$0.5 \leq \frac{t_d}{T} \leq 2.0 ,$$

and

$$\frac{t_d}{T} > 5 .$$

In each of these ranges a somewhat different procedure for constructing the phase planes was used. Whether or not the procedures would apply with the same accuracy to all types of transient pulses that could physically occur for the many different initial conditions was not determined. However, in





mechanical shock testing, acceleration pulse shapes approximating the symmetrical triangles, half-sines, haversines, parabolic cusps, and also the terminal peak sawtooth are most often applied to systems where the relative motion between the mass and support prior to the pulse is zero. Thus, the accuracies in procedures shown for the examples should be representative of accuracies that could be expected in applying the methods to actual problems. (The above statements also apply to undamped two-degree system problems.)

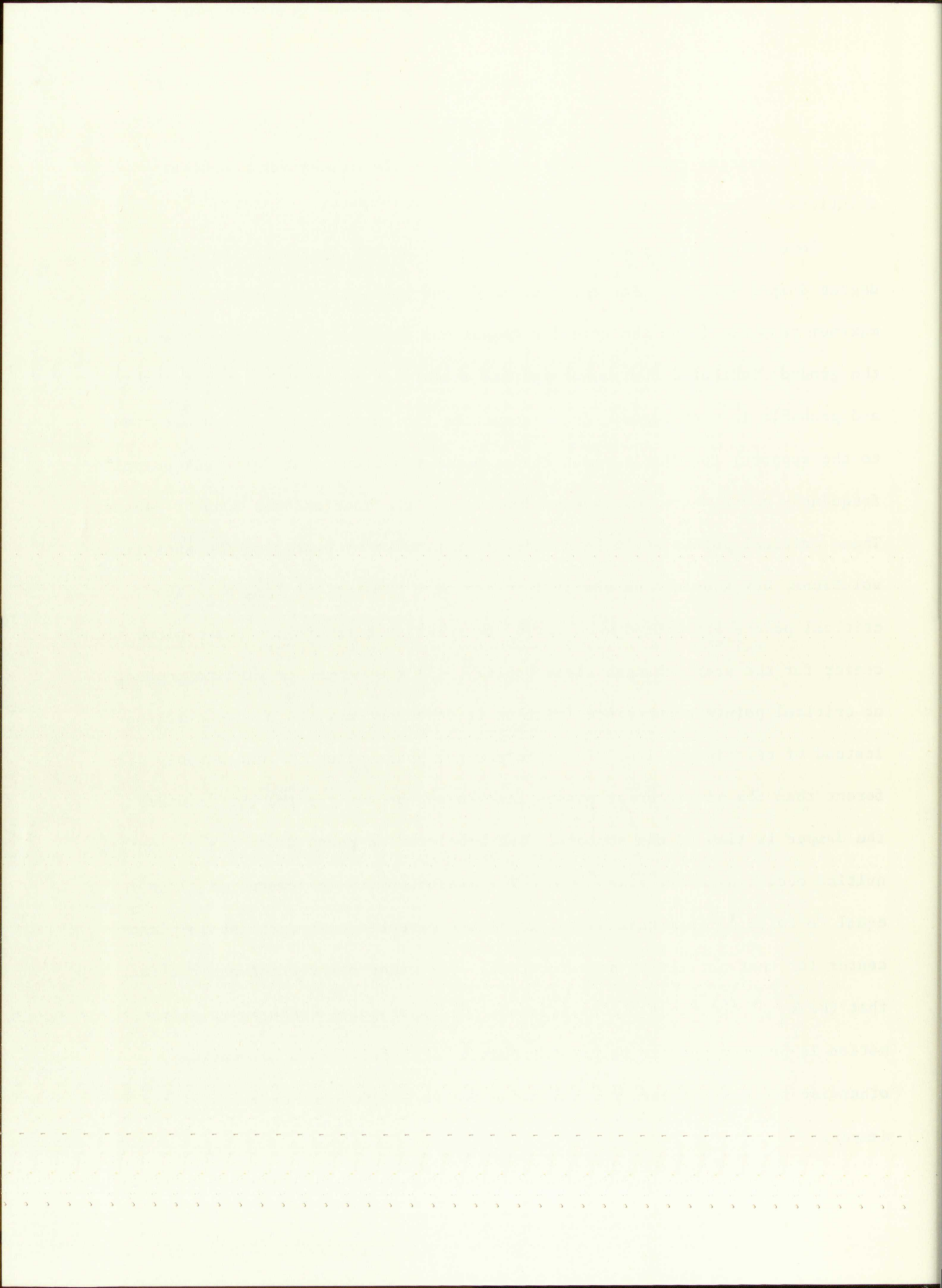
For the condition  $0.5 \leq \frac{t_d}{T} \leq 2.0$ , many steps in the phase-plane construction should be taken. It is in this range that the input pulse shape has the most effect upon the maximum response. Generally, step intervals of  $\frac{t_i}{T} = 0.1$  should not be exceeded. As the slope of the input pulse becomes larger in magnitude, the interval of the step should be lessened. As the ratio  $\frac{t_d}{T}$  exceeds 5 and approaches 10, size of the steps in the phase-plane construction can be increased until a maximum interval of  $\frac{t_i}{T} = 0.5$  is reached but not exceeded. When  $\frac{t_i}{T} = 0.5$  occurs, an actual phase-plane diagram is not needed; the responsive time plot can be made directly with little trouble. When  $\frac{t_d}{T} < 0.2$ , the shape of the input pulse has little effect upon the maximum response; the input pulse is over by the time the mass has reached its maximum response. Only one step having an area equal to the input pulse area is required. As  $\frac{t_d}{T}$  becomes even smaller, say  $\frac{t_d}{T} < 0.07$ , then it is safe to assume that the only effect of the input pulse on the system is to change the starting conditions of the responding mass if time is measured after the pulse is completed. The basic rules for size of the step interval for all the undamped





and damped systems considered are summarized in the Guides for Graphical Solutions in the appendix.

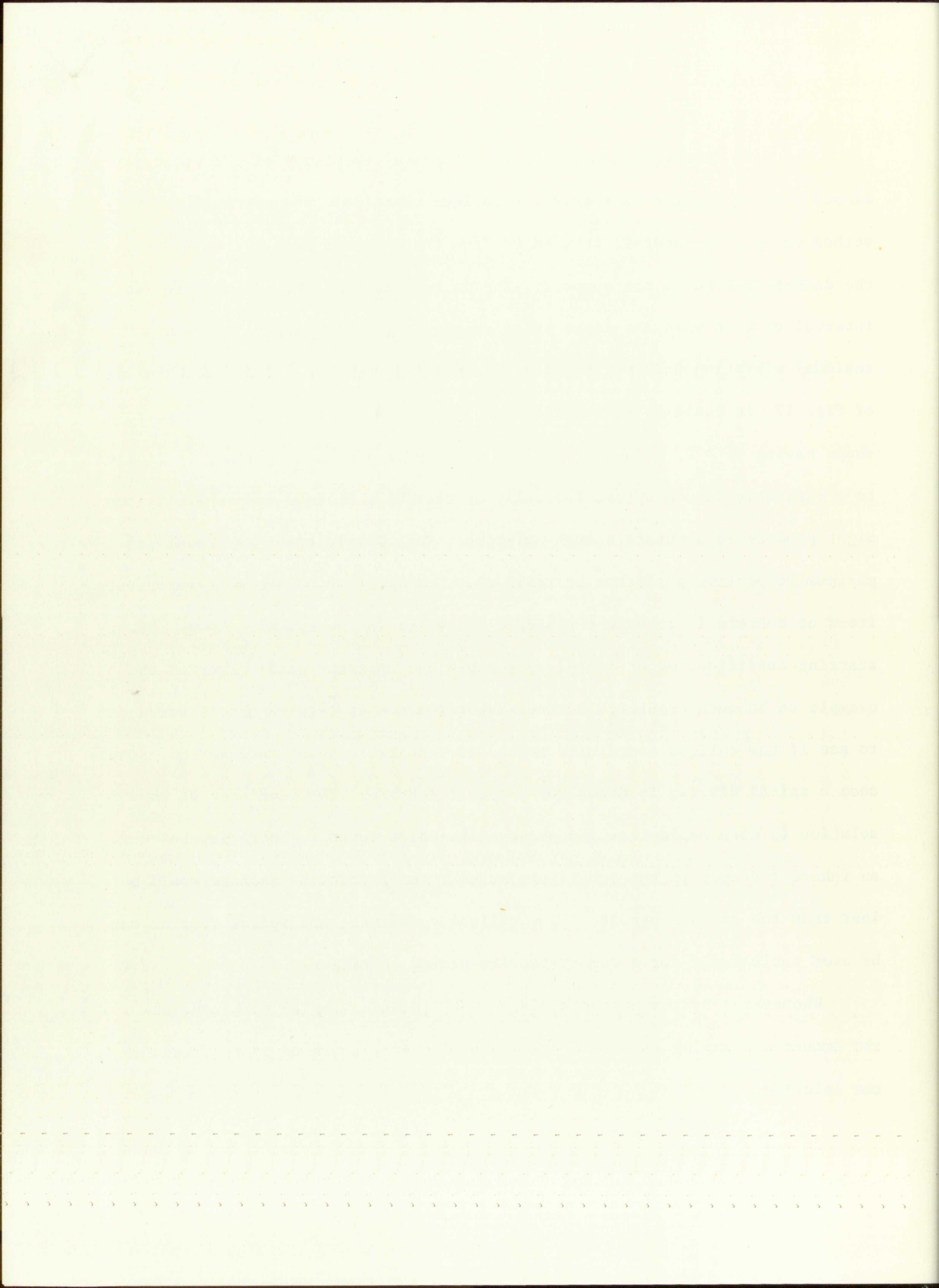
Some interesting phenomena were observed in the investigation of single-degree damped systems. For the coulomb-damped system, a comparison of the maximum response (when the friction damper was fastened to the support or to the ground) indicated that a substantial difference in magnitude was possible, and probable in most cases. In constructing the phase plane (the damper tied to the support) for displacement response, it was found that "critical points" frequently occur where relative motion between the mass and the support ceases. These critical points would be difficult to predict by examining the analytical solutions, but they can be easily foreseen in a phase-plane diagram. The critical points are caused when the  $\Delta_c$  term (which corrects the phase-plane center for the step) changes signs rapidly. If the damper is tied to ground, no critical points occur since friction is dependent only on absolute motion instead of relative motion. The acceleration phase-plane is considerably different than the displacement phase-plane in appearance for the system where the damper is tied to the support. The acceleration-phase plane has discontinuities occurring every time  $\frac{\ddot{x}}{p} = 0$ . The discontinuity (or change in  $\ddot{x}$ ) is equal to twice  $\ddot{\Delta}_c$  in magnitude and is always directed toward the phase-plane center for that particular step interval. One other observation was the fact that the  $\ddot{\lambda}_i$  of the steps at the start of the input pulse (when no relative motion is present) has to be greater than  $\ddot{\Delta}_c$  (the friction acceleration), otherwise the mass appears rigidly connected to the support by means of the damper.





The main observation noted in the graphical solutions of the viscously damped systems was the fact that the oblique coordinate and spiral diagram method cannot, in general, be used to find the response of a system where the damper is tied to the support. The method can be used, however, for any interval of time when the input pulse amplitude is not changing or when residual vibration information after the pulse is desired. From the example of Fig. 17, it could be speculated that in some cases, namely, when a pulse shape having  $\frac{t_d}{T} > 2$ , a damping ratio  $< 0.2$ , and a finite rise time, is applied to a viscously damped system initially at rest, the oblique coordinate system might produce an accurate enough solution. Very little error was found in maximum responsive amplitude or residual vibration (two of the most important items of concern in transient response analysis) in the example shown. Other starting conditions might conceivably cause the apparent small error of the example to be much greater. Further investigation in this regard is warranted to see if the oblique coordinate method is a suitable substitute method, since once a spiral diagram is drawn for a specific system, the remainder of the solution is more rapid than the phase-plane-delta method. There is, however, an inherent danger in the substitute method; the predicted response would be less than the actual response. The oblique coordinate and spiral diagram can be used exclusively for a damper-tied-to-ground condition.

Whenever a system has both viscous and coulomb damping combined, and the amount of damping is known, the phase-plane-delta method is required for the solution.





In extending the phase-plane-delta methods developed for single-degree systems to two-degree systems having support excitations, several interesting observations were made. Solving for the response of each undamped mass by graphical methods first requires describing the motion and configuration of the system in its natural modes of vibration. Then a phase-plane diagram has to be drawn for each mode, all the conditions of each mode being analogous to conditions of the undamped single-degree system. Data from each mode are then combined in some fashion to finally describe the motion of each mass separately. It was found that a single-support excitation permits a phase-plane diagram to be easily drawn, while a two-support excitation permits a phase-plane diagram to be easily drawn only in special cases. The two-support excitations have to have their amplitudes equal to some arbitrary constant ratio which requires the amplitudes to also be either 0 or 180 degrees out of phase. The addition of coulomb friction further complicates the problem because friction effects are simulated by additional support deflections. So, for friction damping to be included as a condition where a phase-plane solution is possible, only one mode of vibration can be excited, and the friction displacements of the support(s) have to be identical.

Viscous damping in a two-degree system also was shown to create problems in that, generally speaking, the two modes of vibration are not independent. Independence of modes is required for phase-plane construction. Damped two-degree systems transient responses were thus considered impractical for solution by graphical techniques.





The experimental investigation brought out two pertinent facts:

(1) the phase-plane method is more accurate than actual determination of the parameters of a linear spring-mass system; (2) natural frequency, and the amount and type of damping in a system, can be found accurately enough in a vibration test to warrant using the information to predict a transient response of the system during a shock test.

To make this thesis more usable in solving the types of problems that occur frequently in mechanical shock testing, an appendix has been included which presents phase-plane construction details. These details are shown for the response history desired for the undamped single- and two-degree lumped-mass system, the single-degree coulomb-damped system, and the single-degree viscously damped system when the type of support excitation is known.





### BIBLIOGRAPHY

1. Timoshenko, S., and Young, D. H. Vibration Problems in Engineering, 3rd Ed. D. Van Nostrand Co., Inc., New York. 1955.
2. Jacobsen, L. S., and Ayre, R. S. Engineering Vibrations, McGraw-Hill Book Co., Inc., New York. 1958.
3. Harris, C. M., and Crede, C. E. Shock and Vibration Handbook, Vol. I. McGraw-Hill, New York. 1961.
4. Jacobsen, L. S. "On A General Method Of Solving Second-Order Ordinary Differential Equations By Phase-Plane Displacements." Journal Of Applied Mechanics, pp. 543-553. Dec. 1952.
5. Bishop, R. E. D. "On The Graphical Solution Of Transient Vibration Problems." Proceedings Institute Mechanical Engineers (London). Vol. 168, No. 10, pp. 299-322. 1954.
6. Timoshenko, S., and Young, D. H. Advanced Dynamics, 1st. Ed. McGraw-Hill Co., Inc., New York. 1948.
7. Ayre, R. S. "Transient Vibration Of Linear Multi-Degree-Of-Freedom Systems By The Phase-Plane Method." Journal Of Franklin Institute, pp. 153-166. Feb. 1952.





8. Chu, W. H., and Abramson, H. N. "Application Of The Generalized Phase-Plane-Delta Method To Multi-Degree-Of-Freedom Vibrating Systems." Journal Of Applied Mechanics, pp. 580-582. Sept. 1962.
9. Mindlin, R. D. "Dynamics of Package Cushioning." Bell System Technical Journal, Vol. 24, pp. 353-461. July-Oct. 1945.
10. Hill, G. A. "Velocity Shock Transmission," Machine Design, pp. 141-144. Mar. 1962.
11. Brooks, R. O. Shock Testing Methods, Sandia Corp. Technical Memorandum SCTM 172-62(73), pp. 14, 58-65. Aug. 1962.





## APPENDIX

The following guides summarize conditions that are needed to construct phase-plane diagrams for transient response of linear, undamped, single- and two-degree lumped spring-mass-systems, and linear, single-degree viscous, and coulomb-damped systems. The type of excitation and initial conditions selected are those that are most generally found in mechanical shock testing. However, other starting conditions are possible. Displacement excitation has been included because acceleration-time data of the input pulse can be graphically integrated to obtain it. (To find spring deflections in a two-degree system problem, the input displacement must be known. Spring deflections cannot be determined merely from acceleration data of each mass.) The velocity input and velocity response determination of a system by phase planes could have been included in the list, but was not, mainly because there is no accurate way to measure velocity directly in shock testing; the information is generally obtained by the integration of acceleration-time histories or by the differentiation of displacement-time histories.



GUIDE FOR GRAPHICAL SOLUTION OF LINEAR SINGLE-DEGREE  
UNDAMPED SYSTEM PROBLEM - SUPPORT EXCITATION

Guide No.	Type Support Excitation	Type Response	Phase-Plane Construction Details
1	Acceleration $\ddot{\lambda}(t)$  (Pulse shape symmetrical, no dwell)	Absolute acceleration, $\ddot{x}$  (Forced vibration)	Coordinates: rectangular, $\ddot{x}$ and $\ddot{x}/p$ . Most probable mass starting conditions: * $\ddot{x}_0 = \ddot{x}_0 = 0$ . Suitable step intervals: ** $t_i/T = 0.5$ for $t_d/T \geq 10$ ; $t_i/T = 0.1$ for $0.5 < t_d/T < 2$ ; $t_i/T = t_d/T$ for $t_d/T \leq 0.25$ .  Center of arc: $\ddot{\lambda}_i$  Note: Angle of arc = $(360 t_i/T)$ deg. $pT = 2\pi$
		Relative displacement of mass to support, $u$  (Forced vibration)	Coordinates: rectangular, $-u$ and $-\dot{u}/p$ . Most probable starting conditions: $u_0 = \dot{u}_0 = 0$ . Suitable step intervals: ratios of $t_i/T$ under Guide No. 1 absolute acceleration apply. Center of arc: $\ddot{\lambda}_i/p^2$ . Angle of arc: $(360 t_i/T)$ deg. $pT = 2\pi$ .
2	Velocity step $ \delta\dot{\lambda}_0 $  (Sudden change in velocity to or from zero)	Absolute acceleration, $\ddot{x}$  (Free vibration)	Coordinates: rectangular, $\ddot{x}$ and $\ddot{x}/p$ . Most probable mass starting conditions: $\ddot{x}_0 = 0$ , $\ddot{x}_0 = p^2  \delta\dot{\lambda}_0 $ Center of arc: origin. Angle of arc: $(360 t_i/T)$ deg. $pT = 2\pi$ .
		Relative displacement of mass to support, $u$  (Free vibration)	Coordinates: rectangular, $u$ and $\dot{u}/p$ . Most probable starting conditions: $u_0 = 0$ , $\dot{u}_0 =  \delta\dot{\lambda}_0 $ Center of arc: origin. Angle of arc: $(360 t_i/T)$ deg. $pT = 2\pi$ .
3	Displacement $\lambda(t)$  (Pulse shape symmetrical, no dwell)	Absolute displacement, $x$  (Forced vibration)	All details same as under Guide No. 1 absolute acceleration, except for replacing $\ddot{x}$ by $x$ , $\ddot{\lambda}_i$ by $\lambda_i$ , etc.

\* Other starting conditions for each Guide No. are possible. They would have to be determined from analytical solutions.

\*\* For other input shapes including those having a dwell, these intervals might need modification for particular rise and fall times involved.



GUIDE FOR GRAPHICAL SOLUTION OF LINEAR SINGLE-DEGREE  
COULOMB-DAMPED SYSTEM PROBLEM - SUPPORT EXCITATION  
(Damper Tied to Support; Friction Permits 2 or More Cycles of Free Vibration)

Guide No.	Type Support Excitation	Type Response	Phase-Plane Construction Details
4	Acceleration $\ddot{\lambda}(t)$ (Pulse shape symmetrical, no dwell)	Absolute acceleration, $\ddot{x}$ (Forced vibration)	Coordinates: rectangular, $\ddot{x}$ and $\ddot{x}/p$ Most probable mass starting conditions: $\ddot{x}_0 = \ddot{\Delta}_c$ , $\ddot{x}_0 = 0$ if $\ddot{\lambda}_1 > \ddot{\Delta}_c$ . Until $\ddot{\lambda}_1 > \ddot{\Delta}_c$ , $\ddot{x}$ will follow $\ddot{\lambda}(t)$ curve. Suitable step intervals: See under Guide No. 1. Center of arc: $\ddot{\lambda}_1$ . Angle of arc: $(360 t_i/T)$ deg. $pT = 2\pi$ . Note: Discontinuity in $\ddot{x}$ occurs every time $\text{sgn } \ddot{x}/p$ changes; jump is always toward $\ddot{\lambda}_1$ .
		Relative displacement, $u$ (Forced vibration)	Coordinates: rectangular, $-u$ and $-\dot{u}/p$ . Most probable starting conditions: $u_0 = \dot{u}_0 = 0$ . Suitable step intervals: * $t_i/T = 0.5$ for $t_d/T \geq 10$ ; $t_i/T = 0.1$ for $0.1 \leq t_d/T \leq 2$ ; $t_i/T = t_d/T$ for $t_d/T < 0.1$ (damping ignored) Center of arc: $(\ddot{\lambda}_1/p^2) - \Delta_c \text{sgn } (-\dot{u})$ . Angle of arc: $(360 t_i/T)$ deg. $pT = 2\pi$ .
5	Velocity step $ \delta \dot{\lambda}_0 $ (Sudden change in velocity to or from zero)	Absolute acceleration, $\ddot{x}$ (Free vibration)	Coordinates: rectangular, $\ddot{x}$ and $\ddot{x}/p$ . Most probable mass starting conditions: $\ddot{x}_0 = \ddot{\Delta}_c$ ; $\ddot{x}_0 = p^2  \delta \dot{\lambda}_0 $ . Center of arc: origin. Angle of arc: $(360 t_i/T)$ deg. $pT = 2\pi$ . Note: $\ddot{x}$ reduced by $2\ddot{\Delta}_c$ every time $\text{sgn } \ddot{x}/p$ changes.
		Relative displacement, $u$ (Pseudo free vibration)	Coordinates: rectangular, $u$ and $\dot{u}/p$ . Most probable starting conditions: $u_0 = 0$ ; $\dot{u}_0 = - \delta \dot{\lambda}_0 $ . Center of arc: $\Delta_c = -\text{sgn } \dot{u}$ . Angle of arc: $(360 t_i/T)$ deg. $pT = 2\pi$ .
6	Displacement, $\lambda(t)$ (Pulse shape symmetrical, no dwell)	Absolute displacement, $x$ (Forced vibration)	Coordinates: rectangular, $x$ and $\dot{x}/p$ . Most probable mass starting conditions: $x_0 = \dot{x}_0 = 0$ . Suitable step intervals: ratios of $t_i/T$ under Guide No. 4 relative displacement apply. Center of arc: $\lambda_1 + \Delta_c \text{sgn } (\dot{\lambda} - \dot{x})$ . Angle of arc: $(360 t_i/T)$ deg. $pT = 2\pi$ .

\* For other input shapes including those having a dwell, these intervals might need modification for particular rise and fall times involved.



GUIDE FOR GRAPHICAL SOLUTION OF LINEAR SINGLE-DEGREE  
VISCOUSLY DAMPED SYSTEM PROBLEM - SUPPORT EXCITATION  
(Damper Tied to Support; Damping Ratio,  $\nu \leq 0.2$ )

Guide No.	Type Support Excitation	Type Response	Phase-Plane Construction Details
7	Acceleration, $\ddot{\lambda}(t)$  (Pulse shape symmetrical, no dwell)	Absolute acceleration, $\ddot{x}$  (Forced vibration)	<p>Coordinates: rectangular, <math>\ddot{x}</math> and <math>\ddot{x}/p</math>.</p> <p>Most probable mass starting conditions: <math>\ddot{x}_0 = \ddot{x}'_0 = 0</math>.</p> <p>Suitable step intervals: ratios of <math>t_i/T</math> under Guide No. 4 relative displacement apply.</p> <p>Center of arc: <math>\ddot{\lambda}_i + \ddot{\Delta}_{vi}</math>, where <math>\ddot{\Delta}_{vi} = 2\nu \left( \frac{\ddot{\lambda}_i - \ddot{x}_*}{p} \right)</math>. Angle of arc: <math>(360 t_i/T)</math> deg.</p> <p>Note: Spiral diagram is used when amplitude of input pulse does not change for a time. Then angle of spiral diagram arc = <math>p\sqrt{1 - \nu^2} t_i</math> rad.</p>
		Relative displacement of mass to support, $u$  (Forced vibration)	<p>Coordinates: oblique, <math>-u</math> and <math>-\dot{u}/p</math>.</p> <p>Most probable starting conditions: <math>u_0 = \dot{u}_0 = 0</math>.</p> <p>Suitable step intervals: ratios of <math>t_i/T</math> under Guide No. 4 relative displacement apply.</p> <p>Center of arc: <math>\ddot{\lambda}_i/p^2</math> (on <math>\ddot{\lambda}/p^2</math> oblique axis).</p> <p>Note: Spiral diagram needed. Angle of arc = <math>p\sqrt{1 - \nu^2} t_i</math> rad.</p>
8	Velocity step $ \delta\dot{\lambda}_0 $  (Sudden change in velocity to or from zero)	Absolute acceleration, $\ddot{x}$  (Free vibration)	<p>Coordinates: oblique, <math>\ddot{x}</math> and <math>\ddot{x}/p</math>.</p> <p>Most probable mass starting conditions: <math>\ddot{x}_0 = 2\nu p  \delta\dot{\lambda}_0 </math>. <math>\ddot{x}'_0 = p^2(1 - 4\nu^2)  \delta\dot{\lambda}_0 </math></p> <p>Center of arc: origin.</p> <p>Note: Spiral diagram used. Angle of arc = <math>p\sqrt{1 - \nu^2} t_i</math> rad.</p>
		Relative displacement, $u$  (Free vibration)	<p>Coordinates: oblique, <math>u</math> and <math>\dot{u}/p</math>.</p> <p>Most probable starting conditions: <math>u_0 = 0</math>; <math>\dot{u}_0 = - \delta\dot{\lambda}_0 </math></p> <p>Center of arc: origin</p> <p>Note: Spiral diagram used; Angle of arc = <math>p\sqrt{1 - \nu^2} t_i</math> rad.</p>
9	Displacement $\lambda(t)$  (Pulse shape symmetrical, no dwell)	Absolute displacement, $x$  (Forced vibration)	<p>All details same as under Guide No. 7 absolute acceleration except for replacing <math>\ddot{x}</math> by <math>x</math>, <math>\ddot{\lambda}_i</math> by <math>\lambda_i</math>, etc.</p>



GUIDE FOR GRAPHICAL SOLUTION OF TWO-DEGREE LINEAR UNDAMPED  
SYSTEM PROBLEM - SINGLE-SUPPORT EXCITATION

Guide No.	Type Support Excitation	Type Response	Phase-Plane Construction Details
10	Acceleration $\ddot{\lambda}(t)$ (Pulse shape symmetrical, no dwell)	Absolute acceleration, $\ddot{x}$ and $\ddot{y}$ (Forced vibration)	<p>Coordinates: principal, <math>\ddot{\theta}_I/H_I</math> and <math>\ddot{\theta}_I/p_I H_I</math> for mode I</p> <p><math>\ddot{\theta}_{II}/H_{II}</math> and <math>\ddot{\theta}_{II}/p_{II} H_{II}</math> for mode II.</p> <p>Most probable starting conditions: <math>\ddot{x}_0 = \ddot{y}_0 = \ddot{x}_0 = \ddot{y}_0 = 0</math>; therefore each phase plane starts at origin.</p> <p>Suitable step intervals: Steps <math>t_i/T_I</math> of mode I and <math>t_i/T_{II}</math> of mode II each follow rules under Guide No. 1.</p> <p>Centers of arcs: <math>\ddot{\lambda}_i</math> for both mode I and II. Angles of arcs: <math>(360 t_i/T_I \text{ or } T_{II})</math> deg.</p> <p>Note: Principal coordinates transformed to rectangular coordinates by <math>\ddot{x} = \ddot{\theta}_I + \ddot{\theta}_{II}</math> and <math>\ddot{y} = \alpha_I \ddot{\theta}_I + \alpha_{II} \ddot{\theta}_{II}</math>.</p>
11	Velocity step $ \delta \dot{\lambda}_0 $ (Sudden change in velocity to or from zero)	Absolute acceleration, $\ddot{x}$ and $\ddot{y}$ (Free vibration)	<p>Coordinates: principal, <math>\ddot{\theta}_I</math> and <math>\ddot{\theta}_I/p_I</math> for mode I</p> <p><math>\ddot{\theta}_{II}</math> and <math>\ddot{\theta}_{II}/p_{II}</math> for mode II.</p> <p>Most probable starting conditions: <math>\ddot{x}_0 = \ddot{y}_0 = 0</math>; <math>\ddot{\theta}_I = \ddot{\theta}_{II} = 0</math>; initial jerk <math>\ddot{\dot{x}}_0</math> and <math>\ddot{\dot{y}}_0</math> expressed in principal coordinates are</p> $\ddot{\theta}_I = p_I^2  \delta \dot{\lambda}_0  \left( \frac{1 - \alpha_{II}}{\alpha_I - \alpha_{II}} \right)$ $\ddot{\theta}_{II} = p_{II}^2  \delta \dot{\lambda}_0  \left( \frac{\alpha_I - 1}{\alpha_I - \alpha_{II}} \right)$ <p>Center of arcs: origin Angles of arcs: <math>(360 t_i/T_I \text{ or } T_{II})</math> deg.</p> <p>Note: Principal coordinates transformed to rectangular coordinates by <math>\ddot{x} = \ddot{\theta}_I + \ddot{\theta}_{II}</math>, <math>\ddot{y} = \alpha_I \ddot{\theta}_I + \alpha_{II} \ddot{\theta}_{II}</math></p>
12	Displacement $\lambda(t)$ (Pulse shape symmetrical, no dwell)	Absolute displacement, $x$ and $y$ (Forced vibration)	<p>All details same as in Guide No. 10 except replacing <math>\ddot{\theta}_I</math> by <math>\theta_I</math>, <math>\ddot{x}</math> by <math>x</math>, etc.</p> <p>See example pp. 67-68 to evaluate <math>\alpha_I</math>, <math>\alpha_{II}</math>, <math>p_I</math>, <math>p_{II}</math>, <math>H_I</math>, <math>H_{II}</math>.</p>









